# DEVELOPMENT OF FIBER CEMENT ROOF TILE USING PERLITE, COCONUT FIBER, AND NATURAL LATEX

JIRA PATTHANAVARIT

A THESIS SUBMITTED IN PARTIAL FULFILLMENT OF THE REQUIREMENT FOR
THE DEGREE OF MASTER OF SCIENCE IN APPLIED PHYSICS
DEPARTMENT OF PHYSICS SCHOOL OF SCIENCE
KING MONGKUT'S INSTITUTE OF TECHNOLOGY LADKRABANG
2022

KMITL-2022-SC-M-030-090

| | |
|---|---|
| **หัวข้อวิทยานิพนธ์** | การพัฒนากระเบื้องหลังคาไฟเบอร์ซีเมนต์โดยใช้เพอร์ไลต์ เส้นใยมะพร้าว และน้ำยางธรรมชาติ |
| **ชื่อนักศึกษา** | จิรา พัฒนวริศ |
| **รหัสประจำตัว** | 62605040 |
| **ปริญญา** | วิทยาศาสตรมหาบัณฑิต (ฟิสิกส์ประยุกต์) |
| **ภาควิชา** | ฟิสิกส์ |
| **พ.ศ.** | 2565 |
| **อาจารย์ที่ปรึกษาวิทยานิพนธ์** | ผู้ช่วยศาสตรจารย์ ดร.เมตยา กิติวรรณ |
| **อาจารย์ที่ปรึกษาวิทยานิพนธ์ร่วม** | ดร.นิตยา แก้วแพรก |

## บทคัดย่อ

งานวิจัยนี้มุ่งเน้นการพัฒนาผลิตภัณฑ์กระเบื้องหลังคาไฟเบอร์ซีเมนต์โดยการใช้เส้นใยมะพร้าวมาทดแทนการใช้แร่ใยหิน และเติมวัสดุเพอร์ไลท์เพื่อให้น้ำหนักเบาและเพิ่มความเป็นฉนวนความร้อน นอกจากนั้นยังมีการเติมยางพาราเพื่อป้องการการดูดซึมน้ำของผลิตภัณฑ์อีกด้วย งานวิจัยแบ่งออกเป็น 2 ส่วนหลัก ส่วนแรกจะเป็นการศึกษาเงื่อนไขการเติมปริมาณเพอร์ไลท์ที่เหมาะสมโดยกำหนดอัตราส่วนระหว่างทรายต่อซีเมนต์เป็น 2:1 อัตราส่วนน้ำต่อซีเมนต์เป็น 1:2 และทำการศึกษาการแทนที่ทรายด้วยเพอร์ไลท์ปริมาณ 5–15 เปอร์เซ็นต์โดยน้ำหนักของทราย และศึกษาการใช้แรงอัดขึ้นรูปด้วยแม่พิมพ์ขนาด 15 x 2.5 ตารางเซนติเมตร ด้วยแรงที่ 20 , 30 และ 40 กิโลนิวตัน (5.3, 8.0 และ 10.6 เมกะปาสคาล ตามลำดับ) ในส่วนที่สองจะนำเงื่อนไขที่ดีที่สุดที่ได้จากตอนแรกมาทำการขึ้นรูปชิ้นงานไฟเบอร์ซีเมนต์ และทำการศึกษาปริมาณการเติมเส้นใยมะพร้าวในปริมาณ 2.5–12.5 กรัม และความยาวของเส้นใยมะพร้าว 1–3 เซนติเมตร รวมถึงศึกษาผลของการเคลือบยางพาราบนเส้นใยมะพร้าว ชิ้นงานจะถูกบ่มเป็นเวลา 28 วัน ก่อนนำไปทดสอบสมบัติต่างๆ ผลการวิจัยส่วนแรกพบว่าสามารถขึ้นรูปชิ้นงานซีเมนต์มอร์ต้าผสมเพอร์ไลท์ได้ สูตรที่เหมาะสมจะเติมเพอร์ไลท์ เปอร์เซ็นต์โดยน้ำหนักและใช้แรงอัด 40 กิโลนิวตัน ซึ่งชิ้นงานที่ได้มีความหนาแน่น 1773 กิโลกรัมต่อลูกบาศก์เมตร การดูดซึมน้ำ 14.0 เปอร์เซ็นต์ และความต้านแรงดัดโค้ง 12.65 เมกะปาสคาล จากนั้นจึงนำเงื่อนไขดังกล่าวไปทำการวิจัยต่อในส่วนที่สองคือการเพิ่มเส้นใยมะพร้าวลงไปเพื่อขึ้นรูปเป็นเพอร์ไลท์ไฟเบอร์ซีเมนต์ โดยพบว่าการผลิตชิ้นงานไฟเบอร์ซีเมนต์โดยการใช้เส้นใยมะพร้าวนั้นควรมีการปรับปรุงผิวของเส้นใยด้วยการเคลือบน้ำยางพาราและเพอร์ไลท์ก่อนนำไปขึ้นรูป โดยเส้นใยที่เคลือบนั้นมีข้อดีมากกว่าเส้นใยที่ไม่เคลือบ ถึงแม้จะมีความหนาแน่นเพิ่มขึ้นเล็กน้อยแต่มีค่าการต้านทานแรงดัดโค้งและมีค่าการดูดซึมน้ำที่ดีกว่าตัวอย่างที่ผสมเส้นใยแบบไม่เคลือบ ทั้งนี้ชิ้นงานที่ใช้เส้นใยที่ไม่เคลือบนั้นเมื่อในไปใช้งานจริงอาจมีอายุการใช้งานที่สั้นกว่าเพราะอาจจะเกิดการกัดกร่อนจากความเป็นเบสในปูนซีเมนต์ จากการวิจัยสูตรที่เหมาะสมกับการนำไปใช้งานจริงคือสูตรที่มีการผสมเส้นใยมะพร้าวที่เคลือบยางพาราความยาว

3 เซนติเมตร และผสมลงในปริมาณ 0.005 เปอร์เซ็นของน้ำหนักมวลรวม โดยมีความหนาแน่นอยู่ที่ 1763 กิโลกรัมต่อลูกบาศก์เมตร ค่าการดูดซึมน้ำอยู่ที่ 17.9 เปอร์เซ็นต์ ค่าความต้านทานแรงดัดโค้งอยู่ที่ 6.63 เมกะปาลคาล และมีค่าการนำความร้อน 0.133 วัตต์ต่อเมตร-เคลวิน

**คำสำคัญ:** กระเบื้องหลังคา เพอร์ไลท์ ไฟเบอร์ซีเมนต์ ยางธรรมชาติ เส้นใยมะพร้าว

| | |
|---|---|
| **Thesis Title** | Development of Fiber Cement Roof Tile using Perlite, Coconut Fiber, and Natural Latex |
| **Student Name** | Jira Patthanavarit |
| **Student ID** | 62605040 |
| **Degree** | Master of Science (Applied Physics) |
| **Department** | Physics |
| **Year** | 2022 |
| **Thesis Advisor** | Asst. Prof. Dr. Mettaya Kitiwan |
| **Thesis Co – Advisor** | Dr. Nittaya Keawprak |


## Abstract

This research focuses on the development of fiber cement roof tiles by using coconut fibers instead of asbestos and filled with perlite to make them lighter and increase heat insulation. Natural latex was also added to prevent water absorption of the product. The research was divided into two main parts. The first part was to study the optimum perlite addition. The cement to water ratio of 2:1 was kept constant, while the cement to aggregate ratio of 1:2 was desired. The content of sand was replaced with perlite ranging from 5–15 % by weight. The specimen was pressed in mold size 15 x 2.5 $cm^2$ under the uniaxial force varied from 20, 30, and 40 kN (5.3, 8.0, and 10.6 MPa, respectively). In the second part, the best condition obtained from the first part was used to fabricate the fiber cement. The effects of amount of coconut fibers added 2.5–12.5 g and the length of coconut fibers between 1 and 3 cm were studied. The effect of natural latex coating on coconut fibers was also investigated. The specimens were cured for 28 days before testing for various properties. A cement mortar mixed with perlite was successfully fabricated. The optimum conditions selected were the 10 wt% perlite and compressive molding of 40 kN. The resulting specimen had a density of 1773 $kg/m^3$, water absorption of 14.0%, and flexural strength of 12.65 MPa. These fabrication conditions were then applied for producing perlite fiber cement using coconut fiber. The fiber cement production using coconut fiber should be improved by coating the fibers with natural latex and perlite before molding. The natural latex coated fibers showed advantages over uncoated fibers. Although the density of specimen slightly increased, the

flexural strength and water absorption were better than those of the samples mixed with uncoated fibers. The specimens using uncoated fibers might have a shorter lifetime because the deterioration from by base in cement. In this research, the suitable condition for practical application was using natural latex coated coconut fiber of 3 cm length and mixed in 0.005% by total weight. The obtained fiber cement exhibited density of 1763 kg/m$^3$, water absorption of 17.9%, flexural strength of 6.63 MPa, and thermal conductivity of 0.133 W/m K.

**Keywords:** Roofing tile, perlite, fiber cement, natural latex, coconut fiber

# Acknowledgment

Firstly, this special project would not have been possible and could be accomplished without assistance from Asst. Prof. Dr. Mettaya Kitiwan, principal thesis advisor and lecturer at Department of Applied Physics, Faculty of Science, King Mongkut's Institute of Technology Ladkrabang (KMITL). Author feels very grateful and appreciative to be given the academic knowledge and advice until the completely of this research.

Secondly, thanks also go to co-adviser, Dr. Nittaya Keawprak who is Researcher at Thailand Institute of Scientific and Technological Research (TISTR). Working with Dr.Nittaya Keawprak, who author has been given pretty advice and idea for solving problems this master thesis until this research was successfully completed.

Finally, thank also goes to Thailand Institute of Scientific and Technological Research (TISTR), for providing specific instruments, equipment and facilities required for researching.

Jira Patthanavarit

# Content

บทคัดย่อ ..... i
Abstract ..... iii
Acknowledgment ..... v
Content ..... vi
List of figures ..... ix
List of Table ..... xiii
Chapter 1 ..... 1
Introduction ..... 1
1.1 Research motivation ..... 1
1.2 Objectives of the study ..... 2
1.3 Scopes of the study ..... 2
1.4 Benefits of the study ..... 2
Chapter 2 ..... 3
Theory and literature reviews ..... 3
2.1 Cement ..... 3
2.1.1 Manufacturing processes of cement ..... 3
2.1.2 Chemical composition of cement ..... 4
2.1.3 Main compounds in cement ..... 5
2.1.4 Setting and hardening ..... 6
2.1.5 Hydration reaction ..... 7
2.1.6. Factors that affect the rate of hydration reaction ..... 10
2.1.7. Type of Portland cement ..... 10
2.2 Perlite ..... 11
2.3 Pozzolanic activity ..... 11
2.3.1 Effect of pozzolan particle characteristic ..... 12
2.3.2 Effect of pozzolan compositions ..... 12
2.4 Coconut fiber ..... 13

2.5 Characterization equipment ..... 14
2.5.1 X-ray diffraction (XRD) ..... 14
2.5.2 Fourier-transform infrared spectroscopy (FTIR) ..... 16
2.5.3 Thermal conductivity principle ..... 20
2.6 Literature reviews ..... 24
Chapter 3 ..... 29
Research methodology ..... 29
3.1 Introduction ..... 29
3.2 Research procedure ..... 29
3.2.1 Mortar preparation ..... 29
3.2.2 Fiber preparation ..... 31
3.3 Characterization method ..... 32
3.3.1 Physical properties characterization ..... 33
3.3.2 Thermal conductivity test ..... 34
3.3.3 Mechanical test ..... 35
3.3.4 Accelerated degradation test ..... 36
Chapter 4 ..... 37
Results and Discussions ..... 37
4.1 Investigation of perlite mortar ..... 37
4.1.1 Bulk density of perlite mortar ..... 38
4.1.2 Water absorption of perlite mortar ..... 39
4.1.3 Flexural strength of perlite mortar ..... 41
4.1.4 Thermal conductivity of perlite mortar ..... 42
4.1.5 XRD results of perlite mortar ..... 43
4.1.6 Summary for Mortar conditions ..... 46
4.2 Investigation of coconut fiber ..... 47
4.2.1 Microstructure of coconut fiber ..... 47
4.2.2 FTIR results of coconut fiber ..... 48

4.3 Investigation of perlite fiber cement ..... 51
4.3.1 Physical and mechanical properties of specimens using uncoated coconut fiber (UCF) ..... 51
4.3.2 Physical and mechanical properties of specimens using natural latex coated coconut fiber (CCF) ..... 53
4.3.3 Thermal conductivity of perlite fiber cement ..... 56
4.3.4 Microstructure of perlite fiber cement ..... 57
4.4 Comparison of properties of perlite fiber cements prepared with uncoated coconut fiber (UCF) and coated coconut fiber (CCF) ..... 60
4.4.1 Comparison of bulk density ..... 60
4.4.2 Comparison of water absorption ..... 62
4.4.3 Comparison of flexural strength ..... 64
4.4.4 Comparison of properties with the values in literature ..... 66
4.5 Accelerated degradation test result ..... 68
4.5.1 Bulk density before and after accelerated degradation test ..... 68
4.5.2 Water absorption before and after accelerated degradation test ..... 69
4.5.3 Flexural strength before and after accelerated degradation test ..... 70
4.6 Cost-benefit analysis ..... 71
Chapter 5 ..... 73
Conclusions ..... 73
References ..... 75
Appendix ..... 78

# List of figures

Figure 2.1 Flow diagram of the 2 conditions of cement manufacturing..... 4
Figure 2.2 Microstructure of Tricalcium silicate ($C_3S$) [4]. ..... 5
Figure 2.3 Diagram of setting and hardening of cement. ..... 7
Figure 2.4 The illustration of calcium silicate reaction products [4]..... 8
Figure 2.5 (a) $C_3A$ hydration retardation process and (b) enlarge image of monosulphate hydrate and ettringite [4]. ..... 9
Figure 2.6 Illustration of X-ray diffraction on crystal lattice according to Bragg's Law. [8] ..... 15
Figure 2.7 Electromagnetic spectrum [9]. ..... 16
Figure 2.8 Interaction between infrared light and matter [9]. ..... 17
Figure 2.9 FTIR Spectroscopy functional group correlation table [9]. ..... 17
Figure 2.10 Parts of an FTIR spectrometer with source, interferometer, and detector [9].18
Figure 2.11 The function of timing laser in FTIR. Each data point in the infrared is taken when the laser interferogram has neither constructive nor destructive interference [9]. ..... 19
Figure 2.12 Schematic drawing of (a) THB tandem strip and (b) tandem strips in parallel [10]. ..... 21
Figure 2.13 Circuit diagram of Wheatstone bridge in THB tandem strip [10]. ..... 21
Figure 2.14 Diagram show heat flow from sensor into specimens [10]. ..... 22
**Figure 2.15** Schematic of thermal conductivity by heat flux method [11]. ..... 23

Figure 3.1 (a) Hydraulic pressing machine, and (b) steel mold used in the molding process ..... 30
Figure 3.2 The macrograph of cement mortar specimen. ..... 31
Figure 3.3 Coconut fiber immersed in sodium hydroxide solution. ..... 31
Figure 3.4 Coated coconut fiber preparation in two steps, (a) immersed fiber in natural latex to form an adhesive layer and (b) coated fiber with perlite. ..... 32

Figure 3.5 Schematic procedures to measure the physical properties: (a) cement mortar bar specimens, (b) small specimens cut from bar, (c) drying at 105 °C for 24 h then cooling in desiccator and weighing (dry weight, D), (d) boiling at 100 °C for 2 h, (e) cooling to room temperature and immersing for 24 h, (f) weighing in water (suspended weight, *S*), and (g) weighing in air (saturated weight, *W*). ..... 33
Figure 3.6 Sandwich setup of sample and sensor for testing thermal conductivity. ... 34
Figure 3.7 Photograph of specimen for test thermal conductivity in heat flux technique. ..... 35
Figure 3.8 (a) Schematic drawing of three-point bending figure, and (b) testing apparatus set in Universal testing machine. ..... 35
Figure 3.9 (a) Salt spray machine and (b) specimens during accelerated degradation test. ..... 36

Figure 4.1 Effects of expanded perlite content and compressive force on bulk density of perlite mortar. ..... 39
Figure 4.2 Effects of expanded perlite content and compressive force on water absorption of perlite mortar..... 40
Figure 4.3 Effects of expanded perlite content and compressive force on flexural strength of perlite mortar. ..... 42
Figure 4.4 Effects of expanded perlite content and compressive force on thermal conductivity of perlite mortar..... 43
Figure 4.5 XRD patterns of mortar and perlite mortar..... 44
Figure 4.6 XRD pattern of perlite mortar coataing 10wt% perlite and the characteristic peak mached with the ICDD data. ..... 45
**Figure 4.7** Photomicrographs of (a) coconut fibers before treatment at 10x magnification and (b) 40x magnification, (c) coconut fiber after treatment at 10x magnification, and (c) 40x magnification..... 47

Figure 4.8 Photomicrographs of (a) coconut fibers after coated with natural latex at 10x magnification and (b) 40x magnification, (c) coconut fiber after coated second layer with perlite at 10x magnification and (d) 40x magnification. ..... 48
Figure 4.9 FTIR results of coconut fibers before and after alkaline treatment. ..... 49
Figure 4.10 FTIR result of coconut fibers after coating with natural latex. ..... 50
Figure 4.11 Bulk density of perlite fiber cements prepared with uncoated coconut fiber (UCF). ..... 51
Figure 4.12 Water absorption of perlite fiber cements prepared with uncoated coconut fiber (UCF). ..... 52
Figure 4.13 Flexural strength of perlite fiber cements prepared with uncoated coconut fiber (UCF). ..... 53
Figure 4.14 Bulk density of perlite fiber cements prepared with coated coconut fiber (CCF). ..... 54
Figure 4.15 Water absorption of perlite fiber cements prepared with coated coconut fiber (CCF). ..... 55
Figure 4.16 Flexural strength of perlite fiber cements prepared with coated coconut fiber (CCF). ..... 56
Figure 4.17 Thermal conductivity of perlite fiber cement specimens. ..... 57
Figure 4.18 Photomicrographs of perlite fiber cement prepared from 1 cm uncoated coconut fiber with content of (a) 2.5 g, (b) 5.0 g (c) 7.5 g, (d) 10 g. (At x10 magnification) ..... 58
Figure 4.19 Photomicrographs of perlite fiber cement prepared from (a) uncoated fiber (b) coated fiber. (At magnification x10)..... 59
Figure 4.20 Crack decfects observation in specimen using coated coconut fiber of 1 cm length, (a) and (b) showing the crack at different area in same sample. (At magnification x10)..... 59
Figure 4.21 Optical stereo photographs of non-adherent rubber on fiber surface (a) at magnification x10 and (b) at magnification x40. ..... 60

Figure 4.22 Bulk density of perlite fiber cement prepared with uncoated and coated coconut fibers. ..... 61
Figure 4.23 Water absorption of specimens that contain fiber coated rubber and uncoated rubber. ..... 62
Figure 4.24 Flexural strength of specimens that contain fiber coated rubber and uncoated rubber. ..... 64
Figure 4.25 Comparison of bulk density of specmimens prepared with uncoated and coated coconut fiber before and after accelerated degradation test. ..... 69
Figure 4.26 Comparison of water absorption of specmimens prepared with uncoated and coated coconut fiber before and after accelerated degradation test. ..... 69
Figure 4.27 Comparison of flexural strength of specmimens prepare with uncoated and coated coconut fiber before and after accelerated degradation test. ..... 70

# List of Table

Table 2.1 Main composition of Portland cement. 5

Table 2.2 The chemical composition of expanded perlite. 11

**Table 2.3** Thermo physical properties of coconut fiber. 14

Table 2.4 Summary of literature reviews. 27

Table 2.5 Summary of literature reviews. (continued) 28

Table 3.1 Particles size of expanded perlite. 29

Table 3.2 Mix proportions of cement mortar. 30

Table 4.1 Bulk density of perlite mortar with different perlite content and compressive force. 38

Table 4.2 Water absorption of perlite mortar with different perlite content and compressive force. 40

Table 4.3 Flexural strength of perlite mortar with different perlite content and compressive force. 41

Table 4.4 Thermal conductivity of perlite mortar with different perlite content and compressive force. 43

Table 4.5 Summary properties of perlite mortar with 10% perlite content. 46

Table 4.6 Bulk density of specimens with uncoated coconut fiber and coated coconut fiber. 61

Table 4.7 Percentage of the change in bulk density between specimens prepared with coated coconut fiber and uncoated coconut fiber. 62

Table 4.8 Water absorption of specimens with uncoated coconut fiber (UCF) and coated coconut fiber (CCF). 63

Table 4.9 Percentage of the change in water absorption between specimens prepared with coated coconut fiber and uncoated coconut fiber. 63

Table 4.10 Flexural strength of specimens with uncoated coconut fiber (UCF) and coated coconut fiber (CCF)..... 65
Table 4.11 Percentage of the change in flexural strength between specimens prepared with coated coconut fiber and uncoated coconut fiber..... 65
Table 4.12 Comparison of properties with the values in literature..... 67
Table 4.13 Cost-benefit analysis of perlite fiber cement roof tile..... 72

# Chapter 1
# Introduction

## 1.1 Research motivation

Asbestos is a group of inorganic minerals that occur in nature. Asbestos presents as an extremely fine fiber that possesses high strength and good heat resistance. 90% of asbestos is used for fiber cement products such as roof sheets, tiles, and ceiling tiles [1]. However, asbestos fiber cement is harmful to health when it is damaged. The damaged fiber cement would release tiny dust or fiber into the air. Subsequently, they would be inhaled or ingested by creatures. Unfortunately, the inhaled fibers can cause health problems such as lung cancer or asbestosis, even though they have coalesced in small quantities. Hence, in many developed countries, alternative materials are adopted for replacing asbestos.

Fundamentally, natural fibers can be used as an alternative material. Thailand is an agricultural country that has abundant biomass waste such as rice straw, sugarcane bagasse, coconut fiber, etc. Coconut fiber has many attractive properties, i.e., high tensile strength and low thermal conductivity, to use as a reinforcement of cement product. Using natural materials can also reduce the cost of raw materials. However, natural fiber would be rapidly degraded due to the chemical reaction with cementitious materials which may directly affect the durability of the cement products. Several papers report that silicious materials which consist lastly of silicon dioxide ($SiO_2$) can be used to prevent the degradation of natural fiber in cement products [2].

Perlite is an amorphous volcanic glass containing $SiO_2$ about 75%. Thus, perlite is a promising additive for fiber cement. Moreover, the addition of perlite resulted in improvement of the physical and thermal properties [3] of cement products such as lighter weight and higher thermal insulation. However, perlite could cause high water absorption of cement products which is inappropriate for use as building materials. Therefore, the suitable amount of perlite addition into cement products should be investigated.

Another feasible way for improving the durability of natural fibers is the modification of fiber by rubber coating. The rubber coating could be an intermediate

layer to protect the natural fiber from chemical attack and humidity. The study of the addition of perlite along with coconut fiber has never been reported. Therefore, this research aims to investigate the effect of perlite and coconut fiber addition on the physical, thermal, and mechanical properties of fiber cement products for roof tile application. The utilization of coconut fiber in building materials is not only economical but also eco-friendly. The investigation results in this research would be the guideline of sustainable development for the construction industry.

## 1.2 Objectives of the study

1) Study the effect of perlite addition on physical, thermal, and mechanical properties of Mortar product.
2) Study the effect of coconut fiber addition on physical, thermal, and mechanical properties of fiber cement product.
3) Investigate the optimized compositions and fabrication conditions of perlite-fiber cement to use for roof tile application.

## 1.3 Scopes of the study

This research focuses on the production of fiber cement products that mainly consists of Portland cement, sand, perlite, and coconut fiber.

1) The perlite was applied as a sand-substitutional material. The different fractions of expanded perlite, i.e., 0, 5, 10, 15 wt% of total aggregate mass in the mixture was examined.
2) The coconut fiber was used as reinforcement in perlite cement. The difference fiber length (1–3 cm) and content (2.5–15 g in total mass of 1000 g) were investigated.
3) The degradation of the coconut fiber with and without natural rubber coating was compared.

## 1.4 Benefits of the study

The perlite fiber cement with optimized composition will possess lightweight, low water absorption, high thermal insulation, and high flexural strength, which proper for roof tile application. The knowledge from this research could be a guideline for producing eco-friendly and sustainable building materials.

# Chapter 2
# Theory and literature reviews

## 2.1 Cement

Cement is a chemical or ceramic material that is caused by a chemical reaction between particles that aggregate into a structure, where the chemical reaction is a Hydration reaction. Cement has been used for construction buildings since Roman times. However, when the Roman Empire declined the use of cement ended as well. In 1824, Joseph Aspdin successfully invented cement and obtained a patent for Portland cement manufacturing. Cement was invented in Portland city in England, which is the reason it is called Portland cement. When cement is solidified, it will have a gray color like construction stone.

### 2.1.1 Manufacturing processes of cement

Portland cement contains the following raw materials: (1) Calcareous materials such as Limestone, Chalk, (2) Argillaceous materials such as Silica, Alumina in form of Clay or Shale, and (3) Iron oxide materials such as Iron ore, Laterite Manufacturing processes of cement can be divided into two types according to the characteristic of the material as shown in Figure 2.1.

1. Wet process: Chalk and Clay are mixed in the proper proportion; water is applied to mix them then mill thoroughly. After that, put the mixture into the kiln.

2. Dry process: Limestone and Shale are mixed in a dry condition before putting into the kiln.

When the raw material has been milled thoroughly, the mixture will be put in the kiln which is mostly a rotary kiln. The burning temperature is approximately 1400–1500°C. At this temperature, the raw materials are melted into Clinker. Then, let it cool down and mill again. The gypsum was added while milling to delay the coagulation time of cement.

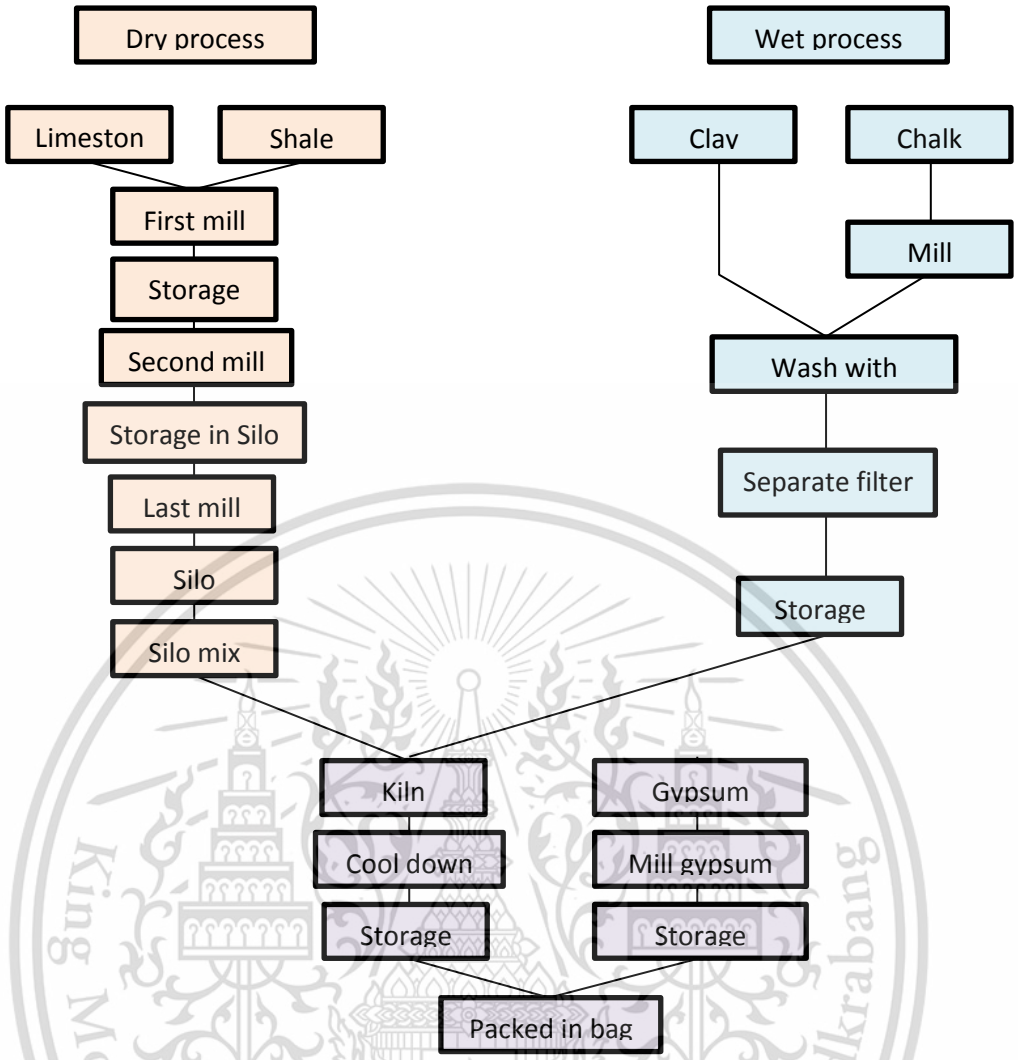


**Figure 2.1** Flow diagram of the 2 conditions of cement manufacturing.

### 2.1.2 Chemical composition of cement

When all raw materials are burned in a kiln, water vaporizes from raw material and $CO_2$ emits from limestone and chalk, then only CaO remains in the mixture. Then, an oxide combination occurred between CaO and $Fe_2O_3$. After the chemical oxide combines, the crystallization of cement compound will form when cool it down. Portland cement oxide composition can be divided into 2 main groups

1. Main oxide such as CaO, $SiO_2$, $Al_2O_3$, $Fe_2O_3$ all together 90% of cement weight

2. Secondary oxide such as MgO, $Na_2O$, $TiO_2$, $P_2O_5$, and gypsum

The main oxide will combine during clinker formation, forming into 4 important compounds as shown in Table 2.1.

**Table 2.1** Main composition of Portland cement.

| Compound name | Chemical composition | Abbreviation |
|---|---|---|
| Tricalcium Silicate | 3 CaO · $SiO_2$ | $C_3S$ |
| Dicalcium Silicate | 2 CaO · $SiO_2$ | $C_2S$ |
| Tricalcium Aluminate | 3 CaO · $Al_2O_3$ | $C_3A$ |
| Tetracalcium Aluminoferrite | 4 Cao· $Al_2O_3$· $Fe_2O_3$ | $C_4AF$ |

### 2.1.3 Main compounds in cement

1. Tricalcium Silicate ($C_3S$)

The morphology of $C_3S$ presents in a hexagon shape and dark gray color as shown in Figure 2.2. When $C_3S$ is mixed with water, it will set in 2–3 h, the strength of $C_3S$ cement extremely increases in the first week. When the reaction occurs, heat is released about 500 J/g. Generally, Portland cement contains $C_3S$ approximately 35–55%.

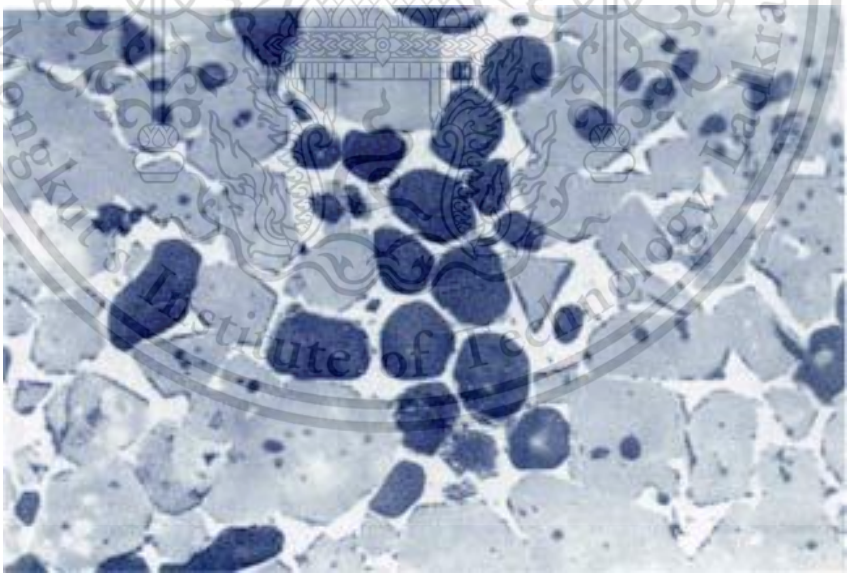

**Figure 2.2** Microstructure of Tricalcium silicate ($C_3S$) [4].

2. Dicalcium Silicate ($C_2S$)

The morphology of $C_2S$ compound exhibits a circle shape. $C_2S$ has many different forms but only $\beta$ -$C_2S$ exists at normal temperature. $\beta$-$C_2S$ has a cohesive property. When mixing with water, it causes a hydration reaction that releases heat of 250 J/g. The setting of $C_2S$ will slowly increase strength but in the long term, the strength of $C_2S$ is comparable with that of $C_3S$. Portland cement contains $C_2S$ approximately 15–35 %.

3. Tricalcium Aluminate ($C_3A$)

The $C_3A$ phase has a faceted shape. $C_3A$ reacts with water immediately which causes rapid setting and release heat of 850 J/g. To prevent flash setting, gypsum is added during the cement milling process. The strength of $C_3A$ cement increases in 1–2 days but their strength of $C_3A$ is quite low. Portland cement has $C_3A$ approximately 7–15%

4. Tetracalcium Aluminoferrite ($C_4AF$)

$C_4AF$ reacts with water rapidly and sets in a few minutes. During the reaction, it releases heat of about 420 J/g. The strength of $C_4AF$ is low. Portland cement has $C_4AF$ approximately 5–10%.

### 2.1.4 Setting and hardening

When mixing cement with water, it will form a cement paste in a liquid state for a short period. The properties of cement paste remained unchanged. This period is called a dormant period. After that, the cement paste begins to set but it still not rigid to be demolded. This period is called the initial set and the duration from the process of mixing cement with water to the initial set is called the initial setting time. The cement paste continues setting till it reaches solid-state or the final set. This period is called the final setting time. However, the paste will continue setting and the strength of cement gradually increases. This final process period is called hardening. The step of setting and hardening of cement paste is shown in Figure 2.3.

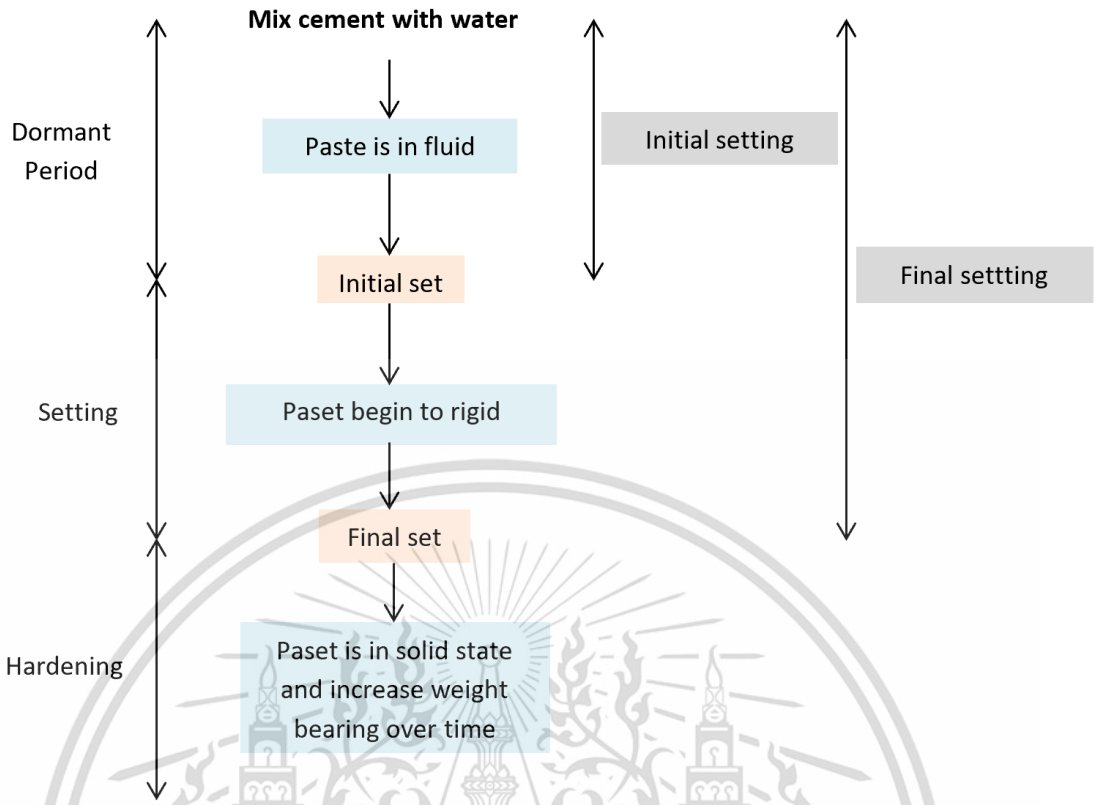


**Figure 2.3** Diagram of setting and hardening of cement.

### 2.1.5 Hydration reaction

The setting and hardening of cement are caused by the hydration reaction of a component in cement. The reaction occurs in two steps: solution formation and solid-state reaction. At the beginning state, cement reacts with water forming a solution that contains many ions, and then the ions combine and form new compounds. After that, a solid-state reaction occurs directly on the surface of the component.

Cement contains many compounds, when hydration reaction occurs, a product may continue to react and create a new product. The hydration reaction of each compound in cement will be described as follows.

1. Hydration reaction of Calcium Silicate ($C_2S$, $C_3S$)

Calcium Silicate reacts with water, forming calcium hydroxide ($Ca(OH)_2$) and calcium silicate hydrate (CHS). These phases perform as a binder. Figure 2.4 shows the illustration of calcium silicate reaction products. The reaction process can be divided into three stages: Stage 1, when $C_3S$ is mixed with water, heat increases rapidly, and then the heat will gradually reduce and stop in 15 minutes. Following

stage 2 or the dormant period, cement is in a plastic state for several hours. At this stage, the cement paste can be poured or molded. At stage 3, the reaction of $C_3S$ will repeat, and the duration of this state is approximately 2–3 h after mixing $C_3S$ with water, corresponding to the initial setting phase. The heat is released during this stage, and the rate of heat generation increases to the maximum value at the aging time of 4–8 h. The initial set starts at this point. The cement paste begins to be hardened and the strength also increases with time. The reaction between $C_2S$ and water is similar to that of $C_3S$ but the reaction of $C_2S$ is slower. Thus, the heat released from $C_2S$ when reacting with water is lower than $C_3S$. The hydration reaction from these compounds also will create a gel on the surface of the component. When it solidifies, two main characteristics which are irregular structure and porosity are obtained.

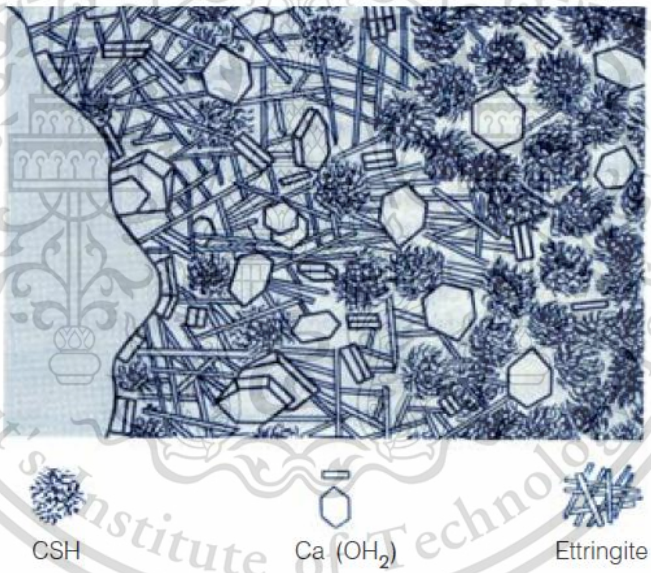


**Figure 2.4** The illustration of calcium silicate reaction products [4].

2. Hydration reaction of Calcium aluminate and Ferrite ($C_3A$)

The hydration reaction of $C_3A$ is instantaneous and causes rapid solidification. To delay the reaction, gypsum is added during cement milling. The gypsum will react with $C_3A$ to form an ettringite layer on the $C_3A$ surface. Ettringite layers delay the setting of $C_3A$ and thus the initial set is dependent on the hydration reaction of $C_3S$ and $C_2S$. However, the formation of ettringite does not affect the hydration reaction of $C_3A$. When ettringite is formed on the $C_3A$ surface, the pressure is generated by

increasing the volume of the $C_3A$ solid. This pressure causes the ettringite layer to rupture and undergo a hydration reaction of $C_3A$. However, a new ettringite can be formed to delay hydration reaction again till the sulfate ions are insufficient to form ettringite. The hydration reaction of $C_3A$ occurs by converting ettringite to monosulphate hydrate as shown in Figure 2.5.

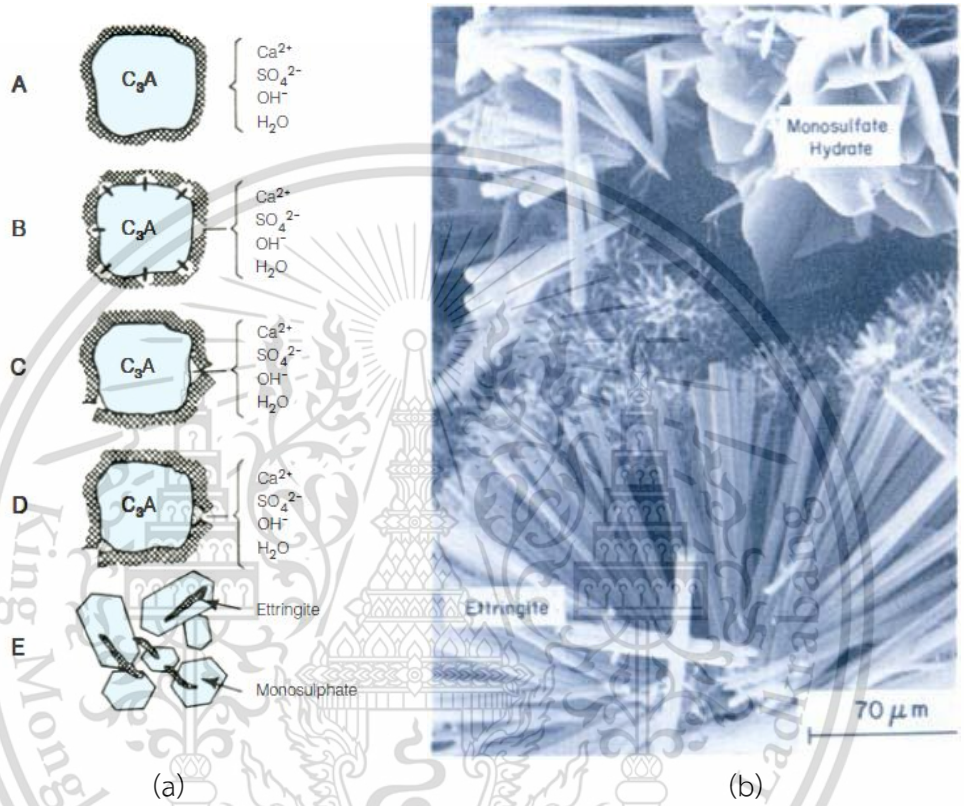


**Figure 2.5** (a) $C_3A$ hydration retardation process and (b) enlarge image of monosulphate hydrate and ettringite [4].

3. Hydration reaction of Calcium aluminate and Ferrite ($C_4AF$)

The reaction of $C_4AF$ is similar to that of $C_3A$, but it occurs more slowly and generates less heat. Iron oxide (F) compounds react like aluminum oxide (A) and can replace them. Gypsum delays the reaction of $C_4AF$ more than $C_3A$. The reaction between $C_4AF$ and gypsum produces sulphoaluminate and sulphoferrite.

### 2.1.6. Factors that affect the rate of hydration reaction

The rate of hydration reaction depends on several factors. The properties of cement depend on the rate of hydration reaction. Therefore, factors affecting the rate of hydration reaction will affect the properties of the hardened cement paste.

1. **Cement component**: The Hydration reaction rate of each compound is different as described previously.
2. **Cement fineness**: High fineness cement will have more surface area to contact with water. As a result, a quick hydration reaction will occur.
3. **Water to Cement ratio**: Initially, the water to cement ratio did not affect the hydration reaction rate. In the latter, the hydration rate is reduced if the water to cement ratio in the mixture is low.
4. **Temperature**: Hydration reaction rate increases with increasing temperature. However, the increasing temperature must not cause the paste to dry.

### 2.1.7. Type of Portland cement

**Type 1** Ordinary Portland cement: This cement is the most widely used, suitable for the normal concrete products.

**Type 2** Modified Portland cement: It is suitable for use in moderate heat and sulphate resistant applications.

**Type 3** High early strength Portland cement: This type of cement provides high early strength, due to fineness than ordinary Portland cement which is suitable for making concrete that needs to be used quickly or to be removed from mold in a short time. This cement type should not be used in large structures, due to heat from hydration reaction is very high will cause the crack of product structures.

**Type 4** Low heat Portland cement: This type is suitable for mass concrete such as dam building. Due to low heat generated from hydration reaction which reduces thermal cracking.

**Type 5** Sulphate resistance Portland cement: This cement is suitable for structural use in sulphate environment. This cement type contains low $C_3A$, to prevent sulphate from outside to destroy concrete. It has a slow rate of increasing strength and low heat generated compared to ordinary Portland cement.

## 2.2 Perlite

Perlite is a glassy volcanic rock with a content of 2-6% water. The average chemical composition of perlite is approximately 74% $SiO_2$ with oxide of Al (13%), K (6%), Na (1%), Ca (1%), Mg (0.3%), Fe (1.5%) and bound water (3.0%) as shown in Table 2.2 [3]. When heated up above 870°C, the perlite becomes soft, and the water trapped inside the rock vaporizes and tries to escape resulting in the expansion of the perlite structure. The expanded perlite is a lightweight material full of tiny little air pockets; it is clean, sterile, and resists compaction. The pockets on the outside absorb water, blocking moisture from entering the center of the perlite pieces. it expands approximately from 4–20 times its original volume [5]. The unique characteristic of expanded perlite is lightweight and thermal insulation properties. As a result of volume increase and its porous structure, water absorption is significantly high. Also, the density of expanded perlite is very low.

Due to its glassy structure and high $SiO_2$ contents, perlite is a pozzolanic material that can cause pozzolanic reaction with hydration reaction in cement. Perlite is being used in different areas such as construction materials, agriculture, medical and chemical industry.

**Table 2.2** The chemical composition of expanded perlite.

| $SiO_2$ | $Al_2O_3$ | $K_2O$ | $Na_2O$ | $Fe_2O_3$ | CaO | $P_2O_5$ | MgO |
|---|---|---|---|---|---|---|---|
| 75 | 14.8 | 4.8 | 2.9 | 1.2 | 0.9 | 0.58 | 0.2 |

## 2.3 Pozzolanic activity

Pozzolanic is a siliceous or silicious/aluminous material that could react with calcium hydroxide in the presence of water to form compounds that possess cementitious properties. Pozzolanic activity is the reaction between a pozzolan and calcium hydroxide in the presence of water. The rate of the pozzolanic reaction is dependent on the intrinsic characteristics of the pozzolan such as the specific surface area, the chemical composition, and the active phase content.

The pozzolanic reaction is the chemical reaction that occurs in Portland cement upon the addition of pozzolan. It is the main reaction involved in the Roman concrete invented in Ancient Rome and used to build, for example, the Pantheon.

The pozzolanic reaction converts a silica-rich precursor with no cementing properties, to a calcium silicate, with good cementing properties.

The pozzolanic reaction is a long-term reaction, which involves dissolved silicic acid, water, and $Ca(OH)_2$ or other pozzolans to form a strong cementation matrix. This process is often irreversible. A sufficient amount of free calcium ion and a high pH of 12 and above is needed to initiate and maintain the pozzolanic reaction. Under these conditions, the solubility of silicon and aluminum ions is high enough to support the pozzolanic reaction.

### 2.3.1 Effect of pozzolan particle characteristic

The particle characteristic of pozzolanic effects on the pozzolanic activity. Grinding of pozzolan results in increased pozzolanic activity by creating a larger specific surface area available for reaction. Moreover, grinding also creates crystallographic defects on the particle surface as well as inside the particle. The dissolution rate of the strained or partially disconnected silicate moieties is strongly enhanced. Materials that are commonly not regarded to behave as a pozzolan, such as quartz, can become reactive when it is ground to have a certain critical particle diameter.

### 2.3.2 Effect of pozzolan compositions

Many pozzolans consist of a heterogeneous mixture of phases of different pozzolanic activity. The content in reactive phases is an important parameter to determine the overall reactivity. Volcanic ash, containing substantial amounts of volcanic glass or zeolites, is more active than quartz sands or detrital clay minerals. In this respect, the thermodynamic driving force behind the pozzolanic reaction serves as a rough indicator of the potential reactivity of silicate material. Similarly, materials showing structural disorder such as amorphous glasses show higher pozzolanic activities than crystalline ordered compounds. The rate of the pozzolanic reaction can also be controlled by external factors such as the mix proportions, the amount of water, formation, and binding of hydration products, and the temperature of the reaction. Therefore, typical blended cement mix design properties such as the replacement ratio of pozzolan for Portland cement, the water to binder ratio, and the curing conditions strongly affect the reactivity of the added pozzolan.

## 2.4 Coconut fiber

There are many natural fibers that are widely used today, such as cotton, hemp, flax, jute, and coconut fiber. These materials have interesting physical and mechanical properties, such as lightweight, low density, and high ductility, compared with other conventional materials, such as steel, plastic, and ceramic [6]. Among these natural fibers, coconut fiber is cheap and easily available.

Coconut fiber has low thermal conductivity in the range of 0.054–0.134 W/m K and has an average density of 386 kg/$m^3$. There are two types of coconut fibers: brown fiber extracted from matured coconuts and white fiber extracted from immature coconuts. Besides, coconut fibers are available in three forms, such as bristle (long fibers), mattress (relatively short), and decorticated (mixed fibers). The physical, chemical, and mechanical properties of coconut fiber are presented in Table 2.3.

Coconut-fiber material offers lower cost and ready availability. These materials have the advantages of being environmentally friendly and biodegradable, along with possible lower processing costs. Besides, these materials can easily be applied to building material as thermal insulation to reduce the temperature in the building and energy consumption. Moreover, using coconut fiber as an insulating material is found to be the most efficient and economical way to reduce residential energy consumption and $CO_2$ emissions. The material has the capability of resulting in a 30–40% reduction in heat loss and a reduction in energy consumption of up to 20–30%.

**Table 2.3** Thermo physical properties of coconut fiber.

| Number | Properties | Measurement |
|---|---|---|
| 1 | Thermal conductivity | high thermal resistance; 0.054–0.143 W/m K |
| 2 | Density | high density; 250–380 kg/$m^3$ |
| 3 | Tensile strength | 15–327 MPa for coconut husk fibers |
| 4 | Water absorptivity | 80–90% water absorption |
| 5 | Thermal and sound insulation | Excellent insulation against temperature and sound |
| 6 | Fire resistance | Good flame-retardant properties compared with other agricultural wastes |
| 7 | Toxicity | No chemical additives, leading to eco-friendly and nontoxic performance |
| 8 | Cost | Coconut husk is an agricultural waste material and is easily available in its natural state at a negligible cost, so the cost of manufacturing the insulation material is low. |
| 9 | Moisture content | It is very tough and durable and unaffected by moisture and dampness |

## 2.5 Characterization equipment

### 2.5.1 X-ray diffraction (XRD)

X-rays were discovered in 1895 by Wilhelm Conrad Rönt-Gen. X-ray is an electromagnetic wave with wavelengths in the range of 10 to 0.01 nm or corresponding to frequencies in the range of 30 to 30,000 PHz. X-rays are often used in medical applications such as diagnostic imaging. The interaction of X-rays with the matter cause different phenomena such as emission, absorbance, and scattering. These phenomena occur depend on the characteristics of each substance when exposed to X-ray. Therefore, X-ray can be used to analyze and identify the type of compound or crystal structure of the compound both qualitatively and quantitative [7].

The wavelength of X-rays is close to the size of an atom. When X-rays incident to a crystal lattice of materials, they diffract from the lattice points. At certain angles of incidence, the diffracted parallel waves constructively interfere and

create detectable peaks in intensity [8]. The diffraction pattern depends on the arrangement of the crystal structure. Therefore, the study of the diffraction pattern from a particular material could be interpreted to its crystal structure.

In 1912, W.L. Bragg and his father W.H. Bragg used X-rays to analyzed the crystal structure of materials and calculate the interatomic distance from X-ray diffraction pattern. They proposed the mathematical equation called Bragg's equation as shown in equation 2.1.

$$2d\ sin\theta = n\lambda \tag{2.1}$$

Where $\mathrm{d}$ = the spacing between a particular set of planes with Miller indices,

$\theta$ = the angle of incidence at which a diffraction peak is measured,

$n$ = an integer that represents the order of diffraction,

$\lambda$ = the wavelength of the X-rays used.

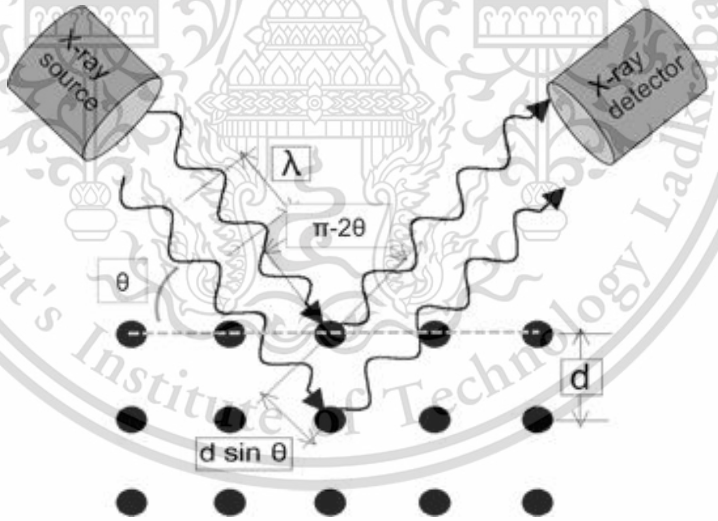


**Figure 2.6** Illustration of X-ray diffraction on crystal lattice according to Bragg's Law. [8]

The X-ray diffraction pattern obtained from the X-ray diffraction analysis is shown in the form of a graph recorded between X-ray intensity (Intensity) with the measured angle (2-theta). If we compare the peak angle in the X-ray diffraction pattern with the peak angle obtained from The Joint Committee Powder Diffraction

Standards (JCPDS files) database, it allows you to determine what element or compound of the substance. In addition, it could be able to identify the crystal structure of that matter and what type of crystal structure.

### 2.5.2 Fourier-transform infrared spectroscopy (FTIR)

FTIR is the most popular type of infrared spectroscopy. It operates on the principle that the IR radiation is absorbed when it passes through a material. The radiation that passes through the sample is then recorded. The spectra can be used to identify and differentiate between molecule since different molecules, due to their various structures, emit various spectra.

The first Infrared spectra were generated using gratings to scan the infrared spectral region, slits to isolate spectral lines, and thermopiles for the detection of infrared light. Fourier Transform Infrared (FTIR) spectrometers do not use gratings, but rather spectra are generated in the time domain, following the position of a moving mirror and the occurrence of constructive and destructive interference. A Fast Fourier Transform (FFT) then converts the signal from time to frequency domain. Since the FFT calculation takes time to compute, the development of commercial FTIR spectroscopy closely followed the trend of the increased power and miniaturization of computers. By the 1980s gratings-based instruments were phased out for the more desirable interferometer type spectrometers. FTIR has three main advantages over gratings-based measurements.

The electromagnetic spectrum consists of different regions corresponding to different energy (E), frequency (**ν**), and wavelength (**λ**) ranges as seen in Figure 2.7. The unit for near-, mid-, and far-infrared, the wavenumber ($cm^{-1}$), is derived from the inverse relationship between wavelength and frequency.

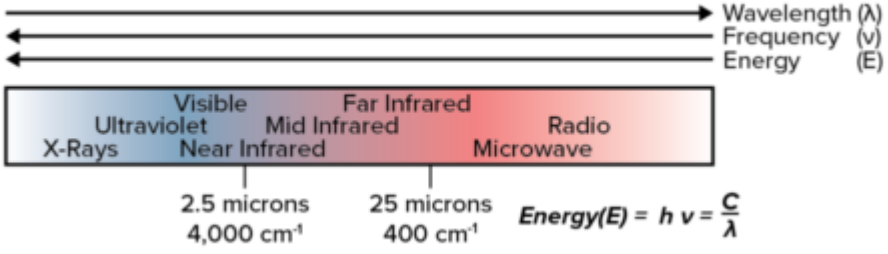


**Figure 2.7** Electromagnetic spectrum [9].

FTIR spectroscopy takes advantage of how IR light changes the dipole moments in molecules (Figure 2.8) that correspond to a specific vibrational energy. Vibrational energy corresponds to two variables: reduced mass (**μ**) and bond spring constant (k). For k constant, we can look at C-C, C=C, and C≡C which show an increase of 800 $cm^{-1}$ across the series. Substituting atoms in a C-C bond with nitrogen and oxygen causes a shift of 100 $cm^{-1}$. By looking at the two series, bond strength alters the wavenumbers more than mass.

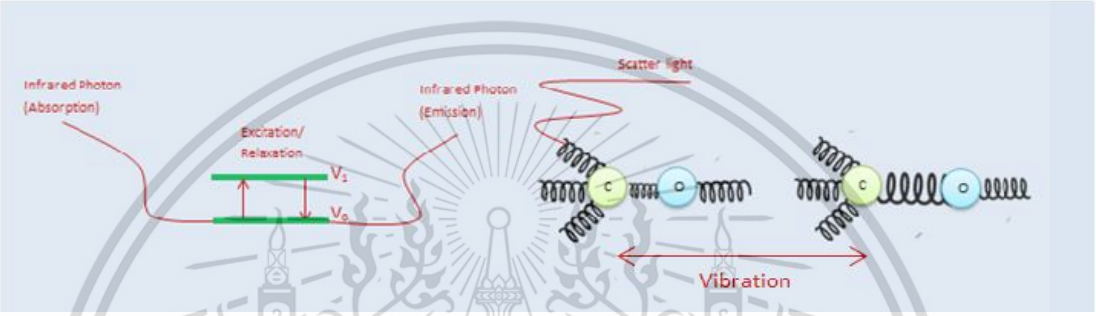


**Figure 2.8** Interaction between infrared light and matter [9].

Since every functional group is composed of different atoms and bond strengths, vibrations are unique to functional groups and classes of functional groups (e.g., O-H and C-H stretches appear around 3200 $cm^{-1}$ and 2900 $cm^{-1}$, respectively). A correlation chart with various functional group vibrations can be seen in Figure 2.9. Since the collection of vibrational energy bands for all the functional groups of a molecule is unique to every molecule, these peaks can be used for identification using library searches of comprehensive sample databases.

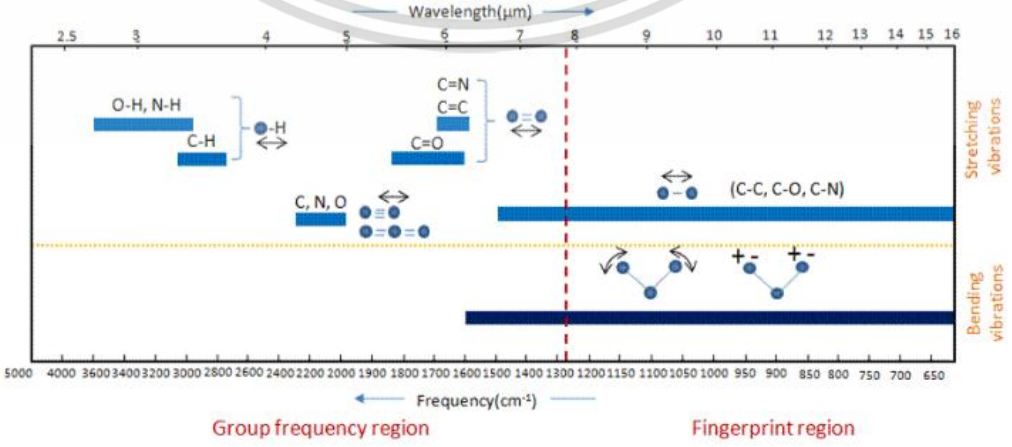


**Figure 2.9** FTIR Spectroscopy functional group correlation table [9].

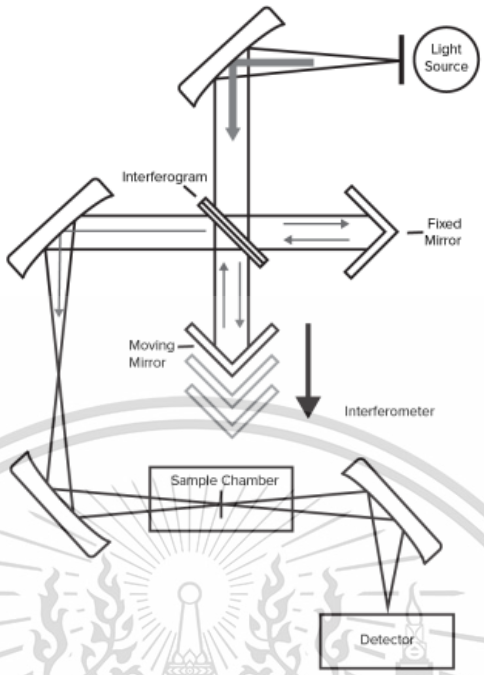


**Figure 2.10** Parts of an FTIR spectrometer with source, interferometer, and detector [9].

The three major parts of FTIR spectrometer are the source, interferometer, and detector as shown in Fig. 2.10. The source is typically a broadband emitter such as a mid-IR ceramic source (50-7,800 $cm^{-1}$), a near-IR halogen lamp (2,200–25,000 $cm^{-1}$) or a far-IR mercury lamp (10-700 $cm^{-1}$). The interferometer is the heart of FTIR and consists of a beam splitter, a stationary mirror, a moving mirror, and a timing laser. The beam splitter splits the light from a source into two paths with half the light going to a stationary mirror and the other half going to a moving mirror. In many FTIR systems, the beam splitter is placed at 45 degrees to the incident beam, but for high throughput applications, a low angle interferometer is preferred as the P and S polarizations converge close to the Brewster's Angle. Common beam splitter materials are KBr (375–12,000 $cm^{-1}$) for mid-IR, Quartz (4,000–25,000 $cm^{-1}$) for near-IR and Mylar (30–680 $cm^{-1}$) for far-IR. The beams from the moving and stationary mirrors are recombined back at the beam splitter and steered toward the sample. The difference in the path of the mirrors causes constructive and destructive interference over the course of time it takes for the moving mirror to make a pass. The signal versus mirror position (and thus, time) is called an interferogram. A laser is used to determine the position of the moving mirror using the precisely known wavelength of

the laser (Figure 2.11). He-Ne lasers are the industry norm due to their excellent wavelength stability compared to solid-state or diode lasers. This laser stability allows for spectral additions, library searches, and other functions that need high wavenumber accuracy (Connes Advantage).

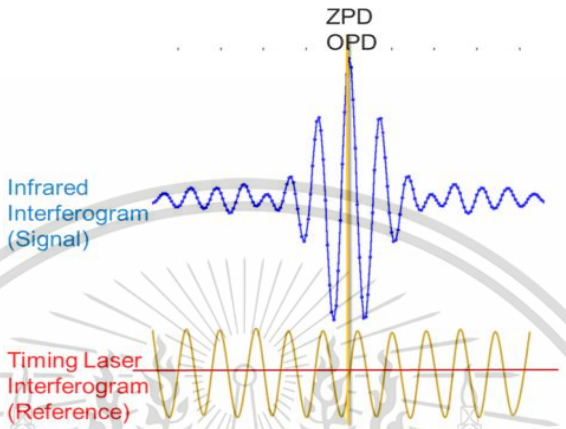


**Figure 2.11** The function of timing laser in FTIR. Each data point in the infrared is taken when the laser interferogram has neither constructive nor destructive interference [9].

Near-IR Spectroscopy: The Near-IR portion of the electromagnetic spectrum falls between 4,000 to 12,800 $cm^{-1}$ this region consists of overtones (two of the same vibrational modes occurring simultaneously) and combinations (two different vibrational modes occurring simultaneously). Since these modes are not strictly quantum mechanically allowed, the intensity of the modes is often quite low. These spectra are often complex, and chemometric techniques, such as multivariate analysis, are used. Despite the drawbacks, there are clear advantages to Near-IR spectroscopy. Firstly, the path length of the light is such that bulk samples can be analyzed with little to no sample preparation. Secondly, water does not affect signal as it does in mid-IR. These two benefits have been of great value to process chemistry and bulk analysis of incoming/outgoing goods.

Far-IR Spectroscopy: The Far Infrared region lies between 10 $cm^{-1}$ and 700 $cm^{-1}$. The bonds that show in this region are 3+ atom functional groups, such as -C-C-C- bending, and lattice vibrations in crystalline materials. Since these are highly

dependent on conformation or crystal structure, materials with the same chemical structure, but different crystal structures may be distinguished using Far-IR. There are two disadvantages to Far IR. Firstly, water absorbs strongly in this region making a purged or evacuated system necessary. Secondly, the intensity of these modes is weak, so sensitive detectors and high-powered sources are needed [9].

### 2.5.3 Thermal conductivity principle

#### 2.5.3.1 Transient hot bridge (THB)

The measurement of thermal conductivity is based on an adaptation of the hot wire technique performed by the Transient Hot Bridge apparatus. The measuring methods mentioned are transient, time dependent measuring methods. This method has much shorter measuring time when compared to another method.

THB is a transient method which uses thermoelectric sensors. A printed circuit foil of nickel is embedded between two polyimide sheets. The layout of the sensor consists of four tandem strips (Figure 2.12 a.) in parallel (Figure 2.12 b.). Each tandem strip comes in two individual strips, a short and a long one.

Two of the tandems are located very close to each other at the center of the sensor and one additional tandem on either edge. All eight strips are symmetrically switched for an equal-resistance Wheatstone bridge (Figure 2.13).

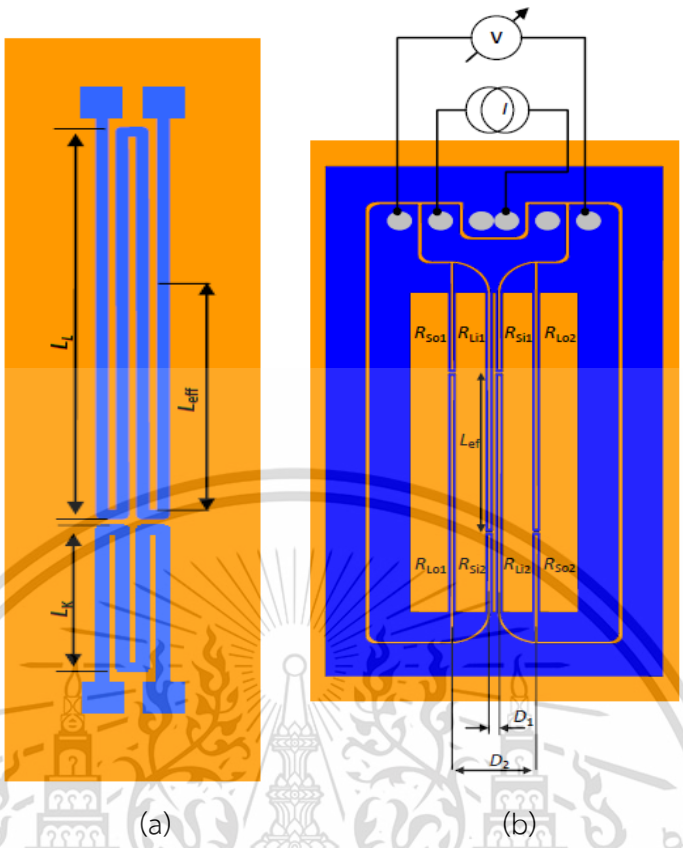


**Figure 2.12** Schematic drawing of (a) THB tandem strip and (b) tandem strips in parallel [10].

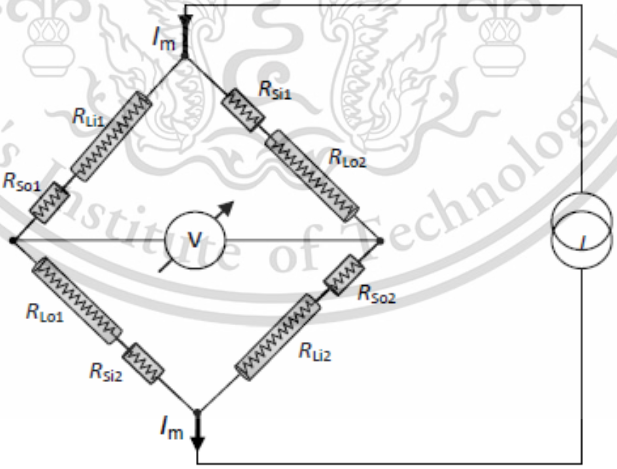


**Figure 2.13** Circuit diagram of Wheatstone bridge in THB tandem strip [10].

At uniform temperature, the bridge is initially balanced, i.e., no nulling is required prior to a run. An electrical current makes the pairwise unequally spaced strips establish a predefined inhomogeneous temperature profile (Figure 2.14.) that

turns the bridge into an unbalanced condition. Then, the sensor produces an almost offset-free output signal of high sensitivity. This voltage rise in time is a measure of the thermal conductivity, thermal diffusivity and volumetric heat capacity of the surrounding specimen.

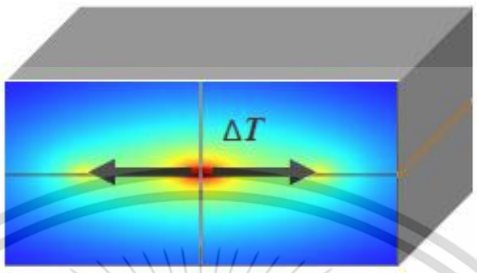


**Figure 2.14** Diagram show heat flow from sensor into specimens [10].

**2.5.3.2 Heat flow apparatus**

There are two methods of testing the thermal conductivity and thermal resistance of insulation: guarded hot plate and heat flow meter. Thermal conductivity is typically measured using the guard hot plate method, which can be used over a wide temperature range. It is quite accurate and can be operated in the wide range between -160 °C and 700°C. However, the drawback is that the exam takes a long time to complete.

Therefore, thermal conductivity test for cement roof tile according to ASTM 518 standard were conducted using principle based on heat transfer from a higher temperature side to a lower temperature side. Heat flow meter measurement techniques are currently applied for the second part in this research. Figure 2.15 shows the schematic of thermal conductivity by heat flux method. The sample is sandwiched between heated and cooled plates. Different temperatures will be established in the system for the two plates. To maintain the stability of the system, insulation is enclosed in the system for both heat sink and sample plates.

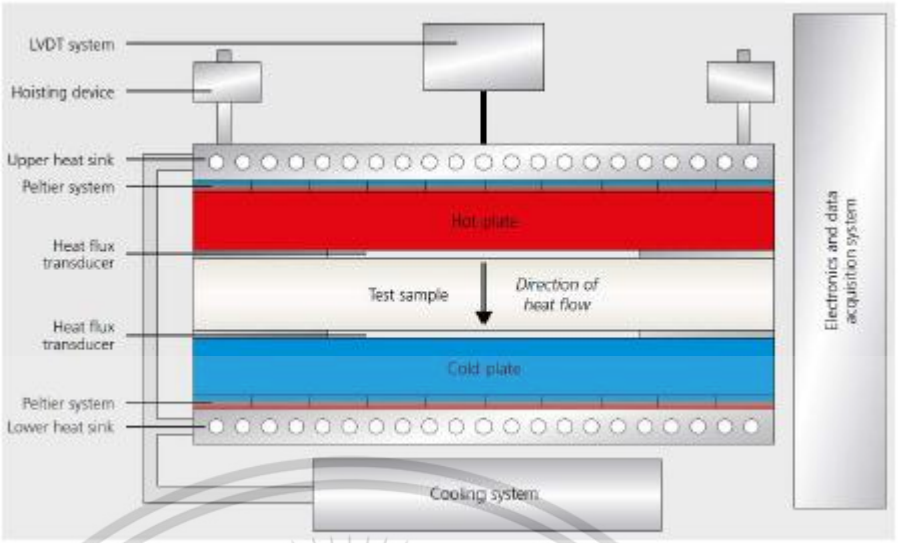


**Figure 2.15** Schematic of thermal conductivity by heat flux method [11].

By detecting the heat flow and the temperature difference between the two plates, the voltage output is determined from a flux sensor that is fixed to the surface of the two temperature plates. The thermal conductivity of sample is assessed when the system is in steady state. The following equation is used to calculate thermal conductivity ($k$) [11].

$$k = Q\frac{\Delta x}{\Delta T} \tag{2.2}$$

Where $Q$ is the amount of heat transferred through the material (W/m$^2$)

$\Delta x$ is the thickness of sample

$\Delta T$ is the difference in temperature (K)

## 2.6 Literature reviews

Several studies have investigated the addition of perlite and fiber in building materials. The literature reviews are as follow.

Akyuncu [12] reported the effect of substitution of sand with perlite coated polysiloxanes at 20–80 vol%. The unit weight of the mortar sample decreases as an increase in perlite. The thermal insulation properties were also improved. However, an increasing amount of coated and uncoated perlite in the mixture caused flexural strength to decrease up to 34% and 38% respectively and water absorption increased up to 141% and 121% respectively.

Sengul et al. [13] reported the effects of expanded perlite on mechanical properties of lightweight concrete. Natural sand was substituted with expanded perlite at 20–100 vol%. The result showed that the thermal conductivity was substantially reduced by replacing sand with expanded perlite. On the other hand, water absorption increased with higher expanded perlite content. The compressive strength is more affected when the replacement ratio is up to 40%.

Erdogan et al. [14] investigated the pozzolanic effect of expanded perlite and chemical activator on cement pastes and mortars. The result showed that ground perlite is an effective natural pozzolan that can be used to replace cement at 25–50% without a significant loss of strength.

Lanzón et al. [15] reported that the addition of expanded perlite above 1.77% by weight leads to a negative effect on mechanical strength and water absorption of lightweight cement mortar.

Lertwattanarul et al. [16] reported the properties of natural fiber cement materials containing coconut fiber for residential building application. Natural fiber was added into mixture at 5% 10% and 15% by the weight of binder. The water to binder ratio was 0.25, which is applicable for fiber cement material in the manufacture of roof sheets and siding. The results showed that flexural strength and thermal conductivity slightly decrease when increase amount of fiber, at lowest value of flexural strength is 84.2 kg/cm$^2$ and lowest thermal conductivity is 0.37 W/m K. Due to lower value of thermal conductivity when compared to standard

specimen, the natural fiber cement sheets can be applied for residential building in that energy efficiency can be improve.

Singh et al. [17] reported the investigation of water/cement ratio on strength development of cement mortar. The specimen with different proportions of water to cement ratio were prepared. Portland cement and river sand with a different w/c ratio at 1:3, 1:4, 1:5, 1:6, 1:7 and 1:8 was investigated. The results show that the compressive strength and split tensile strength of cement mortar decreased with an increase in the w/c ratio. It was suggested that the optimum w/c should be 0.5 to obtain workable cement mortar.

Silva et al. [2] reported a new treatment for coconut fibers to improve the properties of cement-based composites by combining effects of natural latex/pozzolanic materials. When natural fiber was added to cement, the chemical reaction from cement causes a degradation of natural fiber especially after a long curing period. The result of coating fiber with different pozzolans and adherent solution, i.e., silica fume-water (S-A), silica fume-latex (S-L), metakaolin-water (M-A), metakaolin-latex (M-L) were investigated. The flexural strength of fiber cement treated by silica fume-latex showed the highest value at 8.6 MPa. The degradation testing showed a mass loss (%) of fiber. When coating with metakaolin, M-A fibers showed a 13.3% mass loss reduction and M-L fibers 9.4% after 60 testing days. For the silica fume coating agent, 9.3% and 6.4% mass loss were obtained after 60 testing days for S-A and S-L, respectively.

Darsana et al. [18] reported on the development of coir-fiber cement composite roofing tiles. The cement was partially replaced with fiber up to 15% by volume. The result showed that 10% of fiber replacement was an optimum condition in which compressive strength and flexural strength is comparable to control specimen.

Dawood et al. [19] investigated the properties of lightweight concrete containing polystyrene beds and perlite that can be used for production of Canoe. Polystyrene content was 20, 35, 50 and 65%, while the 50% of polystyrene beds perlite content of 10, 20, 30, 40, 50 and 60% were used. The result shows that replacing sand with 50% of polystyrene and 50% of perlite resulted in lightweight concrete that had suitable value of density, compressive strength, and flexural strength of for canoe production.

Oktay et al. [20] reported a mechanical and thermo-physical properties of lightweight aggregate concretes. In this study, experimental investigation is performed for producing new cement-based with relatively high strength, low density, and good thermal properties for energy efficient buildings. Different types of concretes containing silica fume (SF), super-plasticizer (SP) and air-entrained admixtures were prepared with a constant water–cement ratio, and normal aggregates replaced by lightweight aggregates (LWAs) including pumice (PA), expanded perlite (EPA) and rubber aggregates (RA) at different volume fractions of 10, 20, 30, 40, and 50%. The investigation revealed that the addition of PA, EPA and RA reduced the bulk density and compressive strength and improved the insulation characteristics of the composite concretes.

Jedidi et al. [21] reported the effect of expanded perlite aggregate (EPA) dosage on properties of lightweight concrete specimens. Samples were prepared at a water-to-cement ratio of 0.70 with varying replacement percentages of sand by EPA ranging from 0% to 80% by volume of sand. Compressive strength, thermal conductivity and thermal diffusivity were determined over curing age. Unit weights for the mixtures prepared varied between 560 and 1510 kg/m$^3$. Compressive strength decreased when perlite content increased. The test results indicated that replacing natural aggregate by EPA increased the thermal resistance of the lightweight concrete and consequently, improved thermal insulation.

Topçu et al. [22] reported on manufacturing of high heat conductivity resistant clay bricks containing perlite. Clay was replaced with perlite at 0–50%. The results showed that compressive strength decreased but heat conductivity resistance and shrinkage of perlite bricks increase as the replacement ratio of perlite increased. The optimum replacement ratios were obtained with 25% perlite of unit weight.

According to the literature reviews above, it is obviously seen that the addition of perlite benefits lightweight product and improves thermal insulation properties but decrease in the strength of cement product. Therefore, it is important to properly conduct the research on perlite addition for cement roofing tile. Additionally, the use of natural fiber that was treated with a coating agent significantly improve the properties of cement products. However, there has never been reported on coconut fiber coated with natural rubber and perlite.

**Table 2.4 Summary of literature reviews.**

| References | Mixtures | Investigation | Main results |
|---|---|---|---|
| 1. Akyuncu 2014 | Partially replaced sand with uncoated perlite and polysiloxanes coated perlite at 20–80 vol% | Flexural strength<br>Water absorption<br>Thermal conductivity | Thermal conductivity and flexural strength decreased, and water absorption increased as increase in perlite. |
| 2. Sengul 2010 | Water/Cement ratio is 0.55.<br>Replaced sand by expanded perlite at 20–100 vol%. | Compressive strength<br>Thermal conductivity<br>Water absorption | Thermal conductivity and compressive strength decreased as increase in expanded perlite.<br>Water absorption increased as increase in expanded perlite. |
| 3. Erdogan 2012 | Replaced cement by ground perlite at 25–75% | Flexural strength | Increasing the perlite content by 25–50% did not result in a decrease in strength |
| 4. Lanzón 2008 | Adding expanded perlite at 0, 0.59, 1.18, 1.77, 3.54 and 7.08 by weight of total composition | Flexural strength<br>Water absorption | Flexural strength and density decreased as increase in expanded perlite<br>Water absorption increased as increase in expanded perlite. |
| 5. Lertwattanarul 2015 | Adding coconut fiber at 5, 10, and 15% by wt of cement.<br>Water/cement ratio was 0.25 | Flexural strength<br>Thermal conductivity | Flexural strength and thermal conductivity decreased when increasing amount of fiber. |
| 6. Singh 2015 | Study water/cement ratio at 1:2, 1:3, 1:4, 1:5 1:6, 1:7 | Compressive strength | When increased water/cement ratio, compressive strength decrease, and the optimum water/cement ratio was 0.5. |

**Table 2.5 Summary of literature reviews. (continued)**

| References | Mixtures | Investigation | Main results |
|---|---|---|---|
| 7.Sliva 2017 | Coating coconut fiber with silica fume or metakaolin and using water or latex as an adhesive. | Mass loss<br>Flexural strength | Cement composite using coconut fiber coated with silica fume-latex had minimum mass loss and had highest flexural strength. |
| 8. Dasana 2016 | Cement was partially replaced with fiber up to 15 %vol. | Compressive strength<br>Flexural strength | The fiber replacement at 10% was optimum condition. |
| 9. Dawood 2015 | Replaced sand with combination of polystyrene at 20-65% and perlite at 10–50 % | Density<br>Compressive strength<br>Flexural strength | Replacing sand with 50% of polystyrene and 50% of perlite resulted in lightweight concrete that had suitable value of density, compressive strength, and flexural strength. |
| 10. Oktay 2018 | Replaced aggregates with pumice (PA), expanded perlite (EPA) and rubber aggregates (RA) at 10–50 % vol. | Bulk density<br>Compressive strength | Addition of PA, EPA and RA reduced the bulk density and compressive strength but improved the insulation characteristics. |
| 11. Jedidi 2015 | Water-to-cement ratio was 0.70. Replacement of sand by EPA ranging from 0% to 80% by volume of sand. | Compressive strength<br>Thermal conductivity<br>Thermal diffusivity | Compressive strength decreased when perlite content increased. Replacing natural aggregate by EPA increased the thermal resistance. |
| 12. Topçu 2017 | Replace clay with perlite at 0–50%. | Compressive strength<br>Thermal conductivity<br>Shrinkage | Optimum replacement ratios were obtained with 25% perlite of unit weight. |

# Chapter 3
# Research methodology

## 3.1 Introduction

The experiment was divided into two main parts. The first part will be an experiment to find the most effective mortar mixtures. In the mixture of mortar, the content of sand was replaced with perlite ranging from 0 to 15% by weight. The specimen was pressed in mold size 15 x 2.5 under the uniaxial force of 20, 30, and 40 kN (5.3, 8.0, and 10.6 MPa, respectively). In the second part, uncoated coconut fibers and natural rubber coated coconut fibers were added to the perlite cement specimens. The different length and proportion of coconut fiber were investigated.

## 3.2 Research procedure

### 3.2.1 Mortar preparation

In mortar preparation, ordinary Portland cement (Type I) and two aggregate materials consisting of natural sand and expanded perlite (supplied by Klong Yang Limited partnership, Thailand) were used as the raw materials. The Portland cement and natural sand were individually sieved through no. 35 (0.5 mm) and no. 16 (1.99 mm) mesh sieves, respectively, before mixing with expanded perlite. In addition, the particle size distribution of perlites was preliminarily examined by sieves. The result of size distribution is illustrated in Table 3.1.

**Table 3.1 Particles size of expanded perlite.**

| Sieve size (mm) | 0.1< | 0.1-0.3 | 0.3-0.5 | >0.5 |
|---|---|---|---|---|
| Weight fraction | 16.75 | 38.70 | 26.66 | 17.90 |

For all mixtures, the effective cement to water ratio of 2:1 was kept constant, while cement to aggregate ratio of 1:2 was desired. The expanded perlite was applied as a sand-substitutional material. The different fractions of expanded perlite, i.e., 0, 5, 10, 15 wt% of total aggregate mass (sand mass) in the mixture was examined. Hereafter, the experimental cement mortars are referred as P0, P5, P10, and P15 according to the designed compositions. The mixture was blended in a

laboratory vertical-type mortar mixer for 5 min. The mix proportion of cement mortars based on the absolute volume method are listed in Table 3.2.

**Table 3.2 Mix proportions of cement mortar.**

| Specimen code | P0 | P5 | P10 | P15 |
|---|---|---|---|---|
| Cement (kg/m$^3$) | 556 | 556 | 556 | 556 |
| Water (kg/m$^3$) | 228 | 228 | 228 | 228 |
| Natural sand (kg/m$^3$) | 1111 | 1056 | 1000 | 944 |
| Expanded perlite (kg/m$^3$) | 0 | 55 | 111 | 167 |

The rectangular shape specimens were prepared by the compression molding process. An approximate 135 g of mixture was individually put in the steel mold with dimensions of 2.5 cm x 15 cm (width x length), followed by pressing with a hydraulic pressing machine. The specimens were formed at different applied loads at 20, 30, and 40 kN. During pressing, the forces were maintained constant and held for 1 min prior to demolding. Figure 3.1 shows the hydraulic pressing machine and a set of steel mold used in the molding process.

The pressed specimens were cured with wet covering for 28 days, followed by drying in an oven at 90 °C for 24 h. Figure 3.2 shown the example of cement mortar specimen after curing.

(a) (b)

**Figure 3.1** (a) Hydraulic pressing machine, and (b) steel mold used in the molding process.

**Figure 3.2** The macrograph of cement mortar specimen.

### 3.2.2 Fiber preparation

The fibers used for adding into mortar are divided into two types: uncoated coconut fibers (UCF) and natural rubber coated coconut fibers (CCF). For each condition, fibers length of 1, 2, and 3 cm were used, and the addition content was varied from 2.5 g to 15 g.

Coconut fibers were treated before use in the experiment. The coconut fiber was soaked in water to wash the soil and powder from the peeling process. Then, brush the fibers in water to get fibers aligned in the same direction to be convenient for the processing. After that, dried fiber in oven at 60 °C for 20 min then cut into desired length. In the case of coating one, coconut fibers were treated with sodium hydroxide (NaOH) at a concentration of 20%. To prepare NaOH solution, 200 g of solid sodium hydroxide (Merck) was stirred with 800 g water. Then immerse coconut fiber in solution for 1 h (Figure 3.3).

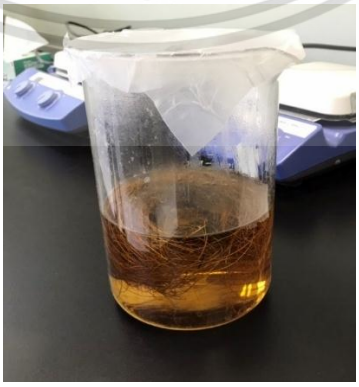

**Figure 3.3** Coconut fiber immersed in sodium hydroxide solution.

After 1 h, the coconut fibers were washed with water mixed with 6-7 drops citric solution until the pH decreased, then washed with water again until clean. After that, dried in oven at 60 °C for 20 min, then coconut fiber is ready for rubber coating process. Coconut fibers were coated in two steps. Firstly, each coconut fiber was immersed in natural latex for 1 min. In this step, the natural latex was coated entirely on the coconut fiber generating adhesive layer. After that, perlite was used as coating agent (Figure 3.4).

After coating, the fiber is ready to add into mortar mixture. The fiber was added into the mixture and homogeneously blended in a laboratory vertical mixer. Then mixture was ready to be fabricated.

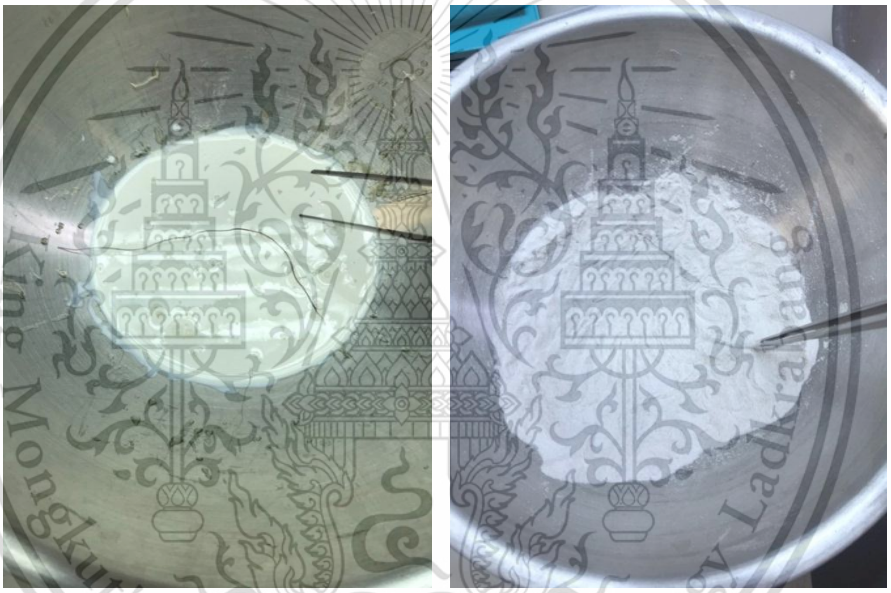

(a) (b)

**Figure 3.4** Coated coconut fiber preparation in two steps, (a) immersed fiber in natural latex to form an adhesive layer and (b) coated fiber with perlite.

### 3.3 Characterization method

In this study, the physical properties i.e., bulk density and water absorption, and flexural strength that are the requirement for fiber cement roof tile were conducted by the method modify from The American Society for Testing and Materials Standard (ASTM). Thermal conductivity, which is one of the important properties for roof tile, was also examined.

### 3.3.1 Physical properties characterization

For physical properties characterization, bulk density and water absorption were determined in accordance with ASTM C20 and ASTM C1185 [12,13]. The procedures to measure the physical properties in this study are shown in Figure 3.5. The small specimens of approximately 2 cm x 2 cm, which were cut from the cement mortar bars, were dried at 105 °C for 24 h then left cool in a desiccator and weighed (dry weight, *D*). After that, the specimens were boiled in deionized water at 100 °C for 2 h. Subsequently, the specimens were cool down to room temperature and immersed in deionized water for 24 h. The weight of specimen while suspended in water was measured and defined as the suspended weight (*S*). Then, the specimens were blotted with the wet cloth prior to weight in the air, this weight is referred to saturated weight (*W*). The volume of specimens (*V*) was derived from *W-S*. The bulk density and water absorption of specimens are expressed as follows.

$$Bulk\ density = \frac{D}{V} \quad (1)$$

$$Water\ absorption = \frac{W-D}{D} \quad (2)$$

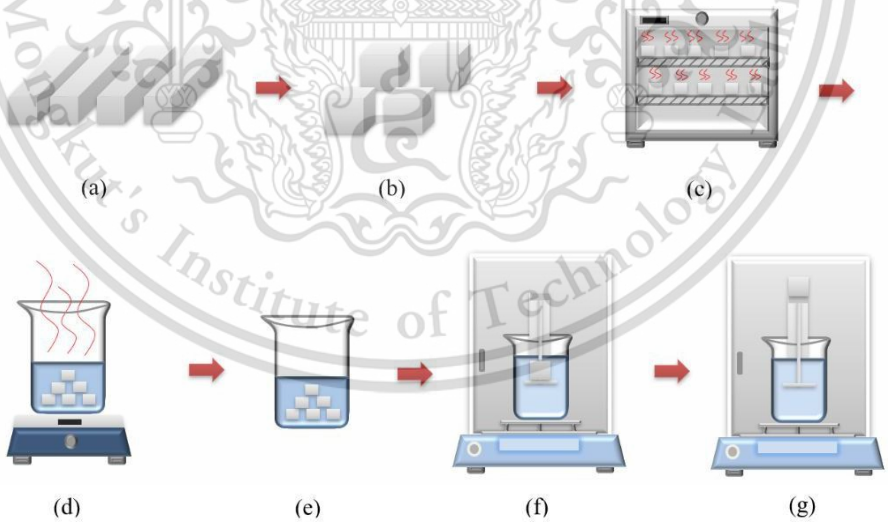


**Figure 3.5** Schematic procedures to measure the physical properties: (a) cement mortar bar specimens, (b) small specimens cut from bar, (c) drying at 105 °C for 24 h then cooling in desiccator and weighing (dry weight, D), (d) boiling at 100 °C for 2 h, (e) cooling to room temperature and immersing for 24 h, (f) weighing in water (suspended weight, *S*), and (g) weighing in air (saturated weight, *W*).

### 3.3.2 Thermal conductivity test

#### 3.3.2.1 Transient Hot Bridge technique

The measurement of thermal conductivity is based on an adaptation of the hot wire technique performed by Transient Hot Bridge (THB) technique (THB-1, LINSEIS). Square pair specimen of 25 x 25 x 12 mm was prepared from each mixture, specimen was dried in an oven at 110 °C for 24 h. After that left to cool down in an auto desiccator. For determination of the thermal conductivity, a sensor is positioned between both sample layers sensor (sandwich-setup shown in Figure 3.6), to ensure contact between specimen surface and the surface of sensor the specimen must be pressed lightly. An electric current is then applied to the sensor, to generate heat which raises an increase in temperature. The increase of temperature will result in heat diffusion into the material which allows the determination of thermal conductivity.

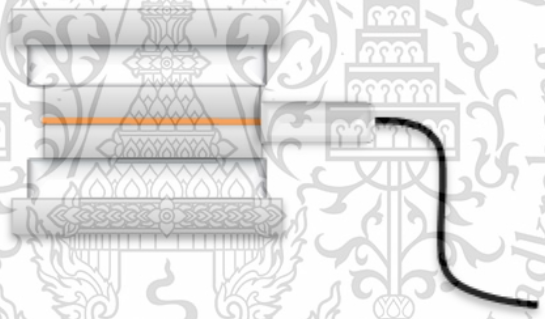

**Figure 3.6** Sandwich setup of sample and sensor for testing thermal conductivity.

#### 3.3.2.2 Heat flux technique

Thermal conductivity measurement was conducted at the Department of Science Service at Thanon Rama VI, Phaya Thai, Ratchathewi, Bangkok. Test procedure was conducted following ASTM C518-15. The thermal conductivity was examined using mass heat-flow apparatus (H1436a, Netzsch). The dimensions of the test specimen are 30 cm x 30 cm in width and length, and approximately 1.5 cm in thickness. The photographs of the specimens for thermal conductivity test are shown in Figure 3.7. One measurement takes 1-2 hours and is repeated until the obtained value is stable.

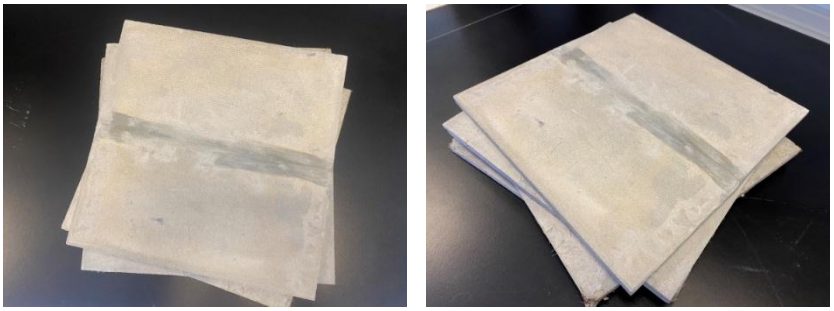

**Figure 3.7** Photograph of specimen for test thermal conductivity in heat flux technique.

### 3.3.3 Mechanical testing

The mechanical property of cement mortar was characterized by a static flexural test. The three-point bending test adapted from ASTM C1185 [24] was performed in order to evaluate the flexural strength. An in-house three-point bending fixture, manufactured with high stiffness materials, was set up in the universal testing machine (Shimadzu AG-X, Japan). A support (span length, *L*) of 100 mm and a constant loading rate of 0.1 mm/min were set for bending tests. The schematic drawing of the three-point bending figure and testing apparatus are shown in Figure 3.7 (a) and (b), respectively. The flexural strength was calculated using equation (3).

$$\sigma = \frac{3PL}{2bd^2} \tag{3}$$

Where **σ** is flexural strength (MPa), *P* is maximum load, *L* is length of span, *b* is width of specimen and *d* is average thickness of specimen.

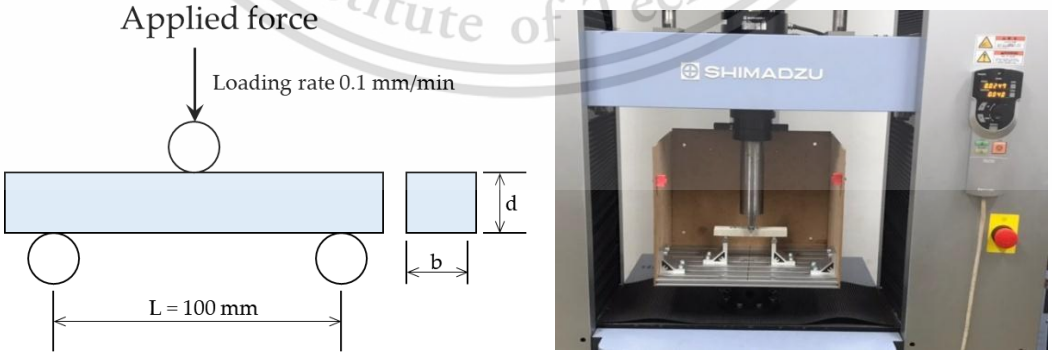


**Figure 3.8 (a)** Schematic drawing of three-point bending figure, and (b) testing apparatus set in Universal testing machine.

### 3.3.4 Accelerated degradation test

Accelerated degradation test was performed to observe degradation of fibers that contain in cement as well as the mechanical strength. The accelerated degradation test method was followed Thai industrial standards 1407-2540 [19]. Salt spray machines model SF/450/CCT/V.H. (Figure 3.8) was used for testing accelerated degradation and using water instead of saline. The accelerated degradation test was procedure by spraying water for 2 h and 50 min, resting for 10 min, then drying at 70±5 °C for 2 h and 50 min, then resting for 10 minutes with a total duration of 6 hours in 1 cycle. The test was repeated for 25 cycles.

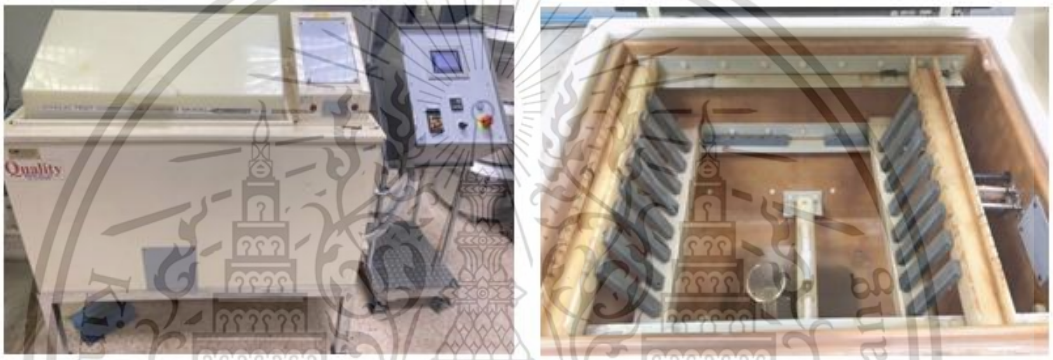

(a) (b)

**Figure 3.9** (a) Salt spray machine and (b) specimens during accelerated degradation test.

# Chapter 4
# Results and Discussions

In this chapter, the results obtained from the experiment of each condition are presented and discussed. After being cured for 28 days, the specimen was ready to be evaluated. The test procedure conducted following the ASTM standard. The experimental results have been divided into five main sections.

First, preliminary research was done on the effects of perlite content on the characteristics of perlite mortar.

Second, the microstructure and chemical analysis of uncoated and coated coconut fiber were investigated.

Third, the effect of addition coconut fiber on the properties of perlite fiber cement was conducted. In this study, the uncoated coconut fiber (UCF) and coated coconut fiber (CCF) with natural latex were used and compared.

Fourth, the comparison of properties of each perlite fiber cement was reported. Also, the comparison with the properties that reported in literature was discussed.

Finally, the durability by accelerated degradation test was reported. In this test, the specimen was aged through wet and dry cycle.

## 4.1 Investigation of perlite mortar

The addition of perlite in building material could reduce unit weight and improve thermal insulation but the excessive amount of expanded perlite could reduce the mechanical strength and increase the water absorption of the products. Therefore, it is necessary to study the addition content of perlite to the cement matrix to optimize the physical and thermal properties. Perlite base building material has been widely studied but the molding processes are mostly performed by casting without compaction. The study of compaction of concrete showed that it tends to reduce water absorption and increase mechanical strength. The molding force for the fabrication of perlite cement composites is also one of the important parameters which should be concerned.

Cement mortar composite mainly contain cement and fine aggregate (natural sand). Various additions such as mineral admixture, fiber, and polymer, can be also employed to enhance the properties of cement mortar composites. The aims of this research are to develop cement mortar composite with a low bulk density and high mechanical strength using substitution of sand with expanded perlite. In this section, the effects of expanded perlite content and molding force on bulk density, water absorption, and flexural strength were investigated.

### 4.1.1 Bulk density of perlite mortar

The effects of expanded perlite content and compressive force on bulk density were shown in Figure 4.1 and the bulk density values are shown in Table 4.1. The bulk densities of cement mortar without perlite were in the range of 2029–2118 kg/m$^3$ while those of specimens containing perlite decreased with increasing expanded perlite content and varied between 1586 kg/m$^3$ and 1933 kg/m$^3$. The increase in compressive molding force resulted in a slight increase in bulk density. When the applied force increases from 20 kN to 40 kN, it causes the bulk density to increase about 4.2–8.8 %.

It is seen that bulk density decreased as the content of perlite increased. For 20 kN specimens, the density value decreased from 2029 kg/cm$^3$ to 1586 kg/cm$^3$. For 30 kN specimens, the density value decreased from 2113 kg/cm$^3$ to 1699 kg/cm$^3$. For 40 kN specimens, the density value decreased from 2118 kg/cm$^3$ to 1739 kg/cm$^3$. The replacement of natural sand by expanded perlite effectively reduced the unit weight of cement mortar. However, the bulk density for all conditions is still higher than the target value (bulk density < 1500 kg/cm$^3$).

**Table 4.1** Bulk density of perlite mortar with different perlite content and compressive force.

| Proportion of perlite (%) | Bulk Density (kg/m³) | | |
|---|---|---|---|
| | 20 kN | 30 kN | 40 kN |
| 0 | 2029 | 2113 | 2118 |
| 5 | 1807 | 1857 | 1933 |
| 10 | 1663 | 1687 | 1773 |
| 15 | 1586 | 1669 | 1739 |

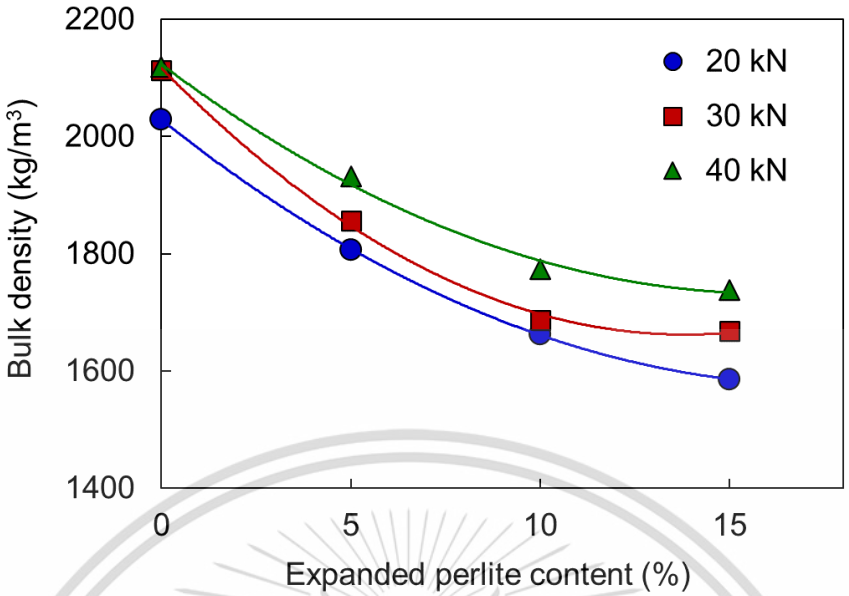


**Figure 4.1** Effects of expanded perlite content and compressive force on bulk density of perlite mortar.

### 4.1.2 Water absorption of perlite mortar

The effects of expanded perlite content and compressive molding force on the water absorption of cement mortar are shown in Figure 4.2 and the water absorption values are shown in Table 4.2. The cement mortar without perlite shows the water absorption of 8.6–7.6%. However, adding expanded perlite caused the water absorption increase to the range of 11.4–18.7%. For 2 kN specimens, water absorption increased from 8.6% to 18.7%. For 3 kN specimens, water absorption increased from 7.6% to 17.1%. For 4 kN specimens, water absorption increased from 7.4% to 15.1%. In general, due to the porous structure of perlite, the water absorption drastically increases with perlite content in the composites. In this study, the water absorption of specimen tended to increase with expanded perlite content which is in accordance with those reported in the literatures.

It should be noted that when the applied force increased, the water absorption of the specimens reduced. During molding, the compressive force applied to the cement mortar could crush expanded perlite to smaller particle size. Additionally, the compressive force could drive the expanded perlite particle to fill in the void between natural sand. The appropriate applied compressive molding force could be an effective way to reduce the water absorption of cement mortar

composites. The values of water absorption of all specimens follow the ASTM standard (water absorption < 25%).

The high-water absorption of perlite is an important disadvantage of building material that contains perlite. In commercial products, coating the surface with water proofing materials could prevent the absorption of water. However, it also increases the cost of building material as well.

**Table 4.2** Water absorption of perlite mortar with different perlite content and compressive force.

| Proportion of perlite (%) | Water absorption (%) | | |
|---|---|---|---|
| | 20 kN | 30 kN | 40 kN |
| 0 | 8.6 | 7.6 | 7.4 |
| 5 | 13.0 | 12.1 | 11.4 |
| 10 | 15.7 | 14.7 | 14.0 |
| 15 | 18.7 | 17.1 | 15.1 |

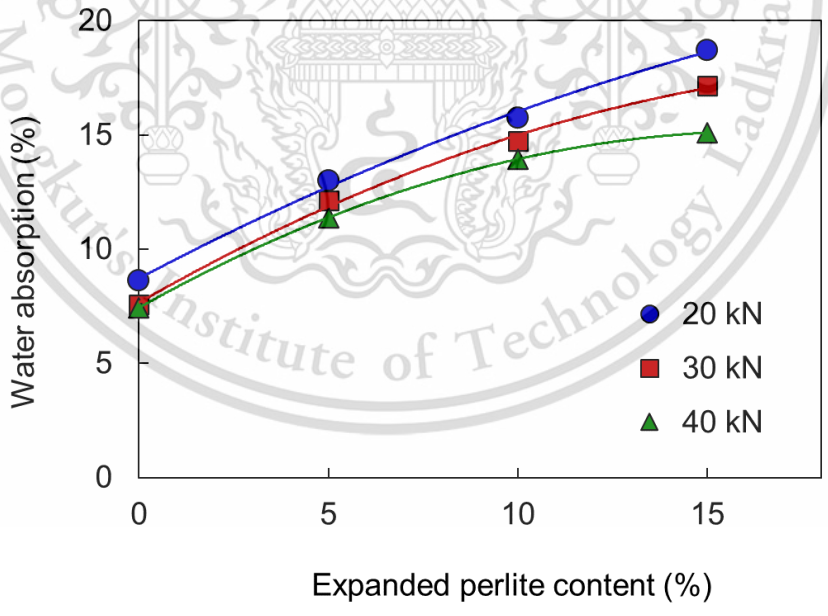


**Figure 4.2** Effects of expanded perlite content and compressive force on water absorption of perlite mortar.

### 4.1.3 Flexural strength of perlite mortar

The effects of expanded perlite content and compressive molding force on the flexural strength of cement mortar are shown in Figure 4.3 and the water absorption values are shown in Table 4.3. The increase in compressive molding force effectively increased the flexural strength of cement mortar composites. For the specimen molding less than 20 kN, the flexural strength of specimen decreases from 10.72 MPa to 7.81 MPa with the increasing expanded perlite content from 0 to 15 wt%. On the other hand, the specimens molding under 30 kN and 40 kN, the flexural strength of perlite-containing specimens showed a maximum value of 10.29 MPa and 12.50 MPa, respectively, at 10 wt% expanded perlite content.

It is general trend that involves expanded perlite in cementitious building materials cause a reduction in strength due to its porous structure. However, some studies reported the positive effect on the strength when expanded perlite is finely ground and added in a suitable amount. The smaller perlite particles responsible for the higher pozzolanic activity which improves the strength of cement composite[26]. The values of flexural strength of all specimens follow the ASTM standard (flexural strength > 4 MPa).

**Table 4.3** Flexural strength of perlite mortar with different perlite content and compressive force.

| Proportion of perlite (%) | Flexural strength (MPa) | | |
|---|---|---|---|
| | 20 kN | 30 kN | 40 kN |
| 0 | 9.70 | 10.75 | 14.50 |
| 5 | 8.17 | 9.30 | 12.15 |
| 10 | 8.60 | 10.64 | 12.65 |
| 15 | 8.20 | 9.22 | 9.98 |

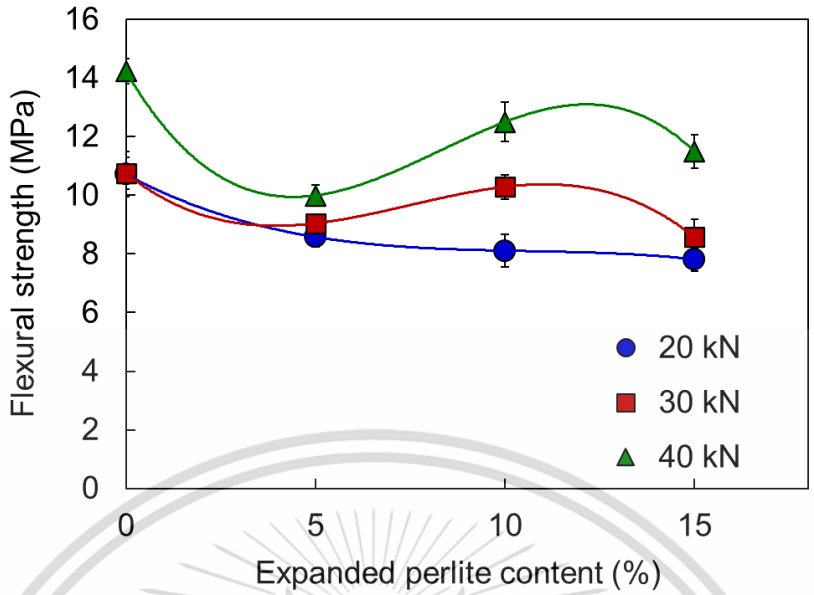


**Figure 4.3** Effects of expanded perlite content and compressive force on flexural strength of perlite mortar.

### 4.1.4 Thermal conductivity of perlite mortar

The effects of expanded perlite content and compressive molding force on the flexural strength of cement mortar are shown in Figure 4.4 and the water absorption values are shown in Table 4.4. All specimens showed a low thermal conductivity in the range of 0.10–0.27 W/m K. In general, due to the porous structure of perlite, the thermal conductivity reduces with increased perlite content in the composites. In this study, the tendency of thermal conductivity was not correlated with expanded perlite content.

It should be noted that the transient hot bridge (THB) method was used to measure the thermal conductivity of perlite mortar in this section and that the surface of the test specimen needed to be smooth. In this study, the roughness of the surface of perlite mortar might lead to the air gap between the layer of specimen and sensor, resulting in lower thermal conductivity. The thermal conductivity measurement by heat flux method will be performed in further study.

**Table 4.4** Thermal conductivity of perlite mortar with different perlite content and compressive force.

| Proportion of perlite (%) | Thermal conductivity (W/m K ) | | |
|---|---|---|---|
| | 20 kN | 30 kN | 40 kN |
| 0 | 0.19 | 0.14 | 0.11 |
| 5 | 0.20 | 0.14 | 0.21 |
| 10 | 0.10 | 0.18 | 0.17 |
| 15 | 0.20 | 0.23 | 0.27 |

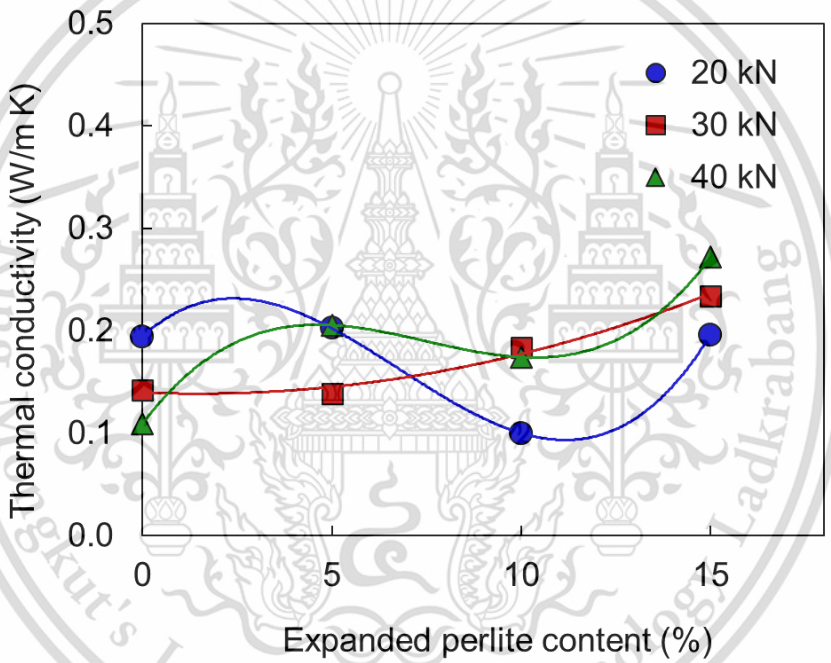


**Figure 4.4** Effects of expanded perlite content and compressive force on thermal conductivity of perlite mortar.

### 4.1.5 XRD results of perlite mortar

This section shows the XRD results of the mortar and perlite mortar. As mentioned previously, sand was replaced with perlite in ratios of 5, 10, and 15% by weight. The XRD pattern of all specimens were investigated, and the characteristic peaks were matched with International Centre for Diffraction Data (ICDD) database to show components contained in the specimens. XRD results are compared for all conditions to observe the intensity of each phase.

Figure 4.4 shows the XRD patterns of perlite mortar with different content of perlite. The specimens with 10% perlite substitution had the highest intensity compared to other conditions. A high intensity indicates a high crystallinity of the specimen, which directly affects the strength of the sample. A chemical reaction between cement and water known as the "hydration reaction" produces calcium silicate hydrate and calcium hydroxide. With suitable proportion of perlite, perlite which mainly contained $SiO_2$, reacted with calcium hydroxide to produce calcium silicate hydrate by pozzolanic reaction. Matrix of the mortar condensed by calcium silicate hydrate from hydration reaction and pozzolanic reaction, so that compressive/flexural strength of concrete will be increased.

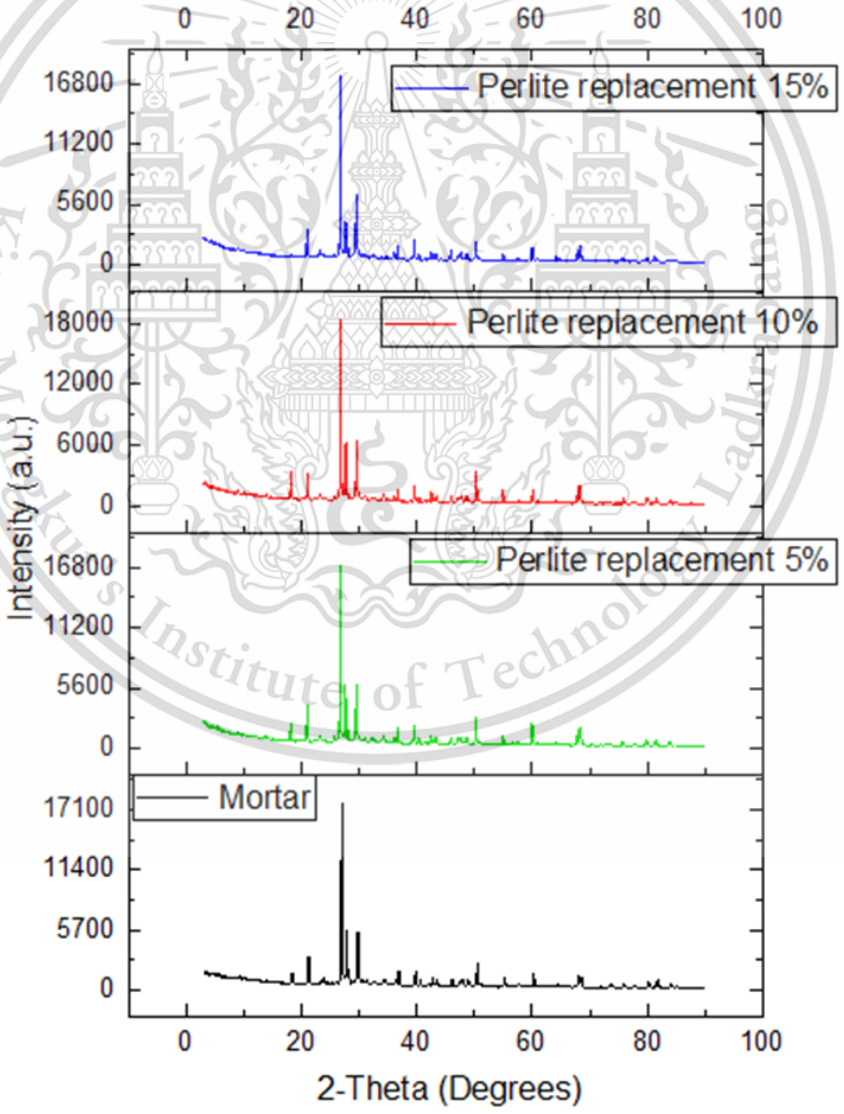


**Figure 4.5** XRD patterns of mortar and perlite mortar.

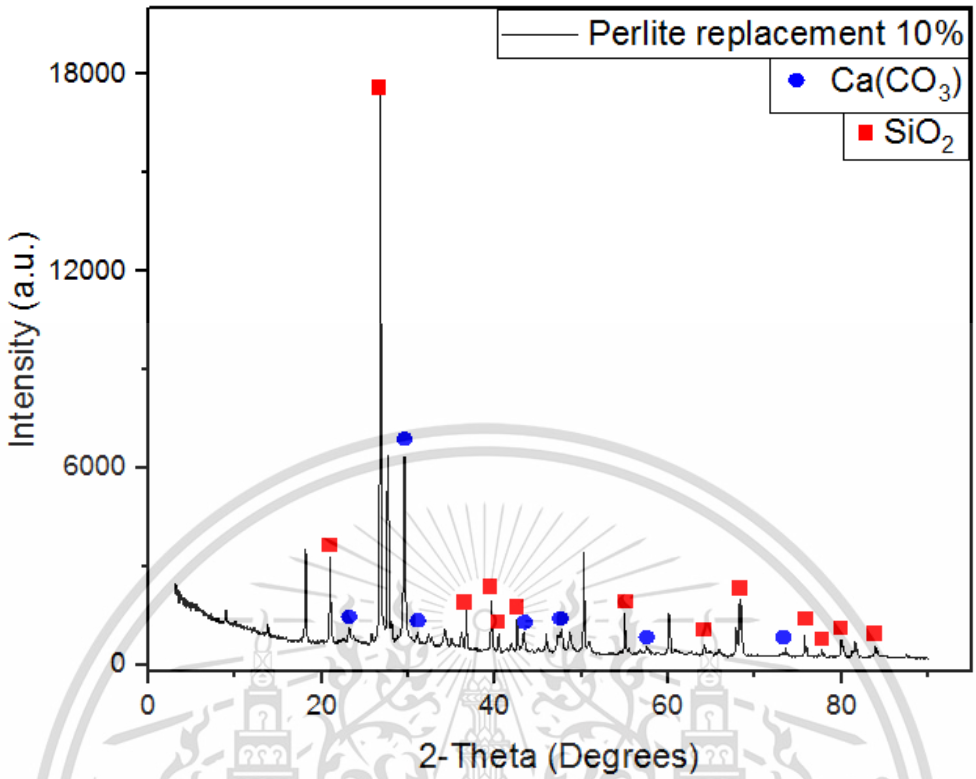


**Figure 4.6** XRD pattern of perlite mortar coataing 10wt% perlite and the characteristic peak mached with the ICDD data.

Fig 4.6 shows XRD pattern of perlite mortar coataing 10wt% perlite and the characteristic peak mached with the ICDD data. It is shown that the specimen mainly contains $SiO_2$ (ICCD no. 46-1045) and $CaCO_3$ (ICCD no. 01-080-9776). Both compounds contributed the strength to the specimens. The effect of $CaCO_3$, so better distribution of cement particles provides more completing hydration reaction And $CaCO_3$ particles which reduce the pores inside the concrete, thus creating better packing of a particle between cement and $CaCO_3$ [27]. $SiO_2$ that contain in the specimen helps the setting process accelerate. On the other hand, the reaction activity of silica with Portland cement minerals results in a slight decrease in porosity and improvement of mechanical properties of cement [28]. With the high intensity of $SiO_2$ and $CaCO_3$ of this condition, as a result, the 10% perlite replacement shows a higher flexural strength higher when compared to other conditions.

### 4.1.6 Summary for Mortar conditions

From the result of physical and mechanical properties conclusions could be drawn as follow:

- Flexural strength of perlite mortar reduced as the content of the expanded perlite increased.
- Bulk density of perlite mortar can be significantly reduced by replacing the expanded perlite to natural sand but slightly increase with a higher compression force
- Water absorption increased with higher expanded perlite content and slightly decreased with a higher compression force.
- All specimens still have a higher density than the target value.

The optimum condition for further research was 10% perlite replacement and compressive forces of 40 kN. The specimen prepared with this condition showed the water absorption and flexural strength followed the ASTM standard. In addition, this specimen had the low thermal conductivity. However, the bulk density was higher than that of the target. In further research, the addition of fiber into mortar was thought to reduce the bulk density of fiber cement specimens.

**Table 4.5** Summary properties of perlite mortar with 10% perlite content.

| Properties | Test result | Target value |
|---|---|---|
| Bulk density | 1773 kg/m³ | < 1500 kg/m³ |
| Water absorption | 13.40% | < 25% (ASTM) |
| Flexural strength | 12.50±1.36 MPa | > 4 MPa (ASTM) |
| Thermal conductivity | 0.17 W/m K | < 0.5 W/m K |

## 4.2 Investigation of coconut fiber

The fibers used for adding into mortar are divided into two types: uncoated coconut fibers (UCF) and natural rubber coated coconut fibers (CCF). Coconut fibers were treated before use in the experiment. The characteristics of coconut fiber were investigated in microstructure and chemical composition.

### 4.2.1 Microstructure of coconut fiber

Prior to use, the coconut fibers underwent an alkaline treatment with a 20% concentration of sodium hydroxide. The surface and microstructure of fibers was observed using stereo microscope (Nikon Z420). Figure 4.7 displays the microstructure of coconut fiber both before and after treatment. Figure 4.7 (a) and (b) illustrate the appearance of coconut fibers before the treatment, which was a yellow color with a woody look. However, after the treatment, the fibers turned to a dark brown color as shown in Figure 4.7 (c) and (d). Additionally, some of surface components were observed to disappear after treatment. Further analyze was described in the section FTIR result.

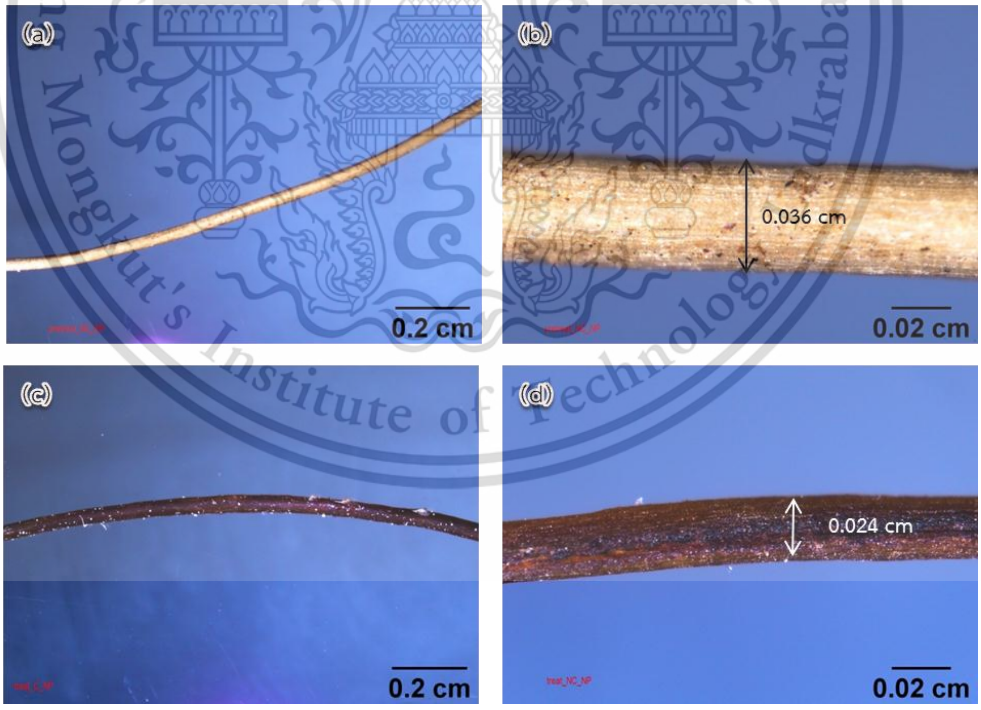


**Figure 4.7** Photomicrographs of (a) coconut fibers before treatment at 10x magnification and (b) 40x magnification, (c) coconut fiber after treatment at 10x magnification, and (c) 40x magnification.

Figure 4.8 shows the microstructure of coconut fiber after coating with natural latex and coconut fiber after coating the second layer with perlite. It can be seen that perlite particles were attached to the coconut fibers by latex bonding. Using this coating technique, coconut fibers were able to reduce the water permeability properties and improve homogeneity in a cement matrix. In addition, due to the high content of silica in perlite, the surface of coconut fiber would allow hydration reaction between cement and perlite and resulted in the bonding of fiber with a cementitious matrix. Additionally, this method can protect the coconut fiber surface from the alkaline attack and prolong degradation of fiber [20].

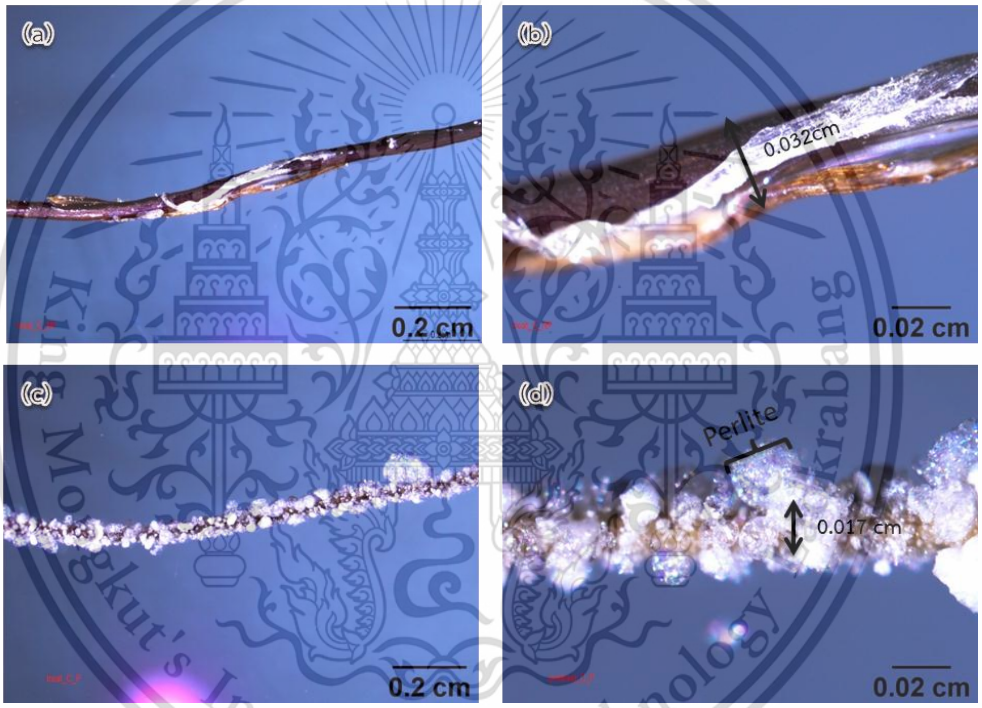


**Figure 4.8** Photomicrographs of (a) coconut fibers after coated with natural latex at 10x magnification and (b) 40x magnification, (c) coconut fiber after coated second layer with perlite at 10x magnification and (d) 40x magnification.

### 4.2.2 FTIR results of coconut fiber

FTIR analysis was used to investigate the organic compounds in the fibers before and after treatment and after coating with natural latex. The FTIR results provide the graph of the functional group, which shows the loss of the functional group after treatment and also the addition function group after coated.

FTIR results of coconut fibers before and after treatments are shown in Figure 4.9. The results of the FTIR analysis show a board peak at 3375 $cm^{-1}$ suggesting OH stretching vibrations from cellulose and lignin [21]. The hemicellulose, lignin, and pectin are identified at peak at 1730 $cm^{-1}$, indicating the C=O stretching of ester and aldehyde [22]. Peak at 897 $cm^{-1}$ is characteristic for ß-linkages, especially for hemicelluloses [23]. IR spectrum of coconut fiber also shows a characteristic C-O-C stretching absorbency peak at 1038 $cm^{-1}$ of cellulose. Absorption peak corresponding to 1250 $cm^{-1}$ is lignin aromatic C-O stretching, and 1509 $cm^{-1}$ is lignin aromatic ring stretching. The characteristic absorbency peak in the wave number of 1608 $cm^{-1}$ is obtained for lignin [24].

The peaks before and after treatment were similar. However, there is the only peak at wavenumber 1740 $cm^{-1}$ that disappeared after the treatment. The missing peak occurred by the disappearance of Hemicellulose on the fiber surface [25]. As a consequence, hemicellulose disappearing resulted in higher fiber tensile properties and improvement of the durability. Furthermore, hemicellulose loss increases the purity of cellulose, which makes fibers have a higher elongation at break. In general, coconut fiber contains high non-cellulosic impurities such as lignin, hemicellulose, wax, and fatty. These components can be found on the outer surface layers of fibers. Therefore, preparing fiber surfaces before being used in other processes must be considered. Alkaline treatment was one of the ways to improve properties and reduce all impurities on the fiber surface. After Fiber treatment results in less wax, fats and exposes the surface pores, which call pits of fiber [32].

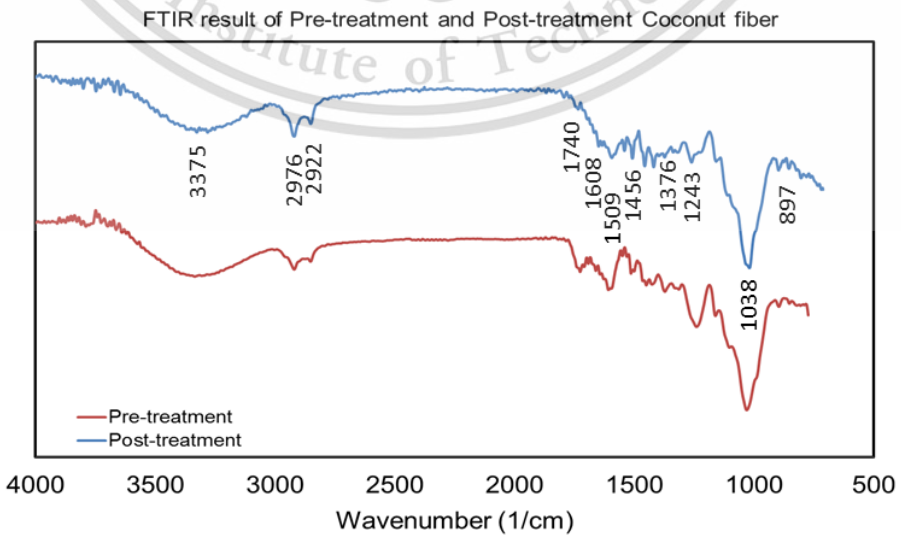


**Figure 4.9** FTIR results of coconut fibers before and after alkaline treatment.

FTIR result of coconut fibers after coating with natural latex are shown in Figure 4.9. The graph shows that the peak of fiber coated with natural latex has a distinct peak when compared to without rubber coating. The peaks that appear are as follows. The cis-1, 4-polyisoprene absorption band of strong amplitude corresponding to C=H bending is observed at 873cm$^{-1}$. The IR spectrum reveals that it has absorbance bands at 1240 cm$^{-1}$, corresponding to O-P-O asymmetric stretching of phospholipids indicating the presence of associated phospholipids at the rubber chain. The absorptions bands at 1375 cm$^{-1}$, 1394 cm$^{-1}$ and 1432 cm$^{-1}$ and 1494 cm$^{-1}$ are characteristics of $CH_2$ deformation. The absorption band at 1647 cm$^{-1}$ correspond to C=C stretching in cis-1,4-polyisoprene. The $CH_2$ symmetric stretching vibrations are observed at the region 2852 cm$^{-1}$, 2925 cm$^{-1}$. Asymmetric stretching in FT-IR of Natural rubber membranes is observed at 2961 cm$^{-1}$ [26].

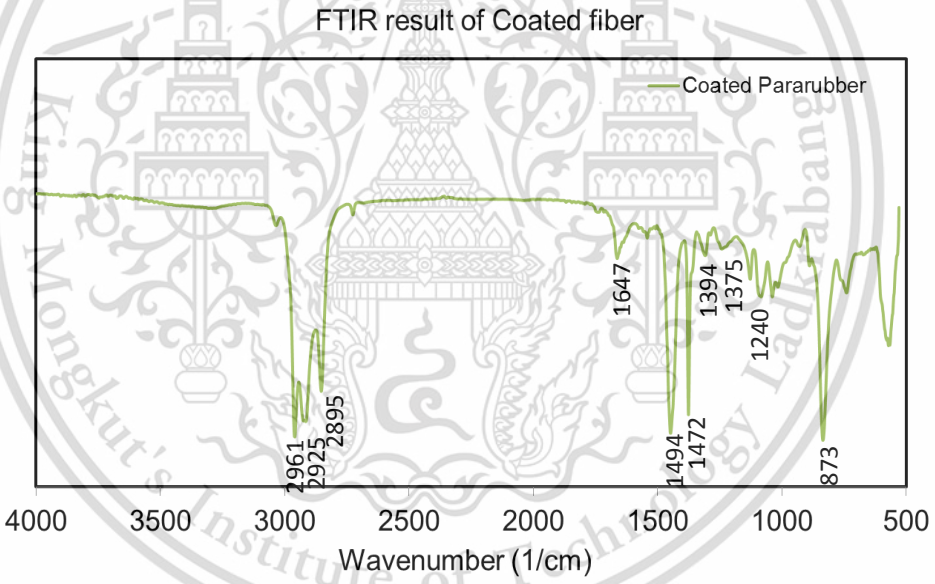


**Figure 4.10** FTIR result of coconut fibers after coating with natural latex.

## 4.3 Investigation of perlite fiber cement

The effects of addition of coconut fiber on the properties of perlite fiber cement were study in this section. The experimental results are divided into two cases: specimen using uncoated coconut fiber (UCF) and specimen using natural latex-coated coconut fiber (CCF). The different length of fibers that are 1, 2 and 3 cm were used. The different contents of coconut fiber i.e., 2.5, 5.0, 7.5, 10, and 12.5 g were also studied. After specimen preparation and curing for 28 days, the investigation of bulk density, water absorption, flexural strength, microstructure, and thermal conductivity were conducted.

### 4.3.1 Physical and mechanical properties of specimens using uncoated coconut fiber (UCF)

Figure 4.11 shows the bulk density of perlite fiber cements prepared with uncoated coconut fiber. When increasing fiber content, the bulk density decreased. For specimens using 1 cm fiber, the density reduced from 1822 kg/m³ to 1684 kg/m³ when the fiber increased from 2.5 g to 12.5 g. For specimens using 2 cm fiber, the density reduced from 1815 kg. /m³ to 1700 kg/m³ when fiber increased from 2.5 g to 10 g, and that of specimens using 3 cm fiber reduced from 1801 kg/m³ to 1720 kg/m³ when fiber increased from 2.5 g to 7.5 g. For the effect of fiber length on density, it was found that the longer fiber resulted in a lower density. The bulk densities of all specimens were still in the range above the target (density < 1500 kg/m³).

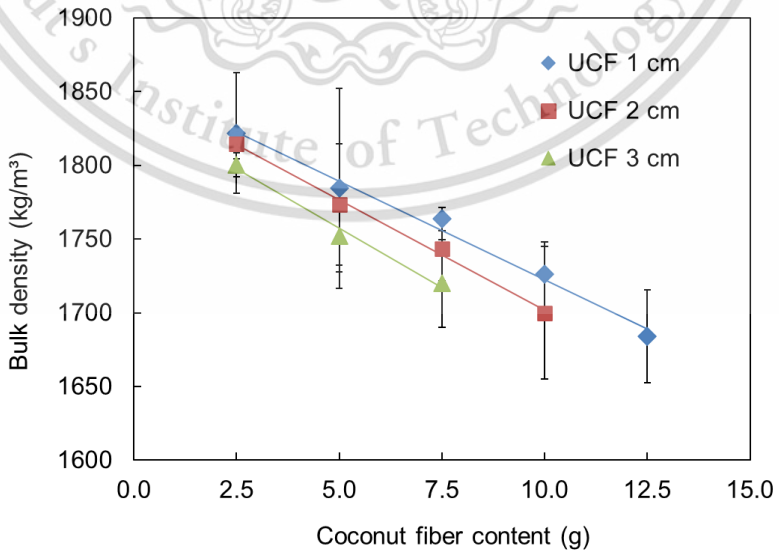


**Figure 4.11** Bulk density of perlite fiber cements prepared with uncoated coconut fiber (UCF).

Figure 4.12 shows the water absorption of the perlite fiber cements prepared with uncoated coconut fiber. It can be seen that the increase in fiber content increased the water absorption value accordingly. For the specimens using 1 cm fiber, water absorption increased from 14.4% to 19.7% when fiber increased from 2.5 g to 12.5 g. For the specimens using 2 cm fiber, water absorption increased from 16.8% to 19.2% when fiber increased from 2.5 g to 10.0 g. For the specimens using 3 cm fiber, water absorption increased from 17.7% to 19.0% when fiber increased from 2.5 g to 7.5 g. It was observed that the longer fiber tended to increase the water absorption of the specimens. The water absorption of all specimens was followed the ASTM standard (water absorption < 25%).

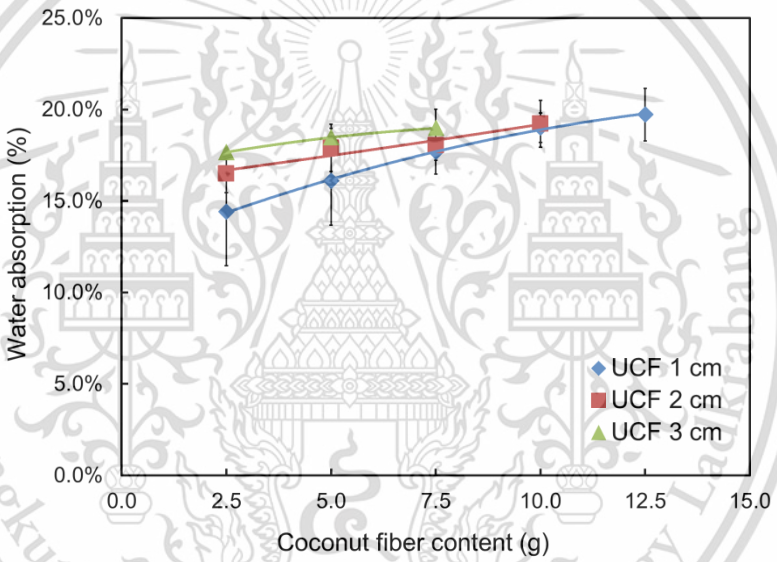


**Figure 4.12** Water absorption of perlite fiber cements prepared with uncoated coconut fiber (UCF).

Figure 4.13 shows the flexural strength of the perlite fiber cements prepared with uncoated coconut fiber. The flexural strength decreased accordingly with fiber content and fiber length. For specimens using 1 cm fibers, the flexural strength reduced from 7.14±0.44 MPa to 1.41±0.13 MPa when fiber content was increased from 2.5 g to 12.5 g. For specimens using 2 cm fibers, the flexural strength decreased from 4.00+2.30 MPa to 1.83±0.32 MPa when the fiber content was increased from 2.5 g to 10 g. For specimens using 2 cm fibers, the flexural strength decreased from 2.49±1.05 MPa to 1.66±0.28 MPa when the fiber content was increased from 2.5 g to

7.5 g. According to the ASTM standard, the flexural strength should higher than 4 MPa. Only samples using 1 cm fibers of 1 cm at 2.5, 5.0, and 7.5 g, and sample using 2 cm at 2.5 g have the flexural strength follow the ASTM standard.

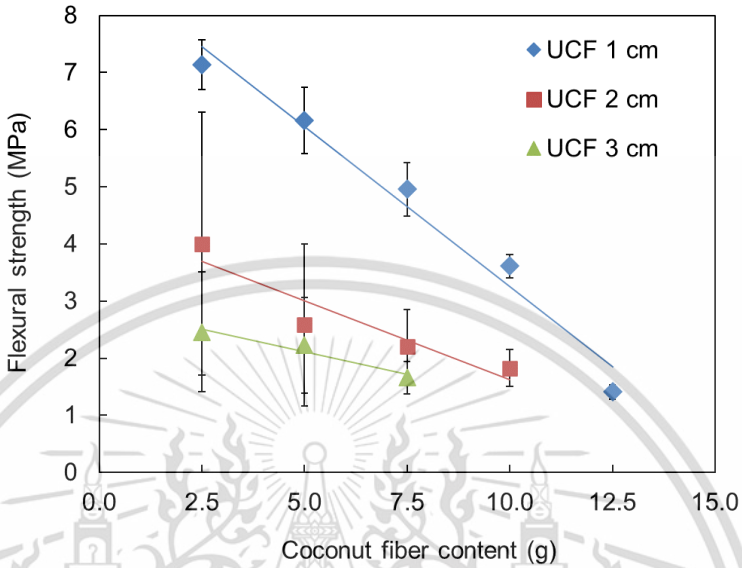


**Figure 4.13** Flexural strength of perlite fiber cements prepared with uncoated coconut fiber (UCF).

### 4.3.2 Physical and mechanical properties of specimens using natural latex coated coconut fiber (CCF)

Figure 4.14 shows the bulk density of perlite fiber cements prepared with natural latex coated coconut fiber. When more fibers were added, the results indicated a proportional drop in bulk density. For specimens using 1 cm fiber, the density was reduced from 1834 kg/m³ to 1725 kg/m³ when the fiber was increased from 2.5 g to 12.5 g. For specimens using 2 cm fiber, the bulk density was reduced from 1821 kg/m³ to 1752 kg/m³ when fiber was increased from 2.5 g to 10 g. For specimens using 3 cm fiber, the bulk density was reduced from 1803 kg/m³ to 1743 kg/m³ when fiber was increased from 2.5 g to 7.5 g. When considering the effect of fiber length on bulk density, it was found that specimens prepared with longer fibers showed a decreased in the bulk density. However, the total target density still showed the value above the target (density < 1500 kg/m³).

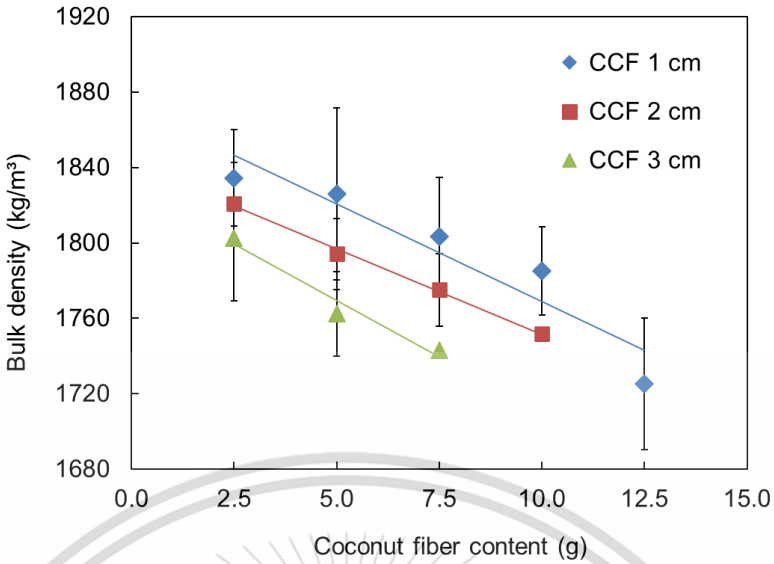


**Figure 4.14** Bulk density of perlite fiber cements prepared with coated coconut fiber (CCF).

Figure 4.15 shows the water absorption of perlite fiber cements prepared with natural latex coated coconut fiber. It was found that water absorption values increased sequentially when increasing the fiber content. The water absorption was increased from 13.7% to 18.3% for specimens using 1 cm fibers when the fiber was increased from 2.5 g to 12.5 g. For specimens using 2 cm fibers, the water absorption was increased from 16.7% to 17.9 % when fiber was added from 2.5 g to 10 g, and specimens using 3 cm fibers had an increase in water absorption from 17.5% to 18.0% when fiber was increased from 2.5 g to 7.5 g. The increase in length of fibers also tended to cause higher water absorption as well. The water absorption values of all samples are in accordance with the standard i.e., the water absorption value does not exceed 25%.

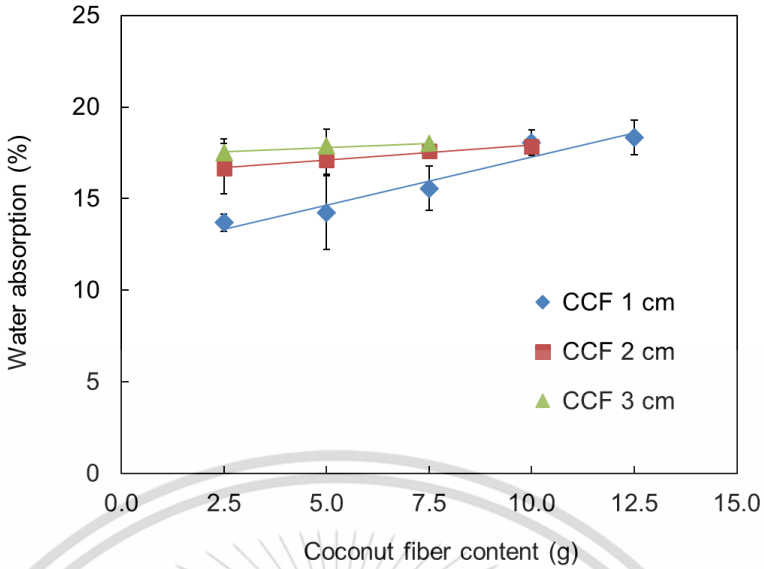


**Figure 4.15** Water absorption of perlite fiber cements prepared with coated coconut fiber (CCF).

Figure 4.16 shows the flexural strength of perlite fiber cements prepared with natural latex coated coconut fiber. As a result, when increasing the content and length of fibers to the sample, the flexural strength values are correspondingly reduced. For specimens using fibers of 1 cm length, the flexural strength decreased from 6.15±1.51 MPa to 2.27±1.27 MPa when the fiber content was increased from 2.5 g to 12.5 g. On the other hand, specimens prepared with the coated fiber lengths of 2 cm and 3 cm, showed an increase in flexural strength compared to that of specimen using 1 cm fibers. For specimens using 2 cm fibers, the flexural strength decreased from 6.57±1.54 MPa to 4.26±1.83 MPa when fiber content was increased from 2.5 g to 10 g. For specimens using 3 cm fibers, the flexural strength was reduced from 6.91+1.83 MPa to 5.33+0.60 MPa as the fiber content increased from 2.5 g to 7.50 g. Compared to the ASTM standard flexural strength target (>4 MPa), there are values according to the standard, including the specimens using coated fibers of length 1 cm in volume not exceeding 7.5 g and specimens using coated fibers of length 2 cm and 3 cm in the amount not exceeding 10 g and 7.5 g, respectively.

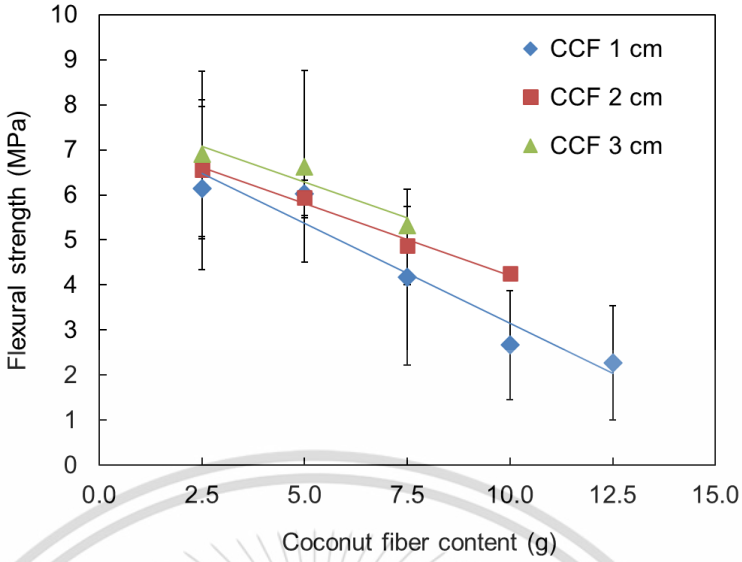


**Figure 4.16** Flexural strength of perlite fiber cements prepared with coated coconut fiber (CCF).

### 4.3.3 Thermal conductivity of perlite fiber cement

This section shows thermal conductivity results. The thermal conductivity of the prototype of perlite mortar, and perlite fiber cements prepared with uncoated and coated coconut fiber were studied. For the perlite fiber cements, the specimens combined with 1 cm and 3 cm of fiber for 5 g were chosen as the fiber condition to be evaluated. The reason for choosing these conditions to measure is because the properties of samples were good in both respects to bulk density, water absorption and flexural strength. The thermal conductivity test by heat flow method was conducted following ASTM C518 [35].

Figure 4.17 shows thermal conductivity of perlite fiber cement specimens prepared from different condition of fiber. The non-fiber contained specimen had a thermal conductivity of 0.147 (W/m K) which is considerably low. As mentioned previously, expanded perlite has high thermal insulating properties due to its porosity. Therefore, it can reduce thermal conductivity when added to the specimen. The uncoated fiber added conditions had a slightly higher thermal conductivity than other conditions. Although coconut fiber has insulating properties, due to the sample density increases, the thermal conductivity also increases. However, compared to the conditions with natural latex coated samples, the thermal conductivity was lower

than that of uncoated conditions. The reason might be because when the fibers are encapsulated by natural rubber, natural rubber will act as the first layer of insulation due to its inherent thermal insulating properties, resulting in lower thermal conductivity.

However, the results show that all specimens had very low thermal conductivity and were in accordance with the target (thermal conductivity < 0.5 W/m K). The perlite fiber cement with 5 g of 3 cm coated coconut fibers exhibited the lowest thermal conductivity of 0.133 W/ m K.

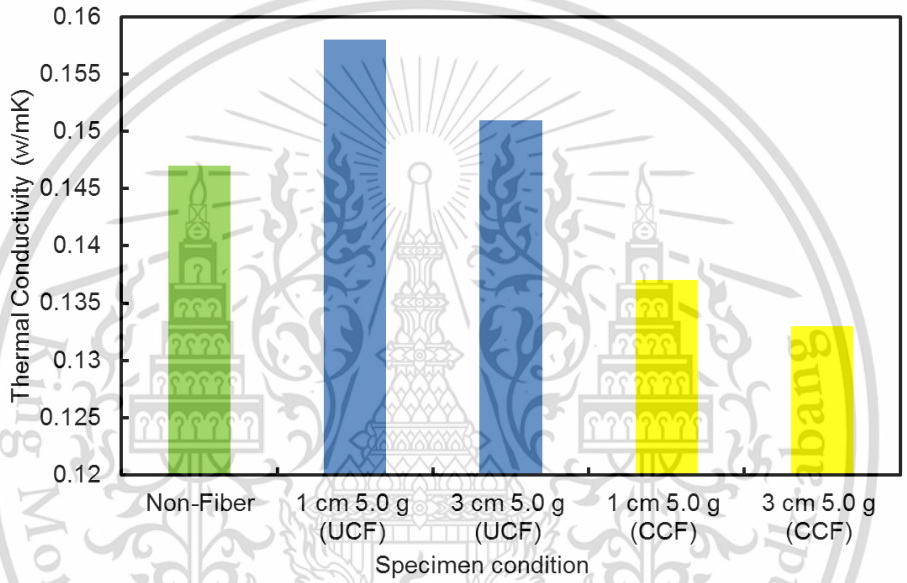


**Figure 4.17** Thermal conductivity of perlite fiber cement specimens.

### 4.3.4 Microstructure of perlite fiber cement

This section shows the microstructure of the specimens in each condition. The cross-sectional images were taken by a stereo camera to observe the microstructure of the specimen. The microstructure images were used as a reference to explain how the bonding between each phase affected the properties of the specimens.

Figure 4.18 shows the microstructure of perlite fiber cement prepared with uncoated coconut fibers at different contents. It can be observed that there was gap at the interface between fiber and cement matrix which left a significant amount of void in microstructure. In addition, the increase in fiber content caused the crack in

specimens. At high fiber content, the fiber had a tendency to overlap leading to inhomogeneous in a cement structure. As a result, the specimen revealed a decrease in density and an increase in water absorption at higher fiber content.

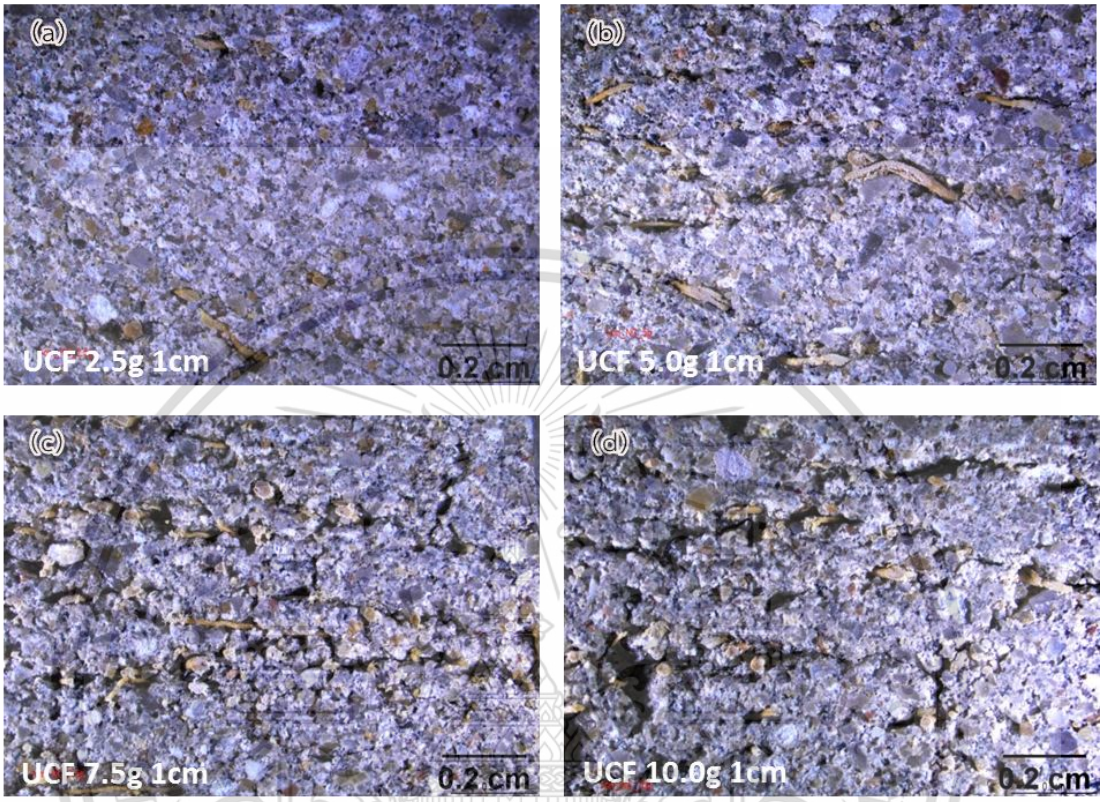


**Figure 4.18** Photomicrographs of perlite fiber cement prepared from 1 cm uncoated coconut fiber with content of (a) 2.5 g, (b) 5.0 g (c) 7.5 g, (d) 10 g. (At x10 magnification)

Figure 4.19 shows the comparison of microstructures of perlite fiber cements prepared with uncoated and coated coconut fibers. Figure 4.19 (a) shows photomicrograph of specimen using uncoated fiber which demonstrates that the fibers were not able to adhere well to the cement. The reason might be because non-cellulosic impurities such as lignin, hemicellulose, wax, and fatty on fiber surfaces restrict the wettability to cement matrix [33]. In Figure 4.19 (b), it is shown that the coating on the fibers with natural latex and perlite improved the adhesion of the fibers to cement matrix thus significantly reduce the voids. The perlite attached to the natural rubber would interact with the cement allowing the fibers to effectively incorporate in the cement structure [2]. Therefore, the specimen with

coated fiber had lower water absorption and increased flexural strength compared to the specimen with uncoated fiber. However, the natural latex also had some negative effects. When natural latex was hardened, it had distinct properties including resilience and elasticity. Due to these characteristics, specimens with 3 cm coated fiber led to cracking during demolding in compression process. This behavior was more severe when using longer fiber.

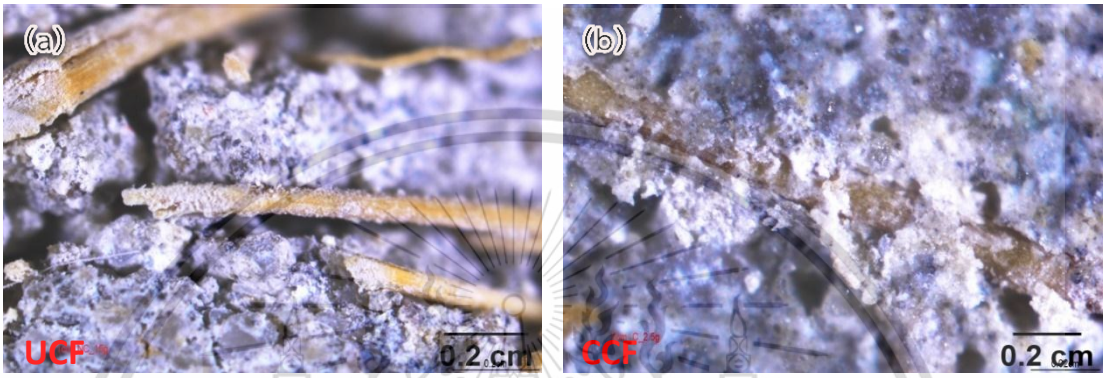


**Figure 4.19** Photomicrographs of perlite fiber cement prepared from (a) uncoated fiber (b) coated fiber. (At magnification x10)

It should be noted that the specimens using coated fiber of 1 cm length, showed the crack defect in their microstructure as shown in Figure 4.20. It was thought that the natural latex used for this condition was degraded. In Figure 4.221, the higher magnification micrograph demonstrated that the coating layer was peeled off from the fiber and dissolved into the cement texture. This crack defect is the explanation for the low mechanical strength for the specimens in this condition.

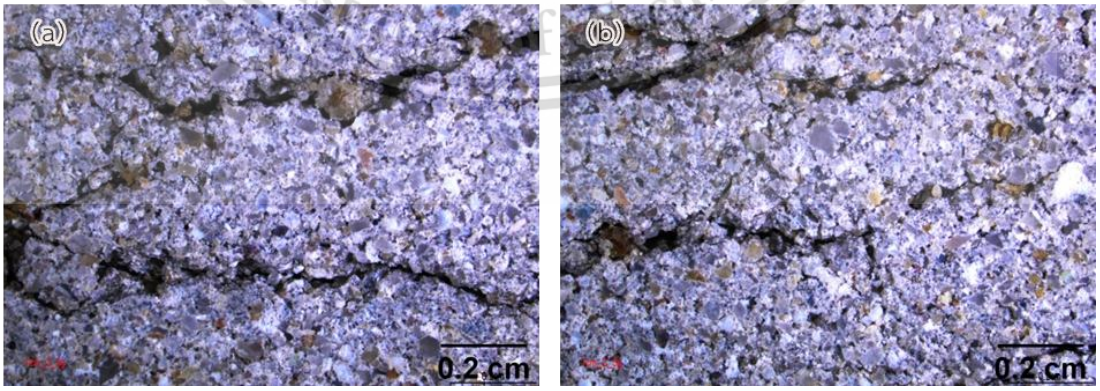


**Figure 4.20** Crack decfects observation in specimen using coated coconut fiber of 1 cm length, (a) and (b) showing the crack at different area in same sample. (At magnification x10)


**Figure 4.21** Optical stereo photographs of non-adherent rubber on fiber surface (a) at magnification x10 and (b) at magnification x40.

## 4.4 Comparison of properties of perlite fiber cements prepared with uncoated coconut fiber (UCF) and coated coconut fiber (CCF)

This section compares and discusses the differences between specimens prepared with uncoated and coated coconut fibers in terms of bulk density, water absorption, and flexural strength. In addition, the results from this research were compared with the experimental results of literatures in order to see the differences and advantages and disadvantages of each process or composition.

### 4.4.1 Comparison of bulk density

Figure 4.22 shows the bulk density of perlite fiber cement prepared with uncoated and coated coconut fibers. It is obviously seen that increasing the proportion of fibers will result in a decrease in bulk density. The density is also influenced by the fiber length, and as the fiber length is increased, the density decreases. When fiber content and/or length increased, more gaps in the cementitious matrix were formed. At higher fiber content, the chunk of fiber layer might be formed in the specimen, causing the cement to disintegrate and crack and resulted in a reduction of bulk density. In addition, the coated condition had a higher density when compared to the uncoated one. It was due to the coated fibers contained a layer of perlite on the surface, the perlite layer will react to the hydration reaction of cement and form a bounding with a cementitious matrix, which reduces the void that occurs when fibers were added in cement.

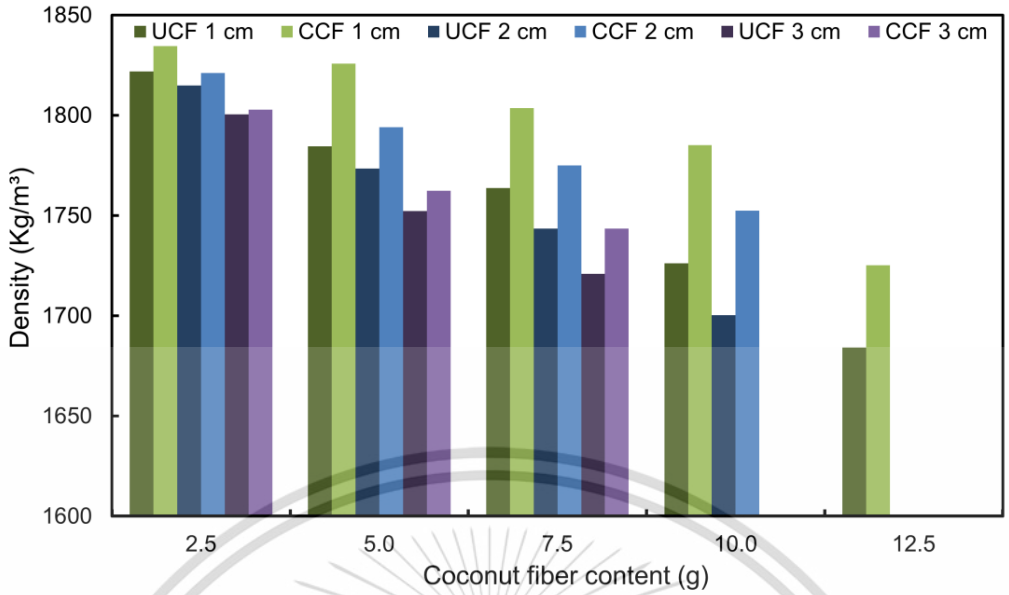


**Figure 4.22** Bulk density of perlite fiber cement prepared with uncoated and coated coconut fibers.

The values of bulk density of specimens with uncoated coconut fiber and coated coconut fiber are shown in Table 4.6. The percentage increase in bulk density of specimens when using coated fibers compared to uncoated fibers are shown in Table 4.7. The increasing values are in the range of 0.11–3.42%. The natural latex coating on the fibers results in better fiber adhesion to cement matrix, as a result, the bulk density of specimens was increased. The specimens with 3 cm coated fibers resulted in the least increase in density due to the crack generation as previously discussed in section 4.3.4.

**Table 4.6** Bulk density of specimens with uncoated coconut fiber and coated coconut fiber.

| Fiber content (g) | Bulk density ($kg/cm^3$) | | | | | |
|---|---|---|---|---|---|---|
| | Uncoated 1 cm | Coated 1 cm | Uncoated 2 cm | Coated 2 cm | Uncoated 3 cm | Coated 3 cm |
| 2.5 | 1822 | 1834 | 1815 | 1821 | 1801 | 1803 |
| 5.0 | 1784 | 1826 | 1773 | 1794 | 1752 | 1762 |
| 7.5 | 1764 | 1804 | 1744 | 1775 | 1721 | 1744 |
| 10.0 | 1726 | 1785 | 1700 | 1752 | - | - |
| 12.5 | 1684 | 1725 | - | - | - | - |

**Table 4.7** Percentage of the change in bulk density between specimens prepared with coated coconut fiber and uncoated coconut fiber.

| Fiber content (g) | Percentage of the change in bulk density (%) | | |
|---|---|---|---|
| | 1 cm | 2 cm | 3 cm |
| 2.5 | +0.66 | +0.33 | +0.11 |
| 5.0 | +2.35 | +1.18 | +0.57 |
| 7.5 | +2.27 | +1.78 | +1.34 |
| 10.0 | +3.42 | +3.06 | - |
| 12.5 | +2.43 | - | - |

### 4.4.2 Comparison of water absorption

Figure 4.23 shows the water absorption of perlite fiber cement prepared with uncoated and coated coconut fibers. The water absorption of specimen tended to increase with fiber content and fiber length. It is also seen that the specimens with coated fibers had lower water absorption than the specimens with uncoated fibers. The reason that coated fiber sample had lower water absorption is due to the properties of the natural latex, when it solidified, rubber reduced water permeability of fiber.

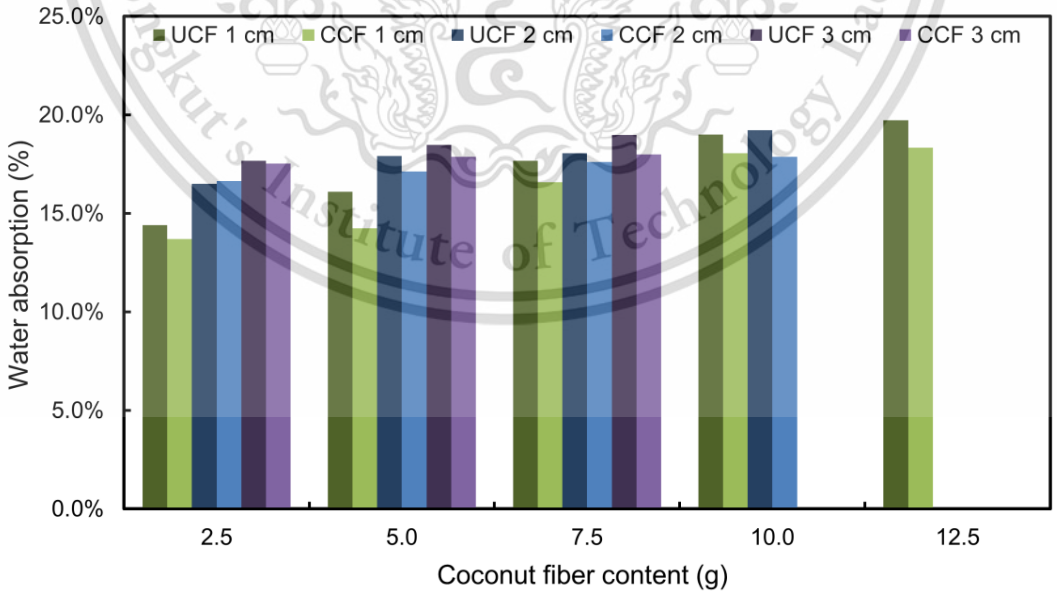


**Figure 4.23** Water absorption of specimens that contain fiber coated rubber and uncoated rubber.

The values of water absorption of specimens with uncoated coconut fiber and coated coconut fiber are shown in Table 4.8. The percentage decrease in water absorption of specimens when using coated fibers compared to uncoated fibers are shown in Table 4.9. The decreasing percentage is in the range of 0.60–11.49%. This result shows the effectiveness of natural latex coating on coconut fiber in preventing water permeability and so reducing the deterioration of coconut fibers.

**Table 4.8** Water absorption of specimens with uncoated coconut fiber (UCF) and coated coconut fiber (CCF).

| Fiber content (g) | Water absorption (%) | | | | | |
|---|---|---|---|---|---|---|
| | Uncoated 1 cm | Coated 1 cm | Uncoated 2 cm | Coated 2 cm | Uncoated 3 cm | Coated 3 cm |
| 2.5 | 14.41 | 13.70 | 16.75 | 16.65 | 17.66 | 17.53 |
| 5.0 | 16.09 | 14.24 | 17.91 | 17.12 | 18.47 | 17.87 |
| 7.5 | 17.68 | 16.57 | 18.05 | 17.61 | 18.98 | 18.00 |
| 10.0 | 19.01 | 18.05 | 19.22 | 17.87 | - | - |
| 12.5 | 19.71 | 18.34 | - | - | - | - |

**Table 4.9** Percentage of the change in water absorption between specimens prepared with coated coconut fiber and uncoated coconut fiber.

| Fiber content (g) | Percentage of the change in water absorption (%) | | |
|---|---|---|---|
| | 1 cm | 2 cm | 1 cm |
| 2.5 | -4.93 | -0.60 | -0.74 |
| 5.0 | -11.49 | -4.41 | -3.25 |
| 7.5 | -6.28 | -2.44 | -5.16 |
| 10.0 | -5.05 | -2.44 | - |
| 12.5 | -6.95 | - | - |

### 4.4.3 Comparison of flexural strength

Figure 4.24 shows the flexural strength of perlite fiber cement prepared with uncoated and coated coconut fibers. With increasing fiber content and fiber length, the flexural strength tended to decline. For specimens using 2 cm and 3 cm fibers with coating, showed a significant increase in flexural strength. It has been clearly demonstrated that the surface treatment of coconut fibers with latex can enhance its adhesion to other elements and increase its strength. On the other hand, the specimens using 1 cm fiber with coating had slightly lower flexural strength values when compared to uncoated specimens. The reason is because the latex used in this condition deteriorated and allowed the latex to be absorbed in the cement rather than coated on the fibers as already mentioned in the earlier section and illustrated in Figure 4.21. As a result, voids and gaps in a cement matrix led to a reduction in flexural strength.

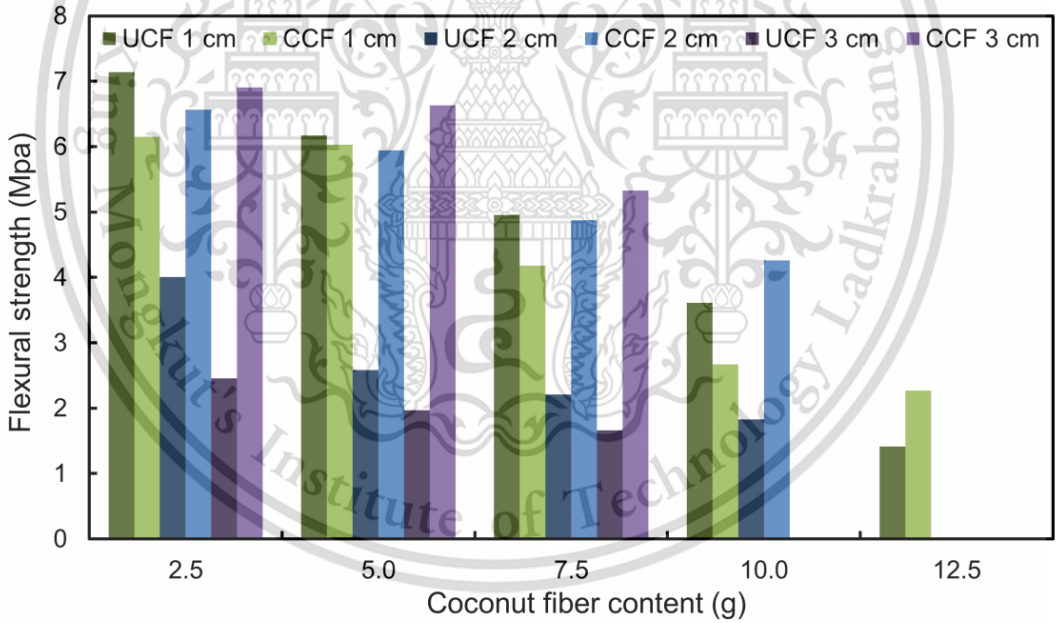


**Figure 4.24** Flexural strength of specimens that contain fiber coated rubber and uncoated rubber.

The values of flexural strength of specimens with uncoated coconut fiber and coated coconut fiber are shown in Table 4.10. The percentage of the change in flexural strength of specimens when using coated fibers compared to uncoated fibers are shown in Table 4.9. Samples using 2.5–10 g of 1 cm fibers had approximately 2.3–26.0% reduction in flexural strength, but when the fiber was increased to 12.5 g,

the flexural strength was as high as 61.1%. Samples with coated fiber with a length of 2 cm and 3 cm resulted in significantly increase the flexural strength. The specimens using 2 cm coated fibers had an increase in flexural strength of 64.3–132.8%, and specimens using 3 cm coated fibers had an increase in flexural strength of 180.9–221.1%.

**Table 4.10** Flexural strength of specimens with uncoated coconut fiber (UCF) and coated coconut fiber (CCF).

| Fiber content (g) | Flexural strength (MPa) | | | | | |
|---|---|---|---|---|---|---|
| | Uncoated 1 cm | Coated 1 cm | Uncoated 2 cm | Coated 2 cm | Uncoated 3 cm | Coated 3 cm |
| 2.5 | 7.14 | 6.15 | 4.00 | 6.57 | 2.46 | 6.91 |
| 5.0 | 6.17 | 6.03 | 2.58 | 5.94 | 2.28 | 6.63 |
| 7.5 | 4.96 | 4.18 | 2.21 | 4.87 | 1.66 | 5.33 |
| 10.0 | 3.61 | 2.67 | 1.83 | 4.26 | - | - |
| 12.5 | 1.41 | 2.27 | - | - | - | - |

**Table 4.11** Percentage of the change in flexural strength between specimens prepared with coated coconut fiber and uncoated coconut fiber.

| Fiber content (g) | Percentage of the change in flexural strength (%) | | |
|---|---|---|---|
| | 1 cm | 2 cm | 1 cm |
| 2.5 | -13.9 | +64.3 | +180.9 |
| 5.0 | -2.3 | +130.2 | +190.8 |
| 7.5 | -15.7 | +120.4 | +221.1 |
| 10.0 | - 26.0 | +132.8 | - |
| 12.5 | +61.0 | - | - |

**4.4.4 Comparison of properties with the values in literature**

In order to compare the differences of each procedure or substance, the experimental results of related studies were compared with the results from this study. Table 4.12 shows the comparison of properties with the values in literature**.**

Lertwattanarul et al. studied the properties of fiber cement using coconut fiber. When coconut fiber is added at 10% ratio of cement mass, it results in the product that had physical and mechanical properties following the standard. The produced specimen had a density of 1098 kg/m$^3$, water absorption of 7.26%, and flexural strength of 8.26 MPa.

Silva et al. studied coconut fiber cement by applying coconut fiber surface with rubber/water combining with silica fume/metakaolin. The study found that coating of coconut fiber with rubber and silica fume resulted in increased strength compared to other conditions, and it showed a flexural strength of 8.5 MPa.

Darsana et al. prepared fiber cement by replacement of sand with coconut fiber. The composite with 10 vol% fiber was considered to be the optimum condition. The product showed water absorption of 6.25% and flexural strength of 4.2 MPa.

Danso et al. studied fiber cement tiles that were mixed with coconut fibers. In this experiment, fibers and limestone additive were added to the mortar. The most proper conditions were 0.2 %wt fiber and 5 %wt limestone of the total mortar weight. The resulting property value were density of 1710 kg/m$^3$, flexural strength of 1.06 MPa and water absorption efficiency of 0.4% (kg/m$^2$*min).

Ramakrishna et al. studied fiber cement by mixing coconut fibers into the prescribed mortar mixture to determine strength. The compositions used were sand to cement ratio of 3:1, w/c of 0.65, and coconut fiber is added at 0.15% of total cement weight. The samples were divided into three different curing conditions. In conditions where the sample was constantly immersed in water showed the highest flexural strength of 4.7 MPa.

Li et al. fabricated fiber cement by mixing coconut fiber into mortar. Mortar composition consisted of cement:sand:water in ratio of 1:3:0.43 by weight. The coconut fiber sheets were put into the composite. With 3-layers fiber sheet addition, the highest flexural strength 6.34 MPa was obtained.

Asasutjarit et al. studied fiber cement containing coconut fibers. The coconut fibers were pre-treated by boiling and washing with water. The length of coconut fiber added was in range of 1-6 cm. The optimum composition ratio was cement:fiber:water at 2:1:2, and it provided density of 1.01 g/cm³, water absorption of 19.9 %, and flexural strength of 19.94 MPa.

Abdullah studied fiber cement containing coconut fiber. The sand to cement ratio was 1:1 and the water to cement ratio was 0.55. The coconut fiber was added to 3-15 wt%. At 9 wt% of coconut fiber, the optimum properties were obtained i.e., density of 1980 kg/m³, water absorption of 2.33%, and flexural strength of 5.24 MPa.

**Table 4.12** Comparison of properties with the values in literature.

| Authors | Flexural strength (MPa) | Water absorption (%) | Bulk density ($kg/m^3$) | Thermal conductivity (W/m K) |
|---|---|---|---|---|
| This study (CCF, 3 cm, 5 g) | 6.63 | 17.9 | 1763 | 0.133 |
| Lertwattanarul | 8.26 | 7.26 | 1980 | 0.38 |
| Silva | 8.50 | - | - | - |
| Darsana | 4.2 | 6.25 | - | - |
| Danso | 1.06 | - | 1710 | - |
| Ramakrishna | 4.7 | - | - | - |
| Li | 6.34 | - | - | - |
| Asasutjarit | 19.94 | 19.65 | 1010 | 0.055 |
| Abdullah [20] | 5.24 | 2.33 | 1980 | - |

From the above experiments in literature, coconut fibers were used to mix in cement products, but different composition and methods were applied. Comparing with the results in this study, the most proper condition was perlite cement mortar prepared with 3 cm coated coconut fibers at 0.005 wt% of total mass. The obtained properties values are density of 1763 kg/m3, water absorption of 17.9%, flexural strength of 6.63 MPa and thermal conductivity of 0.133 W/m K. The flexural strength value was moderate and followed the ASTM standard, while the density was

comparable to most reported in literatures. The water absorption was quite high but still followed the ASTM standard. The thermal conductivity was low, indicating good thermal insulation.

## 4.5 Accelerated degradation test result

The specimens prepared with 3 cm fiber at 5 g were selected to analyze the accelerated degradation. The simulation of aging condition was conducted through wet and dry cycle. The process was carried out by spraying water for 2 h and 50 min, resting for 10 min, then drying at 70±5 °C for 2 h and 50 min, then resting for 10 min. The total duration was 6 h for 1 cycle, and the test was repeated for 25 cycles. Then, the physical and mechanical properties of specimens were examined.

### 4.5.1 Bulk density before and after accelerated degradation test

Figure 4.25 shows the comparison of bulk density of specimens prepared with uncoated and coated coconut fiber before and after accelerated degradation test. The bulk density of specimen significantly reduced after the accelerated degradation test due to the corrosion of the fibers from an alkaline attack which causes the degradation of the fibers resulting in lower density. In addition, the degradation also reduces the fiber's size, which makes the size of the gap between cement and fiber increase, resulting in reduced density. The bulk density of specimen uncoated fibers decreased from 1752 kg/m³ to 1686 kg/m$^3$. After the accelerated degrading test, the bulk density decreased by 3.76%. On the other hand, the specimens prepared with coated fibers showed less reduction in bulk density by 2.89%, from 1762 kg/m³ to 1711 kg/m³.

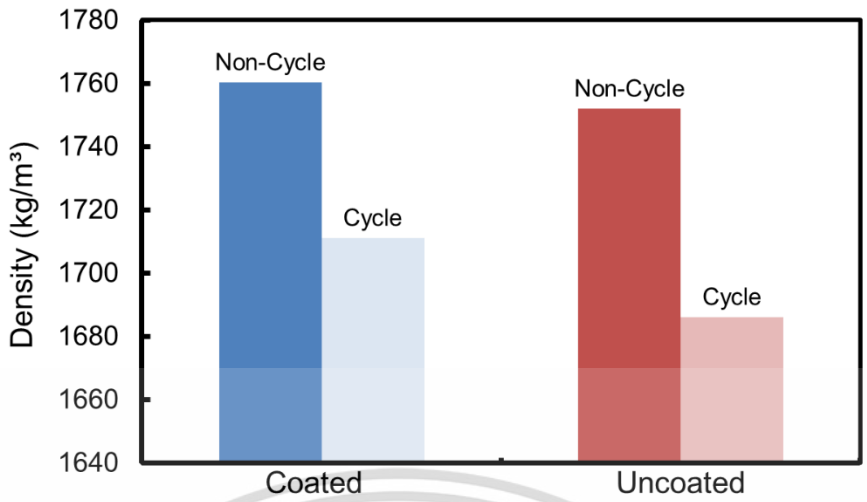


**Figure 4.25** Comparison of bulk density of specmimens prepared with uncoated and coated coconut fiber before and after accelerated degradation test.

### 4.5.2 Water absorption before and after accelerated degradation test

Figure 4.26 shows the comparison of water absorption of specimens prepared with uncoated and coated coconut fiber before and after accelerated degradation test. On the contrary to the bulk density, the water absorption of both specimens increase after the acceleration test. The water absorption decreased from 18.47% to 21.84% in specimen uncoated fibers. The water absorption decreased by 18.25%. The specimens prepared with coated fibers showed the less increased in water absorption by 10.24%, from 17.87% to 19.70%.

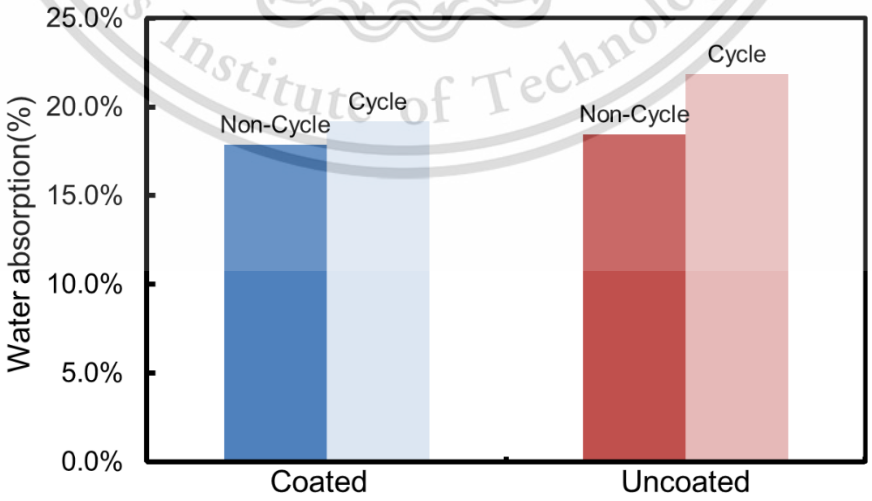


**Figure 4.26** Comparison of water absorption of specmimens prepared with uncoated and coated coconut fiber before and after accelerated degradation test.

### 4.5.3 Flexural strength before and after accelerated degradation test

Figure 4.27 shows the comparison of flexural strength of specimens prepared with uncoated and coated coconut fiber before and after accelerated degradation test. The graph shows that the flexural strength markedly decreased after the accelerated degradation test. In case of specimen with uncoated fibers, the flexural strength decreased from 2.28 MPa to 1.08 MPa which showed a decrease in strength by 52.6%. The specimens prepared with coated fibers showed the less decrease in flexural strength by 39.4%, from 6.63 MPa to 4.02 MPa.

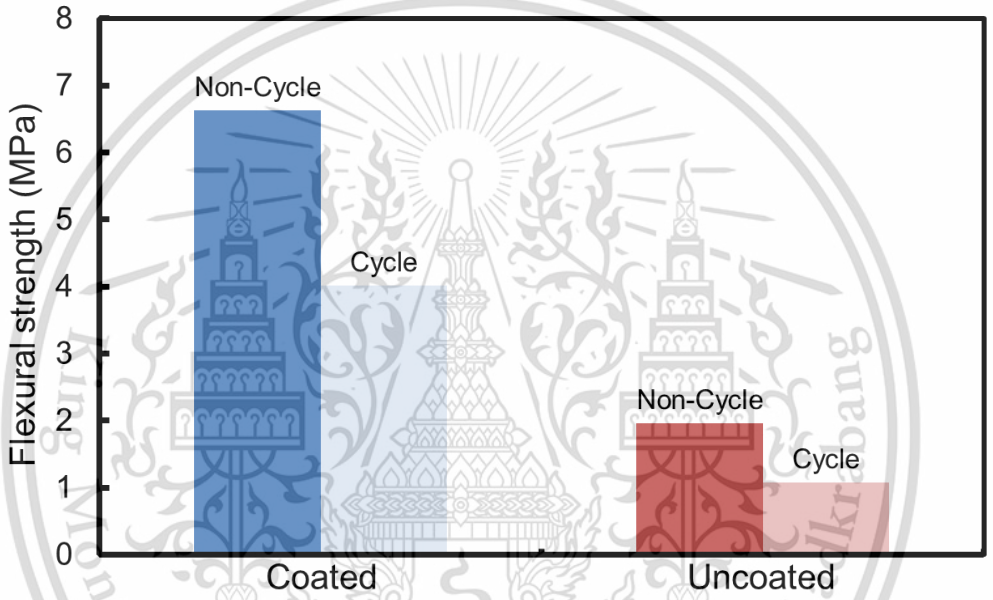


**Figure 4.27** Comparison of flexural strength of specmimens prepare with uncoated and coated coconut fiber before and after accelerated degradation test.

The accelerated degradation results demonstrated that the coated fiber effectively reduced water absorption and retarded the specimens from degradation. The specimen was also able to improve durability with a natural latex coating on fiber. Furthermore, the perlite coating on fiber might have caused pozzolanic reactions, which protected the coconut fibers during the accelerated aging of the specimens. On the other hand, uncoated fibers have lost their ductility. It should be noted that the variation of humidity at high temperature caused by the accelerated aging induced a significant increase in porosity in the fiber-matrix transition zone in the untreated coconut fiber sample [2].

In degradation, the results indicated that a considerable amount of pozzolan adhered to the surface of coconut fibers (due to the latex adhesive layer) may have provided a local pozzolanic effect in the fiber-cement interface. This pozzolanic reaction consumed portlandite (CH) and generates silica and alumina ($SiO_2$ and $Al_2O_3$) which decrease the local pH and increase the resistance and cohesion in the fiber-cement mixture [27].

## 4.6 Cost-benefit analysis

Cost analysis of perlite fiber cement roof tile production was determined from the specimen which contained cement : sand : perlite : coconut fiber (3 cm) coated with Natural latex : water at a ratio of 250 : 450 : 50 : 2.8 : 250, and the results are shown in Table 4.13. The results of the analysis revealed that the selling price of perlite fiber cement roof tile is approximately 46 baht per sheet. The average price of the commercial fiber cement roof tile is 120 baht per sheet. The prototypes produced in this research are 60% cheaper.

**Table 4.13** Cost-benefit analysis of perlite fiber cement roof tile.

| Raw materials | Raw material used for 1 unit (kg) | Cost of raw materials (Bath/kg) | Cost of raw materials for 1 unit (Bath) |
|---|---|---|---|
| Portland cement Type 1 | 0.25 | 1.94 | 0.485 |
| Fine Sand | 0.45 | 0.5 | 0.225 |
| Perlite | 0.05 | 15 | 0.75 |
| Coconut fiber | 0.0028 | 10 | 0.028 |
| Sodium hydroxide | 0.1 | 8 | 0.8 |
| Natural latex | 0.01 | 70 | 0.70 |
| Water | 0.25 | 0.01 | 0.025 |
| Raw materials cost for 1 sheet | | Lab size | 3.01 Bath / 450 $cm^3$ |
| | | Commercial size | 27.02 Bath / 4040 $cm^3$ |
| | | Sum (1) | 27.02 |
| Operation cost (calculate at 30 % of raw materials cost) | | | 8.11 |
| | | Sum (2) | 35.13 |
| Benefits (calculate at 30 % of raw materials and operation cost) | | | 10.54 |
| | | Total | 45.67 |

# Chapter 5
# Conclusions

In this research, coconut fiber was used as a reinforcing material and expanded perlite was applied as an additive material to increase the efficiency of the fiber cement roof tile.

In the first part of the research, expanded perlite was substituted for sand to find a suitable condition before adding fiber, where sand is replaced with perlite in a ratio of 5%, 10%, and 15% by weight. The Specimens were fabricated by compression methods, using force for compaction at 20kN, 30kN and 40 kN. After fabrication, the specimens were cured in water for 28 days. After that, specimens were tested for physical properties and mechanical properties such as density, water absorption and flexural strength. The optimum of the specimen was 40 kN of compression force and 10%wt of perlite replacement, with a comparable flexural strength to cement mortar but less density and had a water absorption following ASTM standard.

In the second part of the research, coconut fibers were added to the optimum cement mortar proportion from the previous study. Two types of coconut fibers were applied: uncoated coconut fibers and natural latex coated fiber. Coconut fibers were treated with alkaline to improve the surface before coating natural latex. After coating with latex as a first layer, it was coated with perlite as a second layer. After specimens, preparation and curing, the specimens were investigated their properties. From the test, the specimens prepared with uncoated fiber had lower performance compared to specimens with coated fiber. When adding uncoated fiber into cement, fiber cannot adhere to the cementitious matrix due to wax and fatty on the surface of fiber resulting in voids and gap in the fiber cement. When applying coated coconut fiber, the bonding between fiber and cement matrix was properly formed. The expanded perlite coated on the surface of coated fiber also contributed to a hydration and pozzolanic reaction in cement that increase the strength of fiber cement. From the accelerated degradation test, rubber-coated fibers had reduced properties from the original but were still acceptable.

In future work, improvements of mortar formula as well as alternative additive materials such as silica fume, metakaolin or fly ash should be considered. The effect of fiber-coated rubber on other fibers with another treatment for improving fiber surface should be investigated.

# References


[1] “การกำจัดโรคที่เกี่ยวข้องกับแร่ใยหิน,” no. 5, pp. 5–8.

[2] E. Jose, M. Lidiane, F. Garcia, C. Fornari, F. Martínez, and M. Mitsuuchi, “A new treatment for coconut fi bers to improve the properties of cement- based composites – Combined e ff ect of natural latex / pozzolanic materials,” *Sustain. Mater. Technol.*, vol. 12, no. February, pp. 44–51, 2017, doi: 10.1016/j.susmat.2017.04.003.

[3] M. Singh and M. Garg, “Perlite-based building materials - a review of current applications,” *Constr. Build. Mater.*, vol. 5, no. 2, 1991, doi: 10.1016/0950-0618(91)90004-5.

[4] ชัชวาลย์ เศรษฐบุตร, “ปูนซีเมนต์,” *คอนกรีตเทคโนโลยี*, pp. 9–24, 2556.

[5] S. Chandra and L. Berntsson, “Production of Lightweight Aggregates and Its Properties,” in *Lightweight Aggregate Concrete*, 2002.

[6] J. Iwaro and A. Mwasha, “Effects of Using Coconut Fiber – Insulated Masonry Walls to Achieve Energy Efficiency and Thermal Comfort in Residential Dwellings,” vol. 25, no. 1, pp. 1–12, 2019, doi: 10.1061/(ASCE)AE.1943-5568.0000341.

[7] ศ. เห็นประเสริฐแท้, “ทำไมต้องมีเทคนิคการเลี้ยวเบนของรังสีเอกซ์.” .

[8] Faisal Alamgir, “X-ray Diffraction Source: Faisal Alamgir, School of Materials Science and Engineering, Georgia Institute of Technology, Atlanta, GA.” .

[9] Jascoinc, “Introduction to FTIR Spectroscopy and How it’s work?” .

[10] L. Messgeraete, “Linseis manuscript,” *https://www.linseis.com/en/products/thermal-conductivity-instruments/thb-transient-hot-bridge/*. .

[11] Department science service (DSS), “Thermal conductivity by Department science service (DSS),” pp. 1–4.

[12] V. Akyuncu and F. Sanliturk, “Investigation of Physical and Mechanical Properties of Mortars Produced by Polymer Coated Perlite Aggregate,” *J. Build. Eng.*, 2021, doi: 10.1016/j.jobe.2021.102182.

[13] O. Sengul, S. Azizi, F. Karaosmanoglu, and M. A. Tasdemir, “Effect of expanded perlite on the mechanical properties and thermal conductivity of lightweight concrete,” *Energy Build.*, 2011, doi: 10.1016/j.enbuild.2010.11.008.

[14] T. K. Erdem, Ç. Meral, M. Tokyay, and T. Y. Erdoğan, "Use of perlite as a pozzolanic addition in producing blended cements," *Cem. Concr. Compos.*, 2007, doi: 10.1016/j.cemconcomp.2006.07.018.

[15] M. Lanzón and P. A. García-Ruiz, "Lightweight cement mortars: Advantages and inconveniences of expanded perlite and its influence on fresh and hardened state and durability," *Constr. Build. Mater.*, 2008, doi: 10.1016/j.conbuildmat.2007.05.006.

[16] P. Lertwattanaruk and A. Suntijitto, "Properties of natural fiber cement materials containing coconut coir and oil palm fibers for residential building applications," *Constr. Build. Mater.*, 2015, doi: 10.1016/j.conbuildmat.2015.07.154.

[17] S. B. Singh, P. Munjal, and N. Thammishetti, "Role of water / cement ratio on strength development of cement mortar," *J. Build. Eng.*, vol. 4, pp. 94–100, 2015, doi: 10.1016/j.jobe.2015.09.003.

[18] P. Darsana, R. Abraham, A. Joseph, A. Jasheela, and P. R. Binuraj, "Development of Coir-Fibre Cement Composite Roofing Tiles," *Procedia Technol.*, vol. 24, pp. 169–178, 2016, doi: 10.1016/j.protcy.2016.05.024.

[19] D. E. Thanon Dawood, "Experimental study of lightweight concrete used for the production of canoe," *AL-Rafdain Eng. J.*, vol. 23, no. 2, pp. 187–197, 2015, doi: 10.33899/rengj.2015.101085.

[20] H. Oktay, R. Yumrutaş, and A. Akpolat, "Mechanical and thermophysical properties of lightweight aggregate concretes," *Constr. Build. Mater.*, vol. 96, no. August 2018, pp. 217–225, 2015, doi: 10.1016/j.conbuildmat.2015.08.015.

[21] M. Jedidi, O. Benjeddou, and C. Soussi, "Effect of expanded perlite aggregate dosage on properties of lightweight concrete," *Jordan J. Civ. Eng.*, vol. 9, no. 3, pp. 278–291, 2015, doi: 10.14525/jjce.9.3.3071.

[22] I. B. Topçu and B. Işikdağ, "Manufacture of high heat conductivity resistant clay bricks containing perlite," *Build. Environ.*, vol. 42, no. 10, pp. 3540–3546, 2007, doi: 10.1016/j.buildenv.2006.10.016.

[23] ASTM C20-00, "Standard Test Methods for Apparent Porosity , Water Absorption , Apparent Specific Gravity , and Bulk Density of Burned Refractory Brick and Shapes by Boiling Water," *Am. Soc. Test. Mater.*, 2015, doi: 10.1520/C0020-00R10.2.

[24] S. Shingles, “Standard Test Methods for Sampling and Testing Non-Asbestos Fiber-Cement Flat,” pp. 1–9.

[25] T. I. Standard, “TIS1407-2540 กระเบื้องซีเมนต์เส้นใยแผ่นลอน.”

[26] L. H. Yu, H. Ou, and L. L. Lee, “Investigation on pozzolanic effect of perlite powder in concrete,” *Cem. Concr. Res.*, 2003, doi: 10.1016/S0008-8846(02)00924-9.

[27] M. Ali, M. S. Abdullah, and S. A. Saad, “Effect of Calcium Carbonate Replacement on Workability and Mechanical Strength of Portland Cement Concrete,” *Adv. Mater. Res.*, vol. 1115, no. June 2020, pp. 137–141, 2015, doi: 10.4028/www.scientific.net/amr.1115.137.

[28] J. Pokorný, M. Pavlíková, M. Záleská, P. Rovnaníková, and Z. Pavlík, “Coagulated silica - A-SiO2 admixture in cement paste,” *AIP Conf. Proc.*, vol. 1752, 2016, doi: 10.1063/1.4955254.

[29] K. Bilba, M. A. Arsene, and A. Ouensanga, “Study of banana and coconut fibers. Botanical composition, thermal degradation and textural observations,” *Bioresour. Technol.*, vol. 98, no. 1, pp. 58–68, 2007, doi: 10.1016/j.biortech.2005.11.030.

[30] A. K. Samanta, G. Basu, and P. Ghosh, “Enzyme and silicone treatments on jute fibre. Part I: Effect on textile-related properties,” *J. Text. Inst.*, vol. 99, no. 4, pp. 295–306, 2008, doi: 10.1080/00405000701478035.

[31] Y. Cao and H. Tan, “Effects of cellulase on the modification of cellulose,” *Carbohydr. Res.*, vol. 337, no. 14, pp. 1291–1296, 2002, doi: 10.1016/S0008-6215(02)00134-9.

[32] L. Mishra and G. Basu, “OR,” no. February, 2020.

[33] D. S. Varma, M. Varma, and I. K. Varma, “Coir Fibers: Part I: Effect of Physical and Chemical Treatments on Properties,” *Text. Res. J.*, vol. 54, no. 12, pp. 827–832, 1984, doi: 10.1177/004051758405401206.

[34] S. K. Sharma *et al.*, “Reinforcement of natural rubber latex using jute carboxycellulose nanofibers extracted using nitro-oxidation method,” *Nanomaterials*, vol. 10, no. 4, 2020, doi: 10.3390/nano10040706.

[35] S. T. Method, “ASTM: C518-15 Standard Test Method for Steady-State Thermal Transmission Properties by Means of the Heat Flow Meter Apparatus,” [Online]. Available: http://www.ansi.org.

# Appendix

งานวิจัยที่ตีพิมพ์ในวารสารระดับนานาชาติ

AIP Conference Proceedings

## Effect of expanded perlite on physical and mechanical properties of cement mortar

Cite as: AIP Conference Proceedings **2397**, 070001 (2021); https://doi.org/10.1063/5.0063810
Published Online: 15 September 2021

Jira Patthanavarit, Mettaya Kitiwan, Nittaya Keawprak, Phacharaphon Tunthawiroon, et al.

View Online Export Citation

ARTICLES YOU MAY BE INTERESTED IN

Mechanical property enhancement of recycled Poly(ethylene terephthalate) with Nylon6
AIP Conference Proceedings **2397**, 070004 (2021); https://doi.org/10.1063/5.0064067

Simulation and analysis of investment casting process on Francis turbine runner
AIP Conference Proceedings **2397**, 020007 (2021); https://doi.org/10.1063/5.0065030

The s-curve model of biodiesel transesterification by numerical methods based on brief experimental data
AIP Conference Proceedings **2374**, 020005 (2021); https://doi.org/10.1063/5.0061169






AIP Publishing

# Effect of Expanded Perlite on Physical and Mechanical Properties of Cement Mortar

Jira Patthanavarit[1, a)], Mettaya Kitiwan[1, b)], Nittaya Keawprak[2, c)] and Phacharaphon Tunthawiroon[3, d)]

[1]*Department of Applied Physics, Faculty of science, King Mongkut's Institute of Technology Ladkrabang, Bangkok 10520, Thailand*
[2]*Expert Centre of Innovative Material, Thailand Institute of Scientific and Technological Research, 35 Mu 3 Khlong Ha, Khlong Luang, Pathumthani, 12120, Thailand*
[3] *School of Engineering, King Mongkut's Institute of Technology Ladkrabang, Bangkok 10520, Thailand*

[a)] 62605040@kmitl.ac.th
[b)] Corresponding author: mettaya.ki@kmitl.ac.th
[c)] nittaya@tistr.or.th
[d)] phacharaphon.tu@kmitl.ac.th

**Abstract.** This study presents an investigation of the physical and mechanical properties of the cement mortar containing expanded perlite as a filler material. The effects of perlite replacement contents and compressive molding force on bulk density, water absorption, and flexural strength were observed. In the mixture of mortar, the content of sand was replaced with perlite ranging from 0 to 15% by weight. The specimen was pressed under the uniaxial force varied from 20 to 40 kN then de-molded and cured in the humidity for 28 days. With the increase in perlite content from 0 to 15 wt%, the bulk density decreased from 2118 kg/m$^3$ to 1586 kg/m$^3$ while the water absorption increased from 7.4% to18.7%. All composites showed a low thermal conductivity in the range of 0.10–0.27 W/m K. The specimen without perlite had a flexural strength in the range of 10.7–14.2 MPa, while that of sample containing perlite was 7.8–12.5 MPa. The cement mortar composite containing 10 wt% expanded perlite and molding at 40 kN showed the highest flexural strength of 12.50±1.36 MPa while the bulk density and water absorption were 1773 kg/m$^3$ and 1.40 %, respectively. The results of this research can be used as a guideline for further development in building materials such as lightweight roof tile, lightweight brick, and ceiling tile.

**Keywords:** Perlite, Expanded perlite, Cement mortar, Mortar, Building materials

## INTRODUCTION

Recently, global warming causes the average temperature to rise in many regions around the world. The demand for the utilization of air-conditioning to manage the hot temperature and high humidity in the residential sector is steadily increased. This leads to considerable energy consumption, especially in the summer. Using insulated building materials is one of the appropriate means to improve the energy efficiency of the resident because it can decrease the heat transfer from outside toward the interior. Several construction materials are practically available to reduce the rate of heat transfer into the building, such as concrete, brick, wood, stone, etc. However, low thermal conductivity and density of building materials are very important properties for this application.

Perlite has been used to enhance various properties in construction materials. Perlite is a siliceous volcanic rock that contains approximately 70–75% of $SiO_2$. Perlite can expand 4–20 times of original volume when heated above 870°C resulting in a porous structure with extremely low density. Perlite can be applied in various areas such as construction materials, horticulture, and chemical industry. In construction, expanded perlite is preferable to use as an additive in cementitious building materials or partially substitution for aggregate because it provides many attractive

*The 7th International Conference on Engineering, Applied Sciences and Technology*
AIP Conf. Proc. 2397, 070001-1–070001-9; https://doi.org/10.1063/5.0063810
Published by AIP Publishing. 978-0-7354-4124-8/$30.00

physical and thermal properties such as lightweight, sound insulation, thermal insulation, fire resistance, and chemical inertness [1,2]. According to a high content of $SiO_2$, expanded perlite can cause a pozzolanic reaction which could improve the durability of cement products in long term [3,4].

Owing to the low specific gravity, increasing in expanded perlite content in the mixture contribute to a reduction in bulk density of cement products [5,6]. In addition, the expanded perlite would decrease the thermal conductivity of cement effectively [5,6]. This attributes to the presence of microporous structure in expanded perlite allowing air to enclose in the structure of composite. Since air has very low thermal conduction, it becomes an effective barrier to heat transfer. Therefore, expanded perlite is a promising additive for building materials such as cement brick, ceiling tile, and gypsum board, to improve physical properties and thermal insulation.

Several studies have investigated the addition of perlite in building materials. Akyuncu and Sanliturk [7] reported the effect of substitution of sand with perlite coated polysiloxanes at 20–80 vol%. The unit weight of the mortar sample decreases as an increase in perlite. The thermal insulation properties were also improved. However, an increasing amount of coated and uncoated perlite in the mixture caused flexural strength to decrease up to 34% and 38% respectively and water absorption increased up to 141% and 121% respectively. Sengul et al. [5] reported the effects of expanded perlite on mechanical properties of lightweight concrete. Natural sand was substituted with expanded perlite at 20–100%. The result showed that the thermal conductivity was substantially reduced by replacing sand with the expanded perlite. On the other hand, water absorption increased with higher expanded perlite content. The compressive strength is more affected when the replacement ratio up to 40%. Erdogan et al. [8] investigated the pozzolanic effect of expanded perlite and chemical activator on cement pastes and mortars. The result showed that ground perlite is an effective natural pozzolan that can be used to replace cement at 25–50% without a significant loss of strength. Lanzón et al. [9] reported that the addition of expanded perlite above 1.77% by weight leads to a negative effect on mechanical strength and water absorption of lightweight cement mortar.

According to the literature, the addition of perlite in building material reduces unit weight and improve thermal insulation but the excessive amount of expanded perlite could reduce the mechanical strength and increase the water absorption of the products. Therefore, it is necessary to study the addition content of perlite to the cement matrix to optimize the physical and thermal properties. Moreover, it is found that the fabrication method of perlite-modified building materials directly influenced some crucial properties. Tuncan et al. [10] reported that molding of cement mortar under compaction would enhance strength and reduce water absorption. Thus, the molding force for the fabrication of perlite cement composites might be one of the important parameters which should be concerned. Nonetheless, the study on the effect of perlite concentration together with the molding force to fabricate perlite-modified cement mortar is limited.

This research aims to develop cement mortar composite with a low bulk density and high mechanical strength using substitution of sand with expanded perlite. Cement mortar composite mainly contains cement and fine aggregate (natural sand). Various addition such as mineral admixture, fiber, and polymer, can be also employed to enhance the properties of cement mortar composites. In this study, the effects of expanded perlite content and molding force on bulk density, water absorption, thermal conductivity, and flexural strength of cement mortar were investigated. The experimental results of this research can be used as a guideline for further development in insulating building materials such as lightweight roof sheets, lightweight brick, and ceiling tiles.

## MATERIALS AND METHOD

### Materials, Mixing, and Molding

In this study, ordinary Portland cement (Type I) and two aggregate materials consisting of natural sand and expanded perlite (supplied by Klong Yang Limited partnership, Thailand) were used as the raw materials. The Portland cement and natural sand were individually sieved through a No. 35 (0.5 mm) and No. 16 (1.99 mm) mesh sieves, respectively, before mixing with expanded perlite. The chemical compositions of as-received perlite analyzed via X-ray fluorescence (XRF; Bruker, S8 TIGER), were listed in Table 1 as oxide compounds and their concentrations. In addition, the particle size distribution of perlites was preliminarily examined by sieves. The result of size distribution is illustrated in Table 2. For all mixtures, the effective cement to water ratio of 2:1 was kept constant, while cement to aggregate ratio of 1:2 was desired. The expanded perlite was applied as a sand-substitutional material. The different fractions of expanded perlite, i.e., 0, 5, 10, 15 wt% of total aggregate mass in the mixture was examined. Hereafter, the experimental cement mortars are referred as P0, P5, P10, and P15 according to the designed compositions. The

mixture was blended in a laboratory vertical-type mortar mixer for 5 min. The mix proportion of cement mortars was based on the absolute volume method as listed in Table 3.

The rectangular cross-section specimens were prepared by the compression molding process. An approximate 135 g of mixture was individually charged in the steel mold with dimensions of 2.5 cm × 150 cm (width × length), followed by pressing with a hydraulic pressing machine. The thickness of the specimens varied from 1.4 to 2.2 cm depending on expanded perlite content and compressive molding pressure. The specimens were formed at different applied loads at 20, 30, and 40 kN. During pressing, the forces were maintained constant and held for 1 min prior to demolding. Figure 1 shows the hydraulic pressing machine and a set of steel mold used in the molding process. The pressed specimens were cured with wet covering for 28 days, followed by drying in an oven at 90 °C for 24 h. Figure 2 illustrates the example cement mortar specimen after curing.

**TABLE 1.** The chemical compositions of expanded perlite analyzed by XRF.

| $SiO_2$ | $Al_2O_3$ | $K_2O$ | $Na_2O$ | $Fe_2O_3$ | CaO | $P_2O_5$ | MgO | $TiO_2$ |
|---|---|---|---|---|---|---|---|---|
| 74.2 | 13.3 | 6.27 | 1.72 | 1.70 | 1.42 | 0.58 | 0.37 | 0.29 |

**TABLE 2.** Particle size distribution analysis of expanded perlite.

| **Sieve size (mm)** | 0.1< | 0.1-0.3 | 0.3-0.5 | >0.5 |
|---|---|---|---|---|
| **weight fraction** | 16.75 | 38.70 | 26.66 | 17.90 |

**TABLE 3.** Mix proportions of cement mortar.

| **Specimen code** | **P0** | **P5** | **P10** | **P15** |
|---|---|---|---|---|
| Cement ($kg/m^3$) | 556 | 556 | 556 | 556 |
| Water ($kg/m^3$) | 228 | 228 | 228 | 228 |
| Natural sand ($kg/m^3$) | 1111 | 1056 | 1000 | 944 |
| Expanded perlite ($kg/m^3$) | 0 | 55 | 111 | 167 |

(a) (b)

**FIGURE 1.** (a) Hydraulic pressing machine, and (b) steel mold used in the molding process.

**FIGURE 2.** The macrograph of cement mortar specimen.

## Physical Properties Characterization

For physical properties characterization, density and water absorption were determined in accordance with ASTM C1185 and ASTM C20 [11,12]. The small specimens, which were cut from the cement mortar bars, were died at 105°C for 24 h then left cool in a desiccator and weighed (dry weight, $D$). After that, the specimens were boiled in deionized water at 100°C for 2 h. Subsequently, the specimens were cool down to room temperature and immersed in deionized water for 24 h. The weight of specimen while suspended in water was measured and defined as the suspended weight ($S$). Then, the specimens were blotted with the wet cloth prior to weight in the air, this weight is referred to saturated weight ($W$). The volume of specimens ($V$) was derived from $W$-$S$. The procedures to measure the physical properties in this study are shown in Fig. 3. The bulk density and water absorption of specimens are expressed as follows.

$$\text{Density} = \frac{D}{V} \tag{1}$$

$$\text{Water absorption} = \frac{W - D}{D} \tag{2}$$

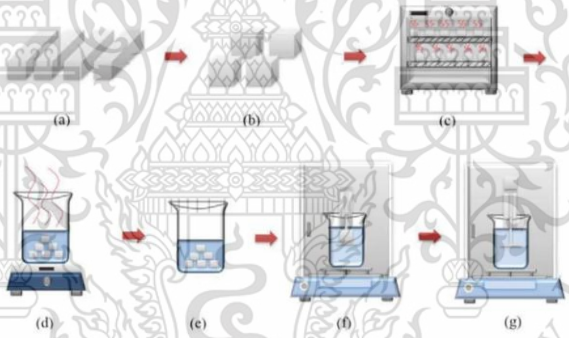


**FIGURE 3**. Schematic procedures to measure the physical properties: (a) cement mortar bar specimens, (b) small specimens cut from bar, (c) drying at 105°C for 24 h then cooling in desiccator and weighing (dry weight, $D$), (d) boiling at 100°C for 2 h, (e) cooling to room temperature and immersing for 24 h, (f) weighing in water (suspended weight, $S$), and (g) weighing in air (saturated weight, $W$).

## Thermal Conductivity Test

The measurement of thermal conductivity is based on an adaptation of the hot wire technique performed by the Transient Hot Bridge apparatus (LINSEIS, THB-1). The pair of specimens of 2.5 cm × 25 cm × 1.2 cm were prepared. The specimen was dried in an oven at 110 °C for 24 h. After that left in an auto desiccator to cool down. For determination of the thermal conductivity, a sensor probe is positioned at the surface between two samples as the sandwich-setup shown in Fig. 4. The specimen was pressed lightly to ensure contact between the surface of specimen and sensor probe. An electric current is then applied to the sensor probe, to generate heats which raises an increase in temperature. The increase of temperature will result in heat diffusion into the material which allows the determination of thermal conductivity.

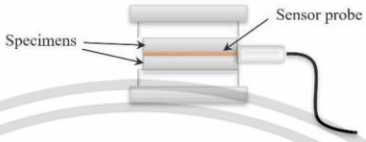


**FIGEURE 4.** Sandwich-setup of samples and sensor probe for testing thermal conductivity

## Mechanical Test

The mechanical property of cement mortar was characterized by a static flexural test. The three-point bending test adapted from ASTM C1185 [11] was performed in order to evaluate the flexural strength. An in-house three-point bending fixture, manufactured with high stiffness materials, was set up in the universal testing machine (Shimadzu AG-X, Japan). A support (span length, $L$) of 100 mm and a constant loading rate of 0.1 mm/min were set for bending tests. The schematic drawing of the three-point bending figure and testing apparatus is shown in Fig. 5(a) and (b), respectively. The flexural strength was calculated using equation (3).

$$\sigma = \frac{3}{2}\frac{PL}{bd^2} \tag{3}$$

Where $\sigma$ is flexural strength (MPa), $P$ is maximum load, $L$ is length of span, $b$ is width of specimen and $d$ is average thickness of specimen.


**FIGURE 5.** (a) Schematic drawing of three-point bending figure, and (b) testing apparatus set in Universal testing machine.

## RESULTS AND DISCUSSION

### Bulk Density and Water Absorption

After 28-day-curing, the bulk density and water absorption of the perlite cement mortar composite were investigated. Figure 6 shows the effect of expanded perlite content and compressive molding force on the bulk density of cement mortar composite. The bulk densities of cement mortar (P0) are in the range of 2029–2118 kg/m$^3$ while those of specimens containing perlite (P5, P10, and P15) decreased with increasing expanded perlite content and varied between 1586 kg/m$^3$ and 1933 kg/m$^3$. The increase in compressive molding force resulted in a slight increase in bulk density. When the applied force increases from 20 kN to 40 kN, it causes the bulk density to increase about 4.2–8.8 %. It is seen that the replacement of natural sand by expanded perlite effectively reduced the unit weight of cement mortar. Although the bulk densities of specimens in this research are higher compare to those report in the literature [5,9,13,14], the result showed a tendency to reduce density by increasing the amount of expanded perlite to higher than 15 wt%.

Figure 7 shows the effect of expanded perlite content and compressive molding force on the water absorption of cement mortar composite. The water absorption of cement mortar (P0) shows the water absorption around 8.6–7.6%. However, adding expanded perlite causes the water absorption increase to the range of 11.4–18.7%. In general, due to the porous structure of perlite, the water absorption drastically increases with perlite content in the composites [2,5,9]. In this study, the water absorption of specimen tended to increase with expanded perlite content which is in accordance with those reported in the literature. It should be noted that when the applied force increased, the water absorption was reduced. During molding, the compressive force applied to the cement mortar could crush expanded perlite to smaller particle size. Additionally, the compressive force could drive the expanded perlite particle to fill in the void between natural sand. The microstructure observation will be carried out to confirm this assumption in further study. To use cement mortar as building materials, the low water absorption is preferable because the high water absorption could deteriorate the construction. The appropriate applied compressive molding force could be an effective way to reduce the water absorption of cement mortar composites.

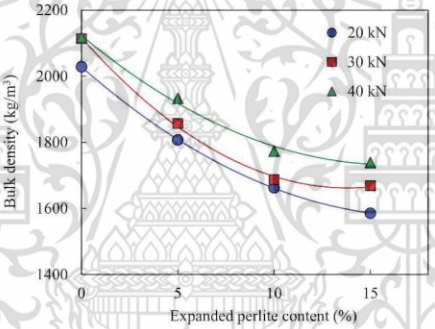


**FIGURE 6.** Effect of expanded perlite content and compressive molding force on the bulk density of cement mortar composite.

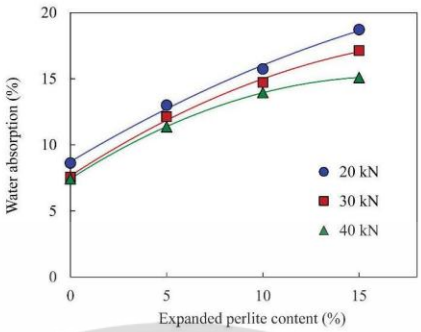


**FIGURE 7.** Effect of expanded perlite content and compressive molding force on the water absorption of cement mortar composite.

## Thermal Conductivity

Figure 8 shows the effect of expanded perlite content and compressive molding force on the thermal conductivity of cement mortar composite. All specimens showed a low thermal conductivity in the range of 0.10–0.27 W/m K. In general, due to the porous structure of perlite, the thermal conductivity reduces with increased perlite content in the composites [5,15,16]. In this study, the tendency of thermal conductivity was not correlated with expanded perlite content. However, the roughness of the surface of specimen might lead to the air gap between the layer of specimen and sensor, resulting in lower thermal conductivity. The thermal conductivity measurement by other methods will be performed in further study for comparison.

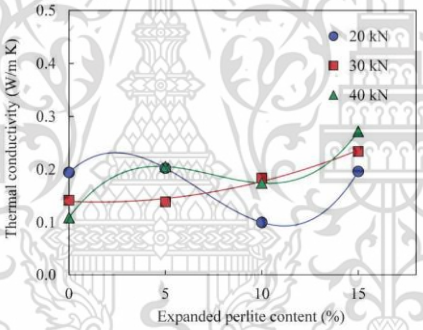


**FIGURE 8.** Effect of expanded perlite content and compressive molding force on the thermal conductivity of cement mortar composite.

## Flexural Strength

Figure 9 shows the effect of expanded perlite content and compressive molding force on the flexural strength of cement mortar composites. The increase in compressive molding force effectively increased the flexural strength of

cement mortar composites. For the specimen molding under 20 kN, the flexural strength of specimen decreases from 10.72±1.55 MPa to 7.81±0.78 MPa with the increasing expanded perlite content from 0 to 15 wt%. On the other hand, the specimens molding under 30 kN and 40s kN, the flexural strength of perlite-containing specimens showed a maximum value of 10.29±0.82 MPa and 12.50±1.36 MPa, respectively, at 10 wt% expanded perlite content. It is general trend that involves expanded perlite in cementitious building materials cause a reduction in strength due to its porous structure. However, some studies reported the positive effect on the strength when expanded perlite is finely ground and added in an appropriate amount [8,16]. The smaller perlite powder responsible for the higher pozzolanic activity which improves the strength of cement composite [16].

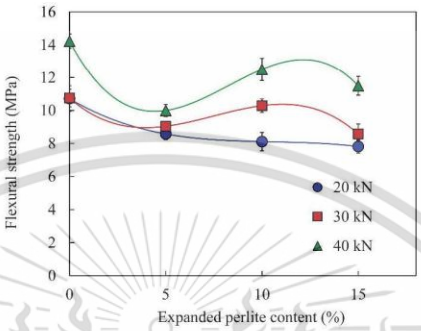


**FIGURE 9.** Effect of expanded perlite content and compressive molding force on the flexural strength of cement mortar composites.

## CONCLUSION

The cement mortar composites containing cement, natural sand, and expanded perlite were prepared by the compressive molding process and curing for 28 days. The effect of replacing natural sand with expanded perlite at 5, 10, and 15 wt%, and compressive molding force at 20, 30, and 40 kN, on the bulk density, water absorption, and flexural strength of cement mortar composites were investigated. The main conclusion from the experimental results of physical and mechanical properties could be drawn as follows:

- The bulk density of cement mortar reduced significantly by replacing natural sand with expanded perlite but slightly increase with a higher compressive molding force.
- The water absorption increased with higher expanded perlite content but slightly decrease with a higher compressive force.
- The thermal conductivities of all composites were low and in the same range.
- The flexural strength of cement mortar containing expanded perlite showed the highest value at 10 wt% expanded perlite content.

From the experimental results, it was found that the optimum content of expanded perlite for sand replacement is 10 wt% and the compressive molding force is 40 kN. With these process parameters, the bulk density, water absorption, and flexural strength of cement mortar composite are 1773 kg/m$^3$, 14.0%, and 12.50±1.36 MPa, respectively.

## ACKNOWLEDGMENTS

This work was funded by National Research Council of Thailand (NRCT). The authors would like to thank Klong Yang Limited partnership for supplying expanded perlite raw material.

## REFERENCES


1. M. Singh and M. Garg, Construction and Building Materials. **5**, 75–81(1991).
2. A.M. Rashad, Construction and Building Materials. **121**, 338–353 (2016).
3. L. H. Yu, H. Ou and L. L. Lee, Cement and Concrete Research. **33**, 73–76 (2003).
4. T. K. Erdem, Ç. Meral, M. Tokyay, T. Y. Erdoğan, Cement and Concrete Composites. **29**, 13–21 (2007).
5. O. Sengul, S. Azizi, F. Karaosmanoglu, and M.A. Tasdemir, Energy and Buildings. **43**, 671–676 (2011).
6. H. Oktay, R. Yumrutaş, and A. Akpolat, Construction and Building Materials. **96**, 217–225 (2015).
7. V. Akyuncu and F. Sanliturk, Journal of Building Engineering. **38**, 102182 (2021).
8. S.T. Erdoğan and A.Ü. Sağlik, Cem. Cement and Concrete Composites. **38**, 29–39 (2013).
9. M. Lanzón and P.A. García-Ruiz, Construction and Building Materials. **22**, 1798–1806 (2008).
10. M. Tuncan, Ö. Arıöz, K. Ramyar, B. Karasu, A. Tuncan, and K. Kılınç, The IV. Ceramic, Glass, Enamel, Glaze and Pigment Seminar with International Participation (SERES 2007), 847–853 (2007).
11. ASTM C 1185-3, "Standard Test Methods for Sampling and Testing Non-Asbestos Fiber-Cement Flat Sheet, Roofing and Siding Shingles, and Clapboards" in *ASTM International* (West Conshohocken, PA, 2016), pp 1–9.
12. ASTM C20-00, Standard Test Methods for Apparent Porosity, Water Absorption, Apparent Specific Gravity, and Bulk Density of Burned Refractory Brick and Shapes by Boiling Water in in *ASTM International* (West Conshohocken, PA, 2015), pp 1–3.
13. D. Kramar and V. Bindiganavile, Material and Structure. **44**, 735–748 (2011).
14. H. Shoukry, M.F. Kotkata, S.A. Abo-EL-Enein, M.S. Morsy, and S.S. Shebl, Construction and Building Materials. **102**, 167–174 (2016).
15. R. Demirboğa and R. Gül, Cement and Concrete Research. **33**, 723–727 (2003).
16. Ł. Kotwica, W. Pichór, and W. Nocuń-Wczelik, Thermal Analysis and Calorimetry. **123**, 607–613 (2016).

# ประวัติผู้วิจัย

| | |
|---|---|
| ชื่อ | นายจิรา พัฒนวริศ |
| วัน เดือน ปีเกิด | 10 สิงหาคม 2540 |
| ที่อยู่ปัจจุบัน | 61/1 หมู่ 7 หมู่บ้านพฤกษา 8/2 ถนน รังสิต-นครนายก ตำบลลำลูกกา อำเภอลำลูกกา จังหวัดปทุมธานี รหัสไปรษณีย์ 12150 |
| ประวัติการศึกษา | (2561) วิทยาศาสตรบัณฑิต สาขา ฟิสิกส์ประยุกต์ เกรดเฉลี่ย 2.81 (สถาบันเทคโนโลยีพระจอมเกล้าเจ้าคุณทหารลาดกระบัง) |
| | (2565) วิทยาศาสตรมหาบัณฑิต สาขา ฟิสิกส์ประยุกต์ เกรดเฉลี่ย 3.81 (สถาบันเทคโนโลยีพระจอมเกล้าเจ้าคุณทหารลาดกระบัง) |
| ทุนการศึกษาที่ได้รับ | ทุนสนับสนุนงานวิจัยทางด้านเกษตรกรรมและอุตสาหกรรม จากสถาบันวิจัยวิทยาศาสตร์และเทคโนโลยี แห่งประเทศไทย |
| ผลงานทางวิชาการ | Jira Patthanavarit, Mettaya Kitiwan, Nittaya Keawprak, Phacharaphon Tunthawiroon, Effects of Expanded Perlite on Physical and Mechanical Properties of Cement Mortar. AIP conference proceedings, 2397, 070001 (2021). |